



The Preserve: Lehigh Library Digital Collections

Elastomeric Films From Structured Latexes.

Citation

He, Yuan. *Elastomeric Films From Structured Latexes*. 1995, <https://preserve.lehigh.edu/lehigh-scholarship/graduate-publications-theses-dissertations/theses-dissertations/elastomeric-0>.

Find more at <https://preserve.lehigh.edu/>

This document is brought to you for free and open access by Lehigh Preserve. It has been accepted for inclusion by an authorized administrator of Lehigh Preserve. For more information, please contact preserve@lehigh.edu.

INFORMATION TO USERS

This manuscript has been reproduced from the microfilm master. UMI films the text directly from the original or copy submitted. Thus, some thesis and dissertation copies are in typewriter face, while others may be from any type of computer printer.

The quality of this reproduction is dependent upon the quality of the copy submitted. Broken or indistinct print, colored or poor quality illustrations and photographs, print bleedthrough, substandard margins, and improper alignment can adversely affect reproduction.

In the unlikely event that the author did not send UMI a complete manuscript and there are missing pages, these will be noted. Also, if unauthorized copyright material had to be removed, a note will indicate the deletion.

Oversize materials (e.g., maps, drawings, charts) are reproduced by sectioning the original, beginning at the upper left-hand corner and continuing from left to right in equal sections with small overlaps. Each original is also photographed in one exposure and is included in reduced form at the back of the book.

Photographs included in the original manuscript have been reproduced xerographically in this copy. Higher quality 6" x 9" black and white photographic prints are available for any photographs or illustrations appearing in this copy for an additional charge. Contact UMI directly to order.

UMI

**A Bell & Howell Information Company
300 North Zeeb Road, Ann Arbor, MI 48106-1346 USA
313/761-4700 800/521-0600**

**ELASTOMERIC FILMS
FROM STRUCTURED LATEXES**

by

Yuan He

A Dissertation

Presented to the Graduate Committee

of Lehigh University

in Candidacy for the Degree of

Doctor of Philosophy

in Polymer Science and Engineering

Lehigh University

1995

UMI Number: 9611123

UMI Microform 9611123

Copyright 1996, by UMI Company. All rights reserved.

**This microform edition is protected against unauthorized
copying under Title 17, United States Code.**

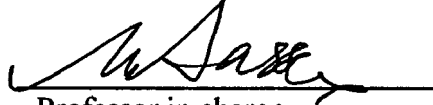
UMI

**300 North Zeeb Road
Ann Arbor, MI 48103**

CERTIFICATE OF APPROVAL

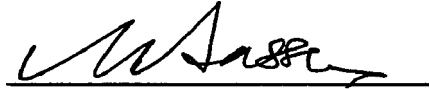
Approved and recommended for acceptance as a dissertation in partial fulfillment of the requirement for the degree of Doctor of Philosophy.


11/10/95
(date)

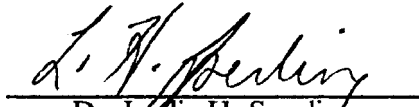

Professor in charge
Dr. Mohamed S. El-Aasser

Accepted 12/8/95
(date)

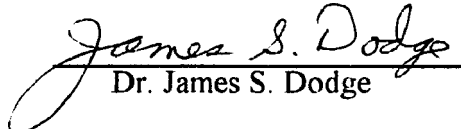
Special Committee Directing the
Doctoral Work of Yuan He


Dr. Mohamed S. EL-Aasser
Chairman, Advisor


Dr. Andrew Klein
Co-Advisor


Dr. Leslie H. Sperling


Dr. Eric S. Daniels


Dr. James S. Dodge

ACKNOWLEDGMENTS

The author wishes to express his sincere and deepest gratitude to his advisors, Dr. M. S. El-Aasser and Dr. A. Klein for their guidance, encouragement and invaluable advice throughout the course of this study.

Sincerest appreciation is given to Dr. E. S. Daniels for his suggestions, discussions and great patience in correcting papers and this dissertation.

The author wishes to thank Dr. L. H. Sperling and Dr. J. S. Dodge for their interest, guidance and willingness to serve on the Dissertation Committee, and the Emulsion Polymers Institute for the financial support for this research work.

Great thanks are also extended to Dr. V. L. Dimonie, Dr. E. D. Sudol, Ms. O. Shaffer and Ms. K. Theodorou for their generous help during all these years of graduate study in EPI.

Special thanks to Ms. D. H. Nyby, Ms. K. Plotts and Ms. R. Snell for their great help with the administrative and paper work.

A warm thank you is expressed to all of my fellow graduate students of EPI for the many wonderful times together.

Finally, the author wishes to express his greatest thanks to his wife, Danni, and his entire family for their love.

Contents

	Page
List of Figures	viii
List of Tables	xiii
Abstract	1
Chapter 1 Introduction	2
1.1 A Brief Overview of Butadiene-Styrene Rubber	2
1.2 The Goal of This Study	7
1.3 Scope of This Dissertation	8
References	10
Chapter 2 Background and Literature Review	11
2.1 Emulsion Polymerization	11
2.1.1 The Harkins-Smith-Ewart (HSE) Theory	12
2.1.2 Medvedev's Particle/Water Interface Initiation Theory	16
2.1.3 The HUFT Theory	18
2.2 Grafting Reaction in Emulsion Polymerization	20
2.3 Film Formation from Latexes	28
2.3.1 Film formation mechanism	28
2.3.2 Molecular interdiffusion	34

	Page
2.3.3 Interfacial Crosslinking	38
References	46
 Chapter 3 Grafting Behavior of n-Butyl Acrylate onto	
 Poly(butadiene-<i>co</i>-styrene) Latexes	55
3.1 Introduction	56
3.2 Experimental	58
3.2.1 Materials	58
3.2.2 Emulsion Polymerization	59
3.2.3 Measurement of the Gel Fraction and Grafting Efficiency using a Solvent Extraction Method	62
3.2.4 Measurement of the Gel Fraction Using a TLC/FID Method	65
3.3 Results and Discussions	66
3.3.1 P(Bd-S) Seed Latex	66
3.3.2 Gel Fraction Measurements	66
3.3.3 Appearance of Latex Films	72
3.3.4 Gel Fraction Measurements During the Second-stage Polymerization	73
3.3.5 Influence of the Type of the Second Stage Monomer and Initiator on the Extent of Grafting/Crosslinking	74

	Page
3.3.6 Morphological Observations of the Development of the Grafting/Crosslinking Interphase Zone using Transmission Electron Microscopy (TEM)	83
3.3.7 P(Bd-S)/PBA Core/Shell Interphase Zone Hardening Process — Comparison with P(Bd-S)/PMMA Core/Shell Systems via Platinum Shadowing TEM Studies	88
3.3.8 DSC Study of the Development of the Core/Shell Interphase Zone	93
3.4 Summary	97
References	99
 Chapter 4 Hydrogenation of Poly(butadiene-<i>co</i>-styrene) in Latex Form	 100
4.1 Introduction	101
4.2 Experimental	103
4.2.1 Materials	103
4.2.2 Preparation of P(Bd-St) Latexes	103
4.2.3 Hydrogenation of P(Bd-S) latexes	105
4.2.4 IR Analysis for Determination of the Degree of Hydrogenation	105
4.3 Results and Discussion	107

	Page
4.3.1 IR Analysis	107
4.3.2 Location and Concentration of Copper Ion	109
4.3.3 Distribution of Double Bonds in the Latex Particles after Hydrogenation	119
4.4 Summary	129
References	130
 Chapter 5 Study of the Consumption of TMI in Latex by Using Attenuated Total Reflectance FTIR (ATR-FTIR)	 132
5.1 Introduction	133
5.2 Experimental	135
5.2.1 Materials	135
5.2.2 Emulsion Polymerization	135
5.2.3 ATR-FTIR Spectroscopy	137
5.2.4 Titration of Isocyanate Groups in P(BA-TMI)	137
5.3 Results and Discussions	138
5.4 Summary	149
References	150

	Page
Chapter 6 Elastomeric Films from Structured Latexes	151
6.1 Introduction	153
6.2 Model Structured Latexes Used for the Study	159
6.3 Experimental	160
6.3.1 Materials	160
6.3.2 Treatments of Hydrogenated P(Bd-S) Seed Latexes	161
6.3.3 Seeded Emulsion Polymerization	164
6.3.4 Preparation of Latex Films	164
6.3.5 Gel Fraction, and Swelling Ratio Measurements	166
6.3.6 Stress-Strain Mechanical Properties	166
6.4 Results and Discussions	167
6.5 Summary and Conclusions	180
References	182
 Chapter 7 Conclusions and Recommendations	 184
 VITA	 190

List of Figures

Chapter 3

- Figure 3-1:** Overall percentage of monomers converted vs. reaction time for SBR latexes prepared at 60, 65, and 70 °C. ---p68
- Figure 3-2:** Gel fractions measured by toluene extraction (filled square) and TLC/FID (empty square) methods for the P(Bd-St) latexes at different conversions of emulsion polymerization. ---p70
- Figure 3-3:** Percentage of second-stage BA monomer converted and total gel fraction of the latex vs. reaction time using the P(Bd-St) seed latex polymerized to 27% (LG SBR, 2% gel-fraction) and 57% (HG SBR, 47% gel-fraction) conversions. ---p75
- Figure 3-4:** Grafting efficiency (GE) for a variety of second stage polymers onto P(Bd-St) latex seed particles after seeded latex emulsion polymerization using a variety of initiators. ---p78
- Figure 3-5:** Gel fraction (GF) of composite latex particles prepared via a P(Bd-St) seeded emulsion polymerization with different second stage monomers. ---p80
- Figure 3-6:** Changes in the gel fraction (GF) of P(Bd-St) seed latexes after the second stage seeded emulsion polymerization was complete for different monomer and initiator systems. ---p82

- Figure 3-7:** The grafting efficiency (GE) of butyl acrylate grafted on P(Bd-St) seed latexes (HG or LG SBR seed) vs. shell/core ratios as determined by solvent extraction measurements. ---p84
- Figure 3-8:** TEM micrographs (cold stage) of LG-SBR/PBA (left) and HG-SBR/PBA (right) composite particles with different core/shell ratios obtained during the second stage semi-continuous polymerization. ---p86
- Figure 3-9:** Schematic illustration of Pt shadowed transmission electron micrograph (TEM) for: (A) soft and (B) hard latex particles. ---p89
- Figure 3-10:** Hardening process for the original soft P(Bd-St) seed latex particle (top) during the seeded emulsion polymerization of MMA (left) and BA (right) as observed by Pt-shadowed TEM micrographs. ---p91
- Figure 3-11:** Changes in the H/R ratio of composite latex particles as determined by Pt-shadowing TEM studies with different shell/core ratios prepared by the P(Bd-St) seeded emulsion polymerization with MMA or BA. ---p92
- Figure 3-12:** DSC curves for the core/shell LG-SBR/PBA latexes prepared with different core/shell ratios; the arrows show the end points of the transitions. ---p95
- Figure 3-13:** Schematic illustration of the development of the core/shell SBR/PBA interphase zone and the formation of PBA phase during the second stage semi-continuous polymerization. ---p98

Chapter 4

- Figure 4-1:** IR spectra of non-hydrogenated P(Bd-St) (a) and partially hydrogenated P((Bd-St) latexes (b). ---p108
- Figure 4-2:** A schematic illustration of the hydrogenation of P(Bd-S) latex particle by the Cu^{2+} catalyzed $\text{H}_2\text{N-NH}_2$ / H_2O_2 redox system. ---p113
- Figure 4-3:** Hydrogenation percentage with different molar concentrations of copper ion in the SP latex system (50 nm). ---p115
- Figure 4-4:** Hydrogenation percentage with different molar concentrations of copper ion in the LP latex system (230 nm). ---p116
- Figure 4-5:** The relationship between the hydrogenation percentage and the surface area density of copper ions at the particle surface (Cu^{2+} / 1000 nm^2) for the SP and LP latex systems. ---p118
- Figure 4-6:** Two models for the distribution of double bonds in hydrogenated P(Bd-S) latex particles: (a) layer model, and (b) uniform model. ---121
- Figure 4-7:** Degree of hydrogenation after each run for three successive 1/1 molar ratio hydrogenations of the high gel (HG) and low gel (LG) latex systems (particle sizes: HG=240 nm; LG=230 nm). ---p122
- Figure 4-8:** Degree of hydrogenation for each type of double bond in the LG P(Bd-St) latex system; particle size = 230 nm. ---p125
- Figure 4-9:** Degree of hydrogenation for each type of double bond in the HG P(Bd-St) latex system; particle size = 240 nm. ---p126

Figure 4-10: TEM micrographs of: (A) non-hydrogenated P(Bd-St) latex, 80 nm-in diameter; (B) completely hydrogenated P(Bd-St) latexes, 80 nm-in diameter; (C) and (D) partially hydrogenated P(Bd-St) latex, 230 and 240 nm, respectively, for LG (C) and HG (D) latexes. ---p128

Chapter 5

Figure 5-1: A schematic illustration for attenuated total reflectance FTIR (ATR-FTIR) for the *in situ* study of the latex film formation process. ---p139

Figure 5-2: Time-dependent ATR-FTIR spectra recorded during the film formation process for 1/1 (w/w) PS/P(BA-TMI) core/shell latex over a 24 h period. ---p140

Figure 5-3: Profiles for the intensities of water, carbonyl (-CO-) and isocyanate (-NCO) functional groups at wavenumbers of 1640, 1750, and 2259 cm^{-1} , respectively, from ATR-FTIR measurements during a 24 h film formation process. ---p142

Figure 5-4: ATR-FTIR absorbance calibration curve for the isocyanate groups in P(BA-TMI) copolymer and its corresponding weight concentration as determined by titration. ---p144

Figure 5-5: ATR-FTIR absorbance profiles of the isocyanate group in P(BA-TMI) (180 nm) latex and a series of PS/P(BA-TMI) core/shell latexes with shell thicknesses of 20, 12, and 7 nm obtained during a 24 h film formation process. ---p145

Chapter 6

Figure 6-1: Schematic representation of : (A) the structured latex particle; and (B) the elastomeric film formed from the particles. ---p156

Figure 6-2: Percentage of second-stage monomers converted, and the total gel fraction of the latex, vs. reaction time obtained using a SBR seed latex (run 1 in Table II) polymerized to 57 % conversion. ---p169

Figure 5-3: Gel fractions and swelling ratios of the films cast from latexes obtained by using the different seed latexes. ---p170

Figure 5-4: Stress-strain behavior for HSBR/P(BA-TMI) structured latex films and P(Bd-St) latex film; solid lines, fresh latex film; dash line, latex film after aging. (Swelling ratios of the fresh latex films are shown in Table III). ---p174

Figure 6-5: Stress-strain behavior for HSBR/P(BA-TMI)-1 structured latex films cast at various film formation temperatures with film formation times as: 4 days at 25 °C, 1 day at 45 °C and 65 °C. ---p178

Figure 6-6: ATR-FTIR absorbance profiles of water and isocyanate groups in the HSBR/P(BA-TMI)-3 latex system during a 24 h film formation process. ---p179

List of Tables

Chapter 3

Table 3-1	Recipe Used for the Preparation of the P(Bd-S) Seed Latex	---p60
Table 3-2	Recipes for the Second Stage Polymerization Using P(Bd-S) as Seed Latexes	---p61

Chapter 4

Table 4-1	Recipes for the Preparation of P(Bd-S) Latexes	---p104
Table 4-2	Recipe Used for the Hydrogenation of P(Bd-S) Latexes with Different Copper Ion Concentrations	---p106

Chapter 5

Table 5-1	Emulsion Polymerization Recipes Used to Prepare Latex Samples Used in the ATR-FTIR Film Formation Study	---p136
------------------	--	---------

Chapter 6

Table 6-1	Characteristics of Seed Latexes	---p162
Table 6-2	Recipe for the Second-Stage Polymerization at 40 °C	---p165
Table 6-3	Film Swelling Ratios for Samples Used in Stress-Strain Measurements (24 h in toluene)	---p175

Abstract

A model structured latex which is capable of forming a self-curable elastomeric film at low temperatures was developed. In this model, a small amount of dimethyl meta-isopropenyl benzyl isocyanate (TMI[®], Cytec Industries) was copolymerized with n-butyl acrylate (BA) onto poly(butadiene-*co*-styrene) (P(Bd-S)) seed latex particles. In the final stage of the film formation process, a crosslinked PBA network in the shell phase was formed by isocyanate groups through a moisture-curing mechanism.

A series of studies indicated that a portion of the second-stage monomer was consumed to form a highly grafted/crosslinked P(Bd-S)/PBA core/shell interphase zone when applying this model directly to a P(Bd-S)/P(BA-TMI) core/shell latex system.

Reducing the amount of residual double bonds in the P(Bd-S) seed latex particles by hydrogenation was found to be an effective way to reduce the development of the interphase zone and the degree of crosslinking. An elastomeric film was formed with the hydrogenated-P(Bd-S)/P(BA-TMI) structured latex.

Attenuated Total Reflectance-Fourier Transform Infra-Red (ATR-FTIR) spectroscopy was also used to investigate the consumption mechanism of the isocyanate groups from the TMI monomer. It was found that the thickness of the shell in which the isocyanate groups were incorporated would influence the consumption of the isocyanate groups during both polymerization and film formation.

Chapter 1

Introduction

1.1 A Brief Overview of Styrene-Butadiene Rubber (SBR)

SBR is the most commercially important synthetic rubber used nowadays. Large quantities of poly(butadiene-*co*-styrene) [P(Bd-S)], or SBR, is produced in latex form as competitors for ammonia-preserved natural rubber latex.

The butadiene-styrene copolymer prepared from an emulsion polymerization, which was named as “Buna S” was first synthesized by E. Tchunkur et al. in 1929^{1,2}. They discovered that the mixture of butadiene and styrene in a 75/25 ratio can be copolymerized via emulsion polymerization. The resulting rubber products could be more easily processed than the bulk polymerized poly(butadiene) rubber (BR), and they also gave improved vulcanized properties. Early on, SBR was produced at about 50°C (“Hot Rubber”) and was produced on a large scale in Germany in 1937. In 1942, the United States began the construction of government- owned plants to produce the famous “GR-S” (Government Rubber-Styrene). Along with the development of the Hot SBR, the application of redox initiators permitted a lowering of the polymerization temperature to 5 °C. The SBR produced at this lower temperature is called “Cold SBR” and was easier to process. Therefore, by 1953,

Cold SBR had already accounted for about 62% of the total SBR production³.

Varieties of grades of SBR have been produced so far. Depending on the butadiene/styrene ratio, polymerization conditions, and processing conditions, they exhibit different properties for each specific application. For most commercial SBR latexes, the ratio of butadiene to styrene is 76.5 to 23.5 by weight. In some applications that require a lower glass transition temperature, T_g , the butadiene ratio could be up to 90%; i.e., at a 90% bound butadiene level, the T_g of the SBR is about -70°C .

SBR is considered to be a general purpose rubber. Besides its major usage for the production of car and light truck tires, it is widely used in belting, shoe soles, cable insulation and jacketing, hose, surgical, food packaging, etc. In addition to these applications where SBR is used as a self-supporting material, SBR latexes have also found extensive applications in a dispersed form, such as a binder in paper production and as impact modifiers for plastic materials. In 1985, the total annual global production capacity for SBR was about 7 million tons, which is more than half of the total synthetic rubber production capacity.

The whole manufacturing process for rubber products prepared from the original SBR latexes is based on complex flowcharts made up of a number of key processes and operations. In the majority of cases, these flowcharts can be reduced to three fundamental stages: Mix → Shape → Vulcanize. In the first stage, various kinds of additives, e.g., vulcanizing agents, fillers, or softeners and resins, are added to the latex, or to the coagulated rubber crumb followed by a screw extrusion and continuous mixing operation. The quality and uniformity of the mixing exerts a profound influence on the performance of downstream processes. The second stage is to shape the raw rubber by calendering and milling operations. The final stage,

which consists of molding and vulcanization, is accomplished at elevated temperatures, usually higher than 150 °C. During the process prior to the onset of crosslinking, the viscosity of the material is of special importance regarding its processibility. Therefore, the polymerization reactions are usually terminated at relative low monomer conversions. For cold SBR, chain branching and gel formation occurs at about 70% monomer conversion. Thus, the polymerizations are terminated at about 60% monomer conversion through the addition of sodium dimethyldithiocarbamate, dialkylhydroxy amine, or the sodium salt of dithionic acid⁴. For the Hot SBR, the termination conversion is even lower, usually about 40%.

In many applications, such as paints, coatings, and adhesives, it is required that the elastomeric films must be cast directly from latex, and in most of these cases, the elevated temperatures that are necessary for the curing process described above are not feasible. Therefore, in order to obtain an elastomeric material, a certain degree of crosslinking of the SBR latex particles is necessary. However, this intraparticle (inside particles) crosslinking of polymer chains would certainly restrict the interdiffusion of polymer chains between adjacent particles, which is an essential mechanism for latex film formation. To solve this problem, functional groups have been incorporated at the particle surface, and these functional groups are able to interact with each other to connect particles together during the film formation process.

Carboxyl groups are one of the most used functional moieties which can be incorporated at particle surfaces through copolymerization of such monomers as acrylic acid (AA), methacrylic acid (MAA), and itaconic acid (IA). These monomer units are highly

hydrophilic and tend to become concentrated at the latex particle surfaces. In the final stage of film formation, latex particles come in contact with one another and become coalesced. At this stage, the carboxyl groups at the particle surfaces could crosslink through hydrogen bonding or ionic bonding when some multivalent cations, e.g., Ca^{2+} , Zn^{2+} , Al^{3+} , etc., are present in the system. In this way, latex particles are interfacially crosslinked, which could help counteract the interdiffusional restriction of polymer chains caused by the intraparticle crosslinking. However, due to the hydrophilicity of these moieties used to form these kinds of bonds, the films exhibit rather weak resistance to alkaline aqueous solutions, such as detergents. In applications where better environmental resistance and strong elasticity are required, the interfacial crosslinking must be accomplished through a covalent bonding mechanism.

Some of the most common functional monomers used in emulsion polymerization that are capable of self-condensing are N-methylolacrylamide (NMA), N-(isobutoxymethyl) acrylamide (IBMA), and hydroxymethylated diacetone acrylamide^{5,6}. These functional monomers can also react with carboxyl and hydroxy groups. One of the problems for these methylol amide functional groups is that they need a relatively high curing temperature, usually about 80 to 100°C, which is not feasible in a number of applications. Studies^{5,7} have also showed that the distribution of these functional groups in the latex particles, e.g., concentrated in the surface layer or distributed relatively uniformly throughout the particles, is extremely important in influencing the extent of interfacial crosslinking, and consequently, the mechanical properties of the final latex films. In fact, not much interfacial crosslinking could occur when the crosslinkable moieties had a more uniform distribution within the latex

particles⁵.

For hydrophobic functional monomers, a large fraction of the functional moieties incorporated in the particles through copolymerization would become distributed inside the particles rather uniformly. This tendency would be even stronger for SBR latex systems because the interparticle crosslinking restricts the mobility of the polymer chains. In addition to this, due to the lower conversions attained during the emulsion polymerization in the SBR system, the remaining monomers must be removed from the latexes. Some functional monomers have quite high boiling points and are very difficult to completely remove from the system.

The preparation of SBR-based core/shell structured latex particles can be considered as one solution to the problems mentioned above. SBR seed latexes with desired degrees of intraparticle crosslinking are prepared via emulsion polymerization. Another rubbery polymer shell is built up on the SBR seed particles through a seeded emulsion polymerization process. Taking advantage of the phase separation of core/shell polymers, functional groups can be effectively incorporated in the shell layer. This structure is favorable for the latex particles to undergo interfacial crosslinking during the latex film formation process.

Although core/shell rubbery/rubbery structured latex systems have been investigated, and while some of them have been used industrially to produce elastomeric materials⁸, surprisingly, SBR has not been used. As is well known, SBR is an excellent elastomeric material that shows superior properties as compared to acrylic rubbers in many circumstances. More importantly, the price of butadiene is only about one ninth that of most of the acrylic monomers. Therefore, it is very meaningful to investigate the SBR-based structured latex

systems for developing high performance and economical elastomeric materials.

A model structured latex is proposed in the present work. In this model, core/shell structured latex particles were prepared with a certain distribution of functional groups in the shell layer. Dimethyl meta-isopropenyl benzyl isocyanate (TMI[®], Cytac Industries) functional monomer was incorporated in the shell layer through copolymerization with n-butyl acrylate (BA) monomer in the presence of poly(butadiene-styrene) [P(Bd-S)] seed. The isocyanate groups from TMI monomer have been found to be stable against hydrolysis under certain emulsion polymerization conditions⁹. These incorporated isocyanate groups could then crosslink, via a water molecule curing mechanism or by external crosslinkers, during the film formation process.

1.2 The Goal of This Study

The overall objective of this project was to study the interfacial crosslinking behavior of structured latex particles and hence, to develop a high performance elastomeric film. The structured latex particles are comprised of a polybutadiene (PBd)-based core with a poly(n-butyl acrylate) (PBA)-based shell.

A model structured latex system was proposed for producing an elastomeric film which is curable (i.e., via interfacial crosslinking) under mild temperature conditions.

1.3 Scope of This Dissertation

In Chapter 2, some important theoretical aspects and literature which are relevant to this study, such as the emulsion polymerization mechanism, polymer grafting reactions, and latex film formation, are briefly reviewed.

Chapter 3 focuses on the investigation of the grafting behavior for the P(Bd-S)/PBA core/shell system. The formation of a highly grafted/crosslinked core/shell interphase zone was characterized by using such techniques as solvent extraction, film swelling, transmission electron microscopy (TEM), Platinum (Pt)-shadowed TEM, and differential scanning calorimetry (DSC).

In Chapter 4, the hydrogenation of P(Bd-S) in the latex form is described. The mechanism of the hydrogenation and the structure of hydrogenated P(Bd-St) [H-P(Bd-S)] latexes are determined with FTIR and TEM.

In Chapter 5, the consumption mechanism of the isocyanate groups is analyzed by using Attenuated Total Reflectance-Fourier Transform Infra-Red (ATR-FTIR) spectroscopy. The amount of isocyanate groups reacted during each stage, i.e., polymerization and film formation, was determined quantitatively. The relationship between latex particle structure and the reaction of the isocyanate groups is discussed.

In Chapter 6 the model for structured latex particles used to prepare low temperature-curable latex films is described. Using this model, H-P(Bd-S)/P(BA-TMI) structured latex particles were prepared. The mechanical properties of the film were examined.

Finally, in Chapter 7 the major results obtained from the above chapters are

summarized and some recommendations for further study are proposed.

References

1. Tschunker, E., and Back, A., *DRP 570,980* to Farbenindustrie, I. G (1929).
2. Boch, W., and Tschunker, E., *DRP 891,025* to Farbenindustrie, I. G (1939).
3. Hofmann, W., *Rubber Technology Handbook*, p.58, Hanser Publishers, New York, 1989.
4. Pennwalt, *U.S. Pat. No. 3,148,225* (1962).
5. Yeliseeva, V. I., *Br. Polym. J.*, 7, 33 (1975).
6. Bassett, H. D., Sherwin, M. And Hager, S., *J. Coatings Technol.*, 51, 65 (1979).
7. Okubo, M., Nakamura, Y., and Matsumoto, T., *J. Polym. Sci., Polym. Chem. Ed.*, 18, 2451 (1980).
8. Fryd, M., Leberzammer, E., and Andries, S., *U.S. Pat. No. 4,956,252* to E.I. duPont Co. (1990).
9. Dexter, R. W., Saxon, R., and Fiori, D. E., *J. Coating Tech.*, 58, 43 (1986).

Chapter 2

Background and Literature Review

2.1 Emulsion Polymerization

Generally speaking, emulsion polymerization is a method of conducting polymerization by mixing monomer(s), initiator, and surfactant(s) with a dispersing medium (usually water), which leads to the formation of a colloidal polymer dispersion with particles of submicron sizes. The initiators used for emulsion polymerization are usually water-soluble, while the monomers are usually sparingly soluble. Surfactant plays a very important role in the emulsion polymerization process. Through the control of the amount and type of surfactants used, one can achieve both a higher polymerization rate and a higher molecular weight at the same time compared to other polymerization process. In addition, temperature and viscosity control during the polymerization process becomes much simpler because of the presence of the large amount of water medium. These are two distinct advantages of the emulsion polymerization over other polymerization methods, such as bulk or solution polymerization. The final product of an emulsion polymerization, referred to as a latex, can be used directly without further separation in such applications as paints, coatings, adhesives,

finishes and floor polishes.

An emulsion polymerization may present different features depending on the solubility of the monomers and polymers. In terms of the solubility, emulsion polymerization (oil-in-water) can be divided into several types: (1) monomers which are highly insoluble in water, such as styrene and butadiene; (2) monomers which have appreciable water solubility, with corresponding polymers which are highly water-insoluble (examples are acrylonitrile and methyl methacrylate); (3) both monomers and polymers are appreciably hydrophilic, of which a typical example is vinyl acetate; and (4) monomers are highly water-soluble and polymers are completely soluble or highly swellable by water (acidic monomers such as acrylic acid and methacrylic acid fall into this category).

2.1.1 The Harkins-Smith-Ewart (HSE) Theory

The theory of emulsion polymerization has been developed starting from the first qualitative study of Harkins¹ and the quantitative treatment of Smith and Ewart² in the late 1940's. Based on the foundations of the Harkins-Smith-Ewart (HSE) theory, subsequent modifications were contributed by other workers³⁻⁷.

The early research conducted by Harkins, Smith and Ewart was focused on the production of styrene-butadiene rubber (trade name: GR-S). The surfactant concentration of their system was well above the critical micelle concentration (CMC). According to the HSE theory, the emulsion polymerization process can be divided into three distinct intervals. Initially, the system consists of dispersed monomer droplets which are stabilized by surfactant

molecules adsorbed on these surfaces. The size of the monomer droplets, depending on the stirring rate, is usually in the range of 1-10 μm or larger. Since the surfactant concentration was above the CMC, there is also a huge number of small micelles formed from aggregates of the excess surfactant molecules in the dispersion system. The size of these micelles was about 2-10 nm and their concentration was 10^{17} - 10^{18} micelles per milliliter⁸. At this stage, more than 95% of monomer was partitioned in the monomer droplets, with less than 5% partitioning in the micelles. After the water-soluble initiator was added, Interval I of the emulsion polymerization process begins. In Interval I, free radicals generated in the aqueous phase react with the small amount of monomer dissolved in the aqueous phase to form oligomeric radicals. The number of monomer units incorporated into the oligomeric radicals increased until the hydrophobic chain lengths were sufficiently high to counter their surface-active properties; these oligomers are capable of entering either monomer droplets or monomer-swollen micelles. However, since the concentration of micelles is overwhelmingly higher than that of monomer droplets (10^{10} - 10^{11} per milliliter), the total surface area of the micelles is larger than that of the droplets by more than two orders of magnitude, i.e., the surface area of the droplets is negligible. Each oligomeric radical captured by the micelles continue to grow until another radical enters and causes termination. Thus, in this interval, monomer-swollen micelles are transformed into monomer-swollen polymer particles of much larger sizes. Monomer that is consumed in the growing particles is supplied from the monomer molecules continuously diffusing from the monomer droplets through the aqueous phase. With the growth in the particle size, more surfactants are needed to stabilize the increased surface area of the polymer particles. Since the colloidal stability of the polymer

particle is much higher than that of the monomer-swollen micelles, micelles that have not captured radicals would dissociate to give up their surfactant to the growing polymer particles. At the end of Interval I, a constant number of polymer particles is reached once all the micelles disappear. Therefore, Interval I is characterized as the micellar nucleation stage. An increase in polymerization rate is observed in this interval. In Interval II, these polymer particles continue to grow with a constant monomer concentration inside the particle until the monomer reservoirs (the monomer droplets) is exhausted. The polymerization rate remains constant in this interval. In Interval III, monomer remaining in the particles is polymerized and the polymerization rate decreases.

According to this mechanism, the rate of polymerization in monomer/polymer particles (R_p) is given by the Smith- Ewart equation as:

$$R_p = \frac{k_p N}{N_A} [M] \bar{n} \quad (2-1)$$

where:

- k_p : propagation rate coefficient.
- N : number of particles.
- N_A : Avogadro's number.
- $[M]$: equilibrium concentration of monomer in particles.
- \bar{n} : average number of radicals per particle.

To find out the number of polymer particles per unit volume formed at the time of consumption of free emulsifier, Smith and Ewart proposed the equation:

$$N = k \left(\frac{R_i}{\mu} \right)^{0.4} (a_s S)^{0.6} \quad (2-2)$$

where μ is the rate of volume increase of a polymer particle; R_i is the rate of radical generation; a_s is the specific area of the surfactant and S is the surfactant concentration. The constant k has 0.37 and 0.53 for its lower and upper limit, respectively.

Combination of Eqs (2-1) and (2-2) gives a relation for the rate of polymerization after the completion of nucleation:

$$N = \frac{k}{2} k_p [M_{eq}] \left(\frac{R_i}{\mu} \right)^{0.4} (a_s S)^{0.6} \quad (2-3)$$

where $[M_{eq}]$ is the equilibrium monomer concentration in monomer/polymer particles.

This theory has been successfully applied for monomers with low water solubility, e.g., styrene. However, this mechanism does not represent general results and is restricted to treating certain cases of emulsion polymerization, i.e., low-water soluble monomer and high surfactant concentration ($>CMC$) systems. This theory has been criticized for several reasons including the observations that: (1) latex particles are produced even in the absence of micelles, i.e., in the cases when the surfactant concentration is below its CMC, and in

surfactant-free emulsion polymerization systems, (2) the particle numbers estimated by this mechanism are usually double those found experimentally, and (3) this theory does not fit more water-soluble monomer systems well.

Several tentative mechanisms to describe particle formation in emulsion polymerization have been postulated to modify the HSE theory^{9,10}. Based on several assumptions, Gardon¹¹⁻¹⁶ modified the micellar model by introducing some new parameters into existing equations. Gardon has reported that only one out of every 100 or 1000 micelles absorbs a radical and becomes a polymer particle and that all other micelles serve as reservoirs of the surfactant. As one of the important parameters in Gardon's modification, the volume fraction of monomer in the monomer-swollen polymer particle, Φ_m , was determined by the particle swelling method in regard to a series of monomers used in emulsion polymerization, e.g., styrene (S), methyl methacrylate (MMA), ethyl methacrylate (EMA), butyl acrylate (BA), etc..

2.1.2 Medvedev's Particle/Water Interface Initiation Theory

As the hydrophilicity of monomer increased, remarkable deviations from the above micellar models (HSE, Gardon) were observed^{17,18}. A new approach to explain some of these experimental results has been presented by Medvedev^{19,20}. He proposed that the surface of a polymer particle is the site of propagation of a polymer chain. Initiation, propagation, and termination all proceed at the polymer particle/water interface. This theory ignores the presence of micelles and considers the surfactant in the reaction system as a whole. The

theory assumes that after the adsorption of an initiator molecule on the surface of monomer/polymer particles, the mechanism of initiation starts to be affected, i.e., monomer molecules are initiated at the interfaces. Interactions between surfactant molecules and initiators lead to an increase in the concentration of primary radicals in the particle surface layer. For an oil-soluble initiator, the overall polymerization rate, R_p , is proportional to the concentration of surfactant $[S]$ to the first power:

$$R_p = k_1[M][S][I_i]^{0.5} ; \quad \overline{P}_n = k_1'[M][I_i]^{-0.5} \quad (2-4)$$

where $[M]$ is the monomer concentration in the effective volume of latex particles, $[I_i]$ is the initiator concentration in the particle/water interphase zone, and \overline{P}_n is the average degree of polymerization.

In emulsion polymerization systems, which are initiated by a water-soluble initiator, the rate of polymerization is proportional to the 0.5 order with respect to the surfactant concentration:

$$R_p = k_2[M][S]^{0.5}[I]^{0.5}, \quad \overline{P}_n = k_2'[M][S]^{0.5}[I]^{-0.5} \quad (2-5)$$

where $[I]$ is the initiator concentration in the aqueous phase.

2.1.3 The HUFT Theory

A more sophisticated and successful theory, known as the HUFT theory, was developed by Hansen & Ugelstad²¹ and Fitch & Tsai²², based on the theory of homogeneous nucleation which was first introduced by Roe.²³

The model of homogeneous nucleation presented in the HUFT theory was formulated on the basis of considerations about the reactions of radicals which may proceed in the aqueous phase. If there is no surfactant in the system, or if the surfactant concentration is below the CMC, the radicals produced by the decomposition of initiator may: (1) add to a monomer dissolved in water; (2) absorb into polymer particles; (3) terminate with other radicals in the aqueous phase; or (4) precipitate from solution as a primary particle, if the radical has reached its critical chain length. The absorption of radicals in particles is a reversible process which depends on the oligomer solubility, reaction rate in particles, and the surface potential. In the HUFT theory, the rate of nucleation (dN/dt) is given as the rate of propagation of the chains of one unit less than the critical chain length:

$$\frac{dN}{dt} = k_p R_{jct-1} [M_a] \quad (2-6)$$

where k_p is propagation constant, $[M_a]$ is the monomer concentration in the aqueous phase, and R_{jct-1} is the concentration of oligomers with one unit less than the critical chain length.

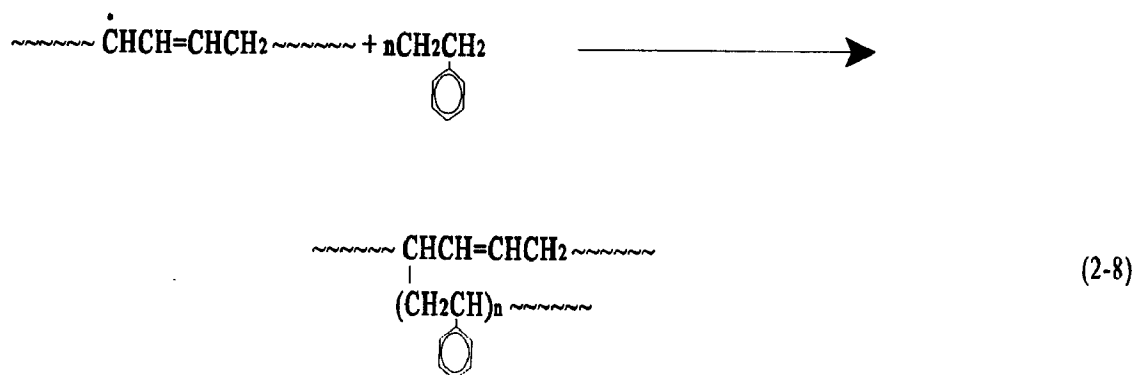
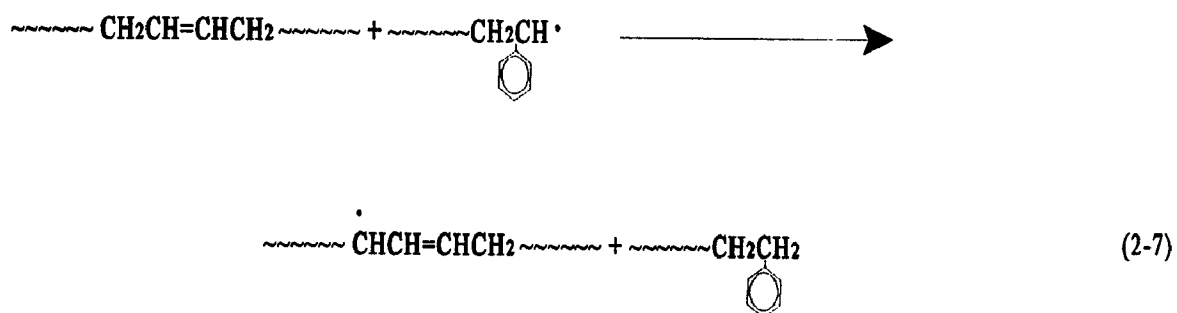
The HUFT coagulative nucleation theory has been supported by a number of

experiments²⁴⁻²⁶.

2.2 Grafting Reactions in Emulsion Polymerization

A graft copolymer contains a long sequence of one monomer (often referred to as the backbone polymer) with one or more branches (grafts) of long sequences of a second monomer. Usually, the synthesis of graft copolymer is a sequential process requiring a second (or multiple step) polymerization scheme. On the basis of the first report on branched polystyrene by Houtz²⁷, and the chain transfer mechanism proposed by Flory²⁸, LeBras²⁹ conducted polymerizations of acrylonitrile in the presence of a rubbery latex, the products of which were called “modified rubber”. The chain transfer mechanism was then expanded to include polymer and monomer of different structural units³⁰. The terms “graft” and “grafting” were first used³¹ to represent polymers in which the backbone polymer and the grafted side polymer chain were composed of different structural units.

Basically, there are three possible radical reactions by which graft copolymers are formed³²⁻³⁵. Consider the polymerization of styrene in the presence of polybutadiene as a typical example. First, a grafting site can be generated via the polymer chain transfer between the propagating styrene radical and the existing polybutadiene polymer:



Second, a grafting site can also be formed by the direct attack on the backbone polymer by primary radicals from the initiator. Finally, for polymers containing double bonds such as polybutadiene, graft polymerization may also involve copolymerization between the polymerizing monomer and the double bonds of the backbone polymers:



or more likely:



since the vinyl double bond is more active to radical reaction.

The production of graft copolymers using emulsion polymerization processes is a common industrial approach. Several such systems are of great commercial significance, such as high-impact polystyrene (HIPS), which is prepared via the polymerization of styrene in the presence of poly(1,3-butadiene), ABS and MBS, which are graft copolymers of styrene-acrylonitrile and methyl methacrylate-styrene, respectively, copolymerized in the presence of

either poly(1,3-butadiene) or poly(styrene-butadiene).

The emulsion polymerization of a second monomer in the presence of a preformed latex particle is called seeded emulsion polymerization, which is the common manufacturing technique used to produce structured latexes as well as graft copolymers. Along with choices in polymerization parameters such as temperature and recipe conditions, there are a number of different emulsion polymerization processes which also offer a variety of ways to influence the outcome of the graft polymerization, and hence, the properties of the final products. Depending on the addition rate of the second stage monomer(s), batch and monomer-starved operations could be considered as two extremes of a general mode of semi-continuous operation. “Batch” operations for seeded emulsion polymerization represent an infinitely fast feed rate while the “monomer-starved” operation represents an addition rate which is so slow that the monomer level within the latex particle is nearly zero. Since the batch operation is usually conducted after swelling equilibrium of the second stage monomer in the seed particles has been reached, a large difference in the monomer concentration, and/or monomer/polymer ratio is expected in the seed particles for these two types of operations. This difference would certainly influence the results of the grafting polymerizations.

Although, theoretically, graft sites can be generated in any polymer backbone via a polymer chain transfer mechanism, significant grafting occurs with those polymers that have active hydrogens, or some more labile atoms, e.g., chlorine atom in chlorinated rubbers³⁶.

Most of the grafting studies have dealt with natural and synthetic rubbers and focused on qualitative interpretation of the modified rubber³⁷⁻⁴³. Conflicting views on the influence of the type of initiator on grafting have been reported. Some studies claimed that, compared with

peroxide-type initiators, azo-type initiators, e.g., azobis(isobutyronitrile) (AIBN), would not produce any grafting,^{33,37,44,45} while others maintain that the use of the azo initiators could generate a small amount of graft sites⁴⁶⁻⁵⁰. By reviewing these works, it can be found that the type of backbone polymer and the polymer/monomer ratio can significantly influence the mechanism of the grafting polymerization. For instance, Brydon³³ stated that cis-1,4-polybutadiene backbone polymer would not produce grafting when AIBN initiator was used. However, it has been shown by Locatelli⁵⁰, that a rather high degree of grafting was attained regardless of the type of initiators, e.g., either benzoyl peroxide (BPO) or AIBN when there was an increased number of vinyl double bonds present in the backbone polymer. Also, more grafting could occur at high polymer/monomer ratios, even with the AIBN initiator.

Since almost all of these studies mentioned above had been conducted in solution polymerization systems, they usually can not be applied directly to an emulsion polymerization system. Chern and Poehlein⁵¹ indicated that the direct attack of initiator on the residual carbon-carbon double bond of the PBd backbone was found to be the most important mechanism for producing grafting sites in solution polymerization. However, when the same modeling study was carried out in emulsion polymerization, chain transfer of a growing polymeric radical to the PBd core by allylic hydrogen abstraction has been found to be dominant. Contrary results have also been found on the influence of the type of initiator on grafting in solution and emulsion polymerization systems. Beati and Peguraro⁵² reported that when AIBN was employed for the emulsion polymerization of MMA using PBd as seed, a higher grafting efficiency was found than when potassium persulfate (KPS) was used. Beati et al. also conducted step-wise seeded emulsion polymerizations. They demonstrated that the

grafting efficiencies decreased in increased steps of the multi-step seeded emulsion polymerization. They concluded that the decreased diffusion of MMA monomer through the seed latex particles was the reason for causing an observed decrease in grafting efficiency.

The heterogeneity of the distribution of monomer throughout the monomer/polymer latex particles in seeded emulsion polymerization has been demonstrated by several researchers.⁵³⁻⁵⁷ A model involving a monomer-rich shell layer for the monomer-swollen latex particles has been proposed, and the monomer-rich “shell” is believed to be main locus of polymerization.

Gasperowicz et al.⁵⁸ have investigated the grafting of styrene onto poly(butyl acrylate) (PBA) seed particles in emulsion polymerization. The grafting efficiency was found to decrease with increasing monomer/polymer ratio, surfactant concentration, and initiator concentration, and was weakly affected by the polymerization temperature.

In accordance with the model developed by Rosen⁵⁹ in a solution polymerization system, Merkel et al.⁶⁰ reported that, at a relatively low polymer/monomer ratio (~30/70), the grafting efficiency decreased with increased conversion of the second stage methyl methacrylate (MMA) monomer. In the high polymer/monomer ratio range (~70/30), a high grafting efficiency (>80%) was found over the entire conversion region. These authors also investigated the influence of the seed surface area and initiator concentration on the degree of grafting. It was found that the grafting efficiency in the PBd/PMMA system decreased with the increased oil-soluble initiator concentration [2,2-azobis(2,4-dimethylvaleronitrile)], and decreased seed surface area, respectively.

Aerdt⁶¹ studied the grafting behaviors of S/MMA copolymer onto PBd seed latex by

solvent extraction combined with a solid state NMR technique. The author demonstrated that there was a sudden increase in the degree of grafting at high conversions (>85%). The cause of this phenomenon was explained by a decrease in the monomer concentration at high conversions, where the probability of chain transfer to PBd polymer was increased.

There are still several other important factors that could alter the outcome of the grafting polymerization. The latex particle morphology can be varied depending on the polymerization process, type of initiator, surfactant concentration, etc.⁶²⁻⁶⁴ Different morphologies would lead to different patterns of phase separation, which could certainly influence the degree of grafting⁶⁵.

Compared with the large number of qualitative studies introduced above, studies aimed at a quantitative prediction of grafting behavior in emulsion polymerization have been relatively sparse. Due to the complexity of emulsion polymerization systems, it has been very difficult to develop a general model to theoretically analyze and predict a grafting reaction for the system. Quantitative models for grafting of styrene monomer onto PBd have been derived by Brydon³³, Ludwico^{34,35}, and Rosen⁵⁹ in solution polymerization systems based on several assumptions. Brydon's model considered that grafts can be formed by both direct attack on the rubber backbone from initiator radicals, and cross-termination from free and grafted polystyrene radical chains. Rosen's model, on the other hand, was set up on the basis of the physical limits of grafting in two-phase polymerization reactions. Regardless of the chemical nature of the grafting process, the physical nature of two-phase polymerization limits the maximum amount of glassy polymer which could possibly be grafted to the rubber. Rosen assumed that all of the styrene which reacted within the monomer-swollen rubber phase was

actually grafted to the rubber, and the grafting efficiency decreased with increasing glassy monomer/rubber ratio and conversion, i.e., most of the grafting is accomplished during the early stages of the reaction.

Sundberg et al.^{66,67} developed a kinetic model describing the grafting reactions in emulsion polymerization. Their work considers that radicals formed in the aqueous phase can initiate both grafted and free second stage polymer chains in the monomer-swollen rubber phase, with the probability of the formation of each different chain being related to a specific initiation rate constant. The chain length of the second stage polymer is predominantly controlled by a chain transfer process rather than by the cross-termination of free and grafted polymer chains. The model was verified for the seeded emulsion polymerization of St monomer in the presence of polybutadiene latex particles by investigating the influence of parameters such as conversion, concentration of chain transfer agent, and temperature, on the grafting efficiency.

In the work of Chern and Poehlein⁶⁸, the concept of a nonuniform distribution of free-radicals in polymerizing latex particles has been incorporated into the development of a kinetic model to describe grafting reactions. This theory permits the prediction of grafting efficiency as a function of reaction conditions. It can also be used for the evaluation of rate constants for the grafting reactions. The authors found that the predominant grafting reaction appears to be the attack of growing polystyrene chains on the allylic hydrogen atoms of polybutadiene. The results further reinforce the hypothesis that the entering oligomeric free-radicals are not distributed uniformly within the particle volume.

An old concept of so-called “trapped radicals”, which was proposed by Miller^{69,70} in

the 1950's, may be suitable for generally describing monomer-starved condition in emulsion polymerization. This theory considered that the “macromolecule free radicals” generated in a highly viscous or crosslinked polymer phase is accompanied by a slowing of the termination reaction due to the reduced mobility. In a seeded emulsion polymerization system, especially in a process that is under “monomer-starved” conditions, the mobility of the “macromolecule free-radicals” in the latex particles is expected to be greatly reduced. Consequently, polymer backbone radicals and postformed polymer radicals would have a longer lifetime and a higher concentration in the particle. Under such circumstances, various reaction mechanisms may occur at the same time, i.e., polymer chain transfer, direct attack of radicals to backbone polymer, and cross termination of radicals. This last mechanism can also introduce crosslinks in the latex particle⁷¹.

To summarize, grafting reactions in emulsion polymerization are rather complicated and still only partially understood. Most of the models which have been developed invoke many assumptions. The grafting behavior of a specific system is not only dependent on the polymerization conditions, but also on the type of the polymer/monomer system. The most often used seed latexes are rubbery polymers such as polybutadiene (PBd), poly(styrene-butadiene) (SBR), poly(butadiene-acrylonitrile) (NBR), and poly(butyl acrylate) (PBA). The second stage monomers are usually those which produce glassy polymers; examples of which are styrene (St), methyl methacrylate (MMA), and acrylonitrile (AN). A combination of rubbery seed/shell monomer which would polymerize to give glassy polymer is the common point in almost all of the published studies relevant to grafting reactions.

In order to produce a high performance elastomeric film from structured latex

particles, the grafting study conducted in the present work was aimed at investigating a system of P(Bd-St)/BA rubbery seed/second stage monomer which would give rubbery polymer. Some unique grafting behaviors that have not been observed in other studies are reported.

2.3 Film Formation from Latexes

Films formed from polymer latexes are of considerable industrial importance. Film-forming polymer latexes have been utilized in a wide variety of applications such as coatings, adhesives, latex paints, membranes, and polymer electrolytes.

2.3.1 Film Formation Mechanism

Generally, the process of film formation from polymer latexes may be divided into three stages⁷²:

1. Concentration of latex particles by evaporation of water until the particles are densely packed;
2. Deformation and coalescence of the polymer particles until a continuous and pore-free polymer film is formed; and,
3. Further gradual coalescence and fusion which occurs by interdiffusion of the polymer chains of adjacent particles.

The first two stages have been studied extensively. In an early attempt to develop a

mechanism for latex film formation, Bradford et al.⁷³⁻⁷⁵ proposed a theory in which viscous flow due to surface tension was postulated to explain latex film formation; this theory is known as the dry sintering theory or “dry caking” theory. According to this theory, following the evaporation of water, latex particles were forced into contact because the surface tension of the polymer, which was exerted as the total surface area of the latex polymer, decreased greatly. Subsequently, the particles underwent dry sintering accompanied by viscous flow and particle deformation. They applied the model developed by Frenkel⁷⁶ to describe the coalescence of spheres due to purely viscous flow:

$$\theta^2 = \frac{3\gamma tR}{2\pi\eta} \quad (2-11)$$

where θ is the degree of coalescence (as measured by the half angle of coalescence), γ is the polymer surface tension, t is the elapsed time, R is the particle radius, and η is the polymer viscosity.

Later, this concept of purely viscous flow was criticized by Brown⁷⁷ based on the following experimental results:

- (1) Since film formation occurred simultaneously with water evaporation from the latex, the polymer/water interfacial tension, instead of the polymer surface tension (i.e., polymer/air interfacial tension), would supply the driving force for particle coalescence;
- (2) The rate of water evaporation influenced the degree of coalescence;
- (3) An incompletely fused film can be produced by maintaining the temperature below

a certain value (later expanded to the concept of the “minimum temperature for film formation”, MFT); and,

(4) Lightly crosslinked latex particles may form continuous films that have low mechanical strength. Purely viscous flow of the polymer can not account for this observation since mutual penetration by sintering is hindered by the crosslinking.

Brown proposed that film formation takes place by capillary pressure which is related to the surface tension at the water/air interface. At the end of the first stage of the film formation process, at which point the particles are densely packed and no longer mobile in the bulk latex, the particles may either deform, leading to film formation, or water may evaporate completely from the channels, without fusion of particles occurring. Obviously, there are two opposite forces that drive the process in two different directions, i.e., either promoting or hindering coalescence.

Brown postulated that the capillary force, F_C which resulted from the surface tension of water when evaporation has caused the formation of very small radii of curvature between the particles is the main driving force for coalescence of the particles. According to this hypothesis, coalescence occurs when F_C exceeds the force resisting deformation, F_G (the Columbic repulsions and van der Waals attractions were considered to be negligible compared with F_C and F_G). This resistance force of a sphere to coalescence (F_G) does not depend on the viscous flow of the material, but primarily on its elastic deformation. It was then concluded that for film formation to occur:

$$G < 35 \gamma_{a/w} / R \quad (2-12)$$

where G is the elasticity modulus of the polymer, $\gamma_{a/w}$ is the air/water surface tension, and R is the particle radius.

Mason⁷⁸ modified Brown's theory and commented that Brown made the erroneous assumption that the capillary pressure is constant throughout the second stage of film formation. Mason pointed out that the capillary pressure is a function of particle deformation and stated that the condition for film formation to occur should be:

$$G < 266 \gamma_{a/w} / R \quad (2-13)$$

Subsequently, Bradford and Brown's theories were extended by Vanderhoff et al.⁷⁹ and the theory that they proposed is known as the "wet caking" theory. According to Vanderhoff's mechanism, at the beginning of the second stage of film formation, particles are brought into close proximity so that their stabilizing layers were in contact, retarding any closer approach. As the water continued to evaporate, the force from the water surface tension pushed the particles together until the stabilizing layers were ruptured, resulting in polymer-polymer contact. The pressure of the particle was then increased by the forces arising from the polymer/water interfacial tension.

One of the reasons for this extension to Brown's theory is the effect of latex particle size. Continuous P(Bd-S) films were formed⁸⁰ from a polymer latex with an average particle size which was larger than the critical condition given by Brown's equation (2-12). Vanderhoff and Bradford proposed that different curvature radii could be involved in the coalescence of two polymer particles. The pressure difference ($P_2 - P_1$), caused by surface

tension, across the area of contact between two coalescing particles is given by:

$$P_2 - P_1 = \gamma (1/r_1 + 1/r_2 + 2/r) \quad (2-14)$$

where γ is the polymer/water interfacial tension and r_1 and r_2 are the principal radii of curvature. Since r_1 is very small in the beginning stages of coalescence, the pressure difference causing coalescence could be very important, even if the particle radius, r , is large. Although this model is still not general because other forces besides interfacial tension may also contribute simultaneously to coalescence, nevertheless, this theory indicates that the forces exerted during the drying of latexes of large particle sizes might be strong enough to cause coalescence.

Based on theories of Bradford, Brown, and Vanderhoff, several more models and theories have been proposed. Kendall et al.⁸¹ developed an equation involving different forces such as columbic repulsions and van der Waals attractions, surface tension, and elastic forces, and stated that all of these forces might act simultaneously during the formation of a latex film. Recently, Eckersley et al.^{82,83} proposed a time-dependent criterion for film formation based on Brown's model and Mason's expression:

$$1/J_c(t) < 34\gamma/R \quad (2-15)$$

where $J_c(t)$ is the time-dependent creep compliance of polymer. This relation was verified

experimentally to be valid when the strain is small. This model was further verified by investigating the minimum film temperature (MFT, defined as the minimum temperature at which a latex cast film becomes continuous and clear) and using scanning electron microscopy (SEM) to examine P(MMA-BA) latex films as a function of particle size, molecular weight and degree of crosslinking. It was concluded that the degree of film fusion was a function of particle size.

The theories introduced above have explained the first two stages of latex film formation from different point of views. Controversies based on experimental results still exist, especially on the relationship between particle size and MFT. Some researchers have implied that the MFT of a particular polymer emulsion should be independent of particle size⁷⁹, while others support Brown's model and have found that the MFT increased as the average particle size increased^{84,85}. The influence of the plasticizer on the MFT of a latex system has also been discussed⁸⁶⁻⁸⁸.

A very important contribution to the understanding of the latex film formation process was made by Voyutskii and Starkh^{89,90} as early as 1954. They observed the time dependence and the irreversibility of the latex film formation process and attributed these properties to the phenomenon of autohesion, i.e., the mutual interdiffusion of free polymer chain ends across the particle-particle interface, which would render the film to be homogeneous. This theory is actually describing the stage which was later on assigned as the third stage of latex film formation.

The third stage of the film formation from latexes is also known as the cohesive strength development stage because films attain their full strength after this stage. Once the

polymer particles are in intimate contact with one another, the cohesive strength development can proceed between adjacent particles. Daniels and Klein⁹¹ have given a rather complete review about this stage of film formation from latexes.

It is generally accepted that there may be three types of basic interparticle interactions in this stage:

- (1) Molecular interdiffusion of macromolecules from particles into their neighbors;
- (2) Interfacial crosslinking through interactions of functional moieties in the particle surface layers; and,
- (3) Interstitial crosslinking by a void-filling polymer, either homogeneous or heterogeneous, which is capable of crosslinking with the particle surfaces.

2.3.2 Molecular Interdiffusion

Historically, due to the lack of sensitive instrumentation, very few papers have been published concerning the interdiffusion of polymer chains between neighboring latex particles after the “autohesive” theory proposed by Voyutskii. This interdiffusion, termed “a further gradual coalescence”, was observed by Vanderhoff⁹² by utilizing electron microscopy and investigating the aging effect of latex film. Conclusive evidence was presented by El-Aasser et al.⁹³ to prove this concept, that the residual structure of the spherical particles in dry films is diminished with aging. The availability of small angle neutron scattering (SANS) sources and other new instrumentations provided a way of tackling this historically difficult problem. Hahn et al⁹⁴⁻⁹⁶ observed an increase in the radius of gyration of deuterated polymer chains as

a function of annealing time using SANS measurements with deuterated n-butyl methacrylate-based copolymer latexes, which led to the conclusion that the coalescence of dried latex films is due to massive interdiffusion in material of different latex particles. Meantime, Linné et al.⁹⁷ made a very detailed study on the initial interdiffusion in deuterated polystyrene (PS) films as a function of the annealing time. High molecular weight PS chains are constrained within small latex particles with radii of gyration four times smaller than that in the relaxed state. Upon annealing at a temperature 50°C above the glass transition temperature, the radii of gyration increased with time as segmental diffusion proceeds during film formation, via a relaxation diffusion mechanism. Subsequently, Yoo et al.⁹⁸ have investigated the relationship between the depth of interdiffusion measured by SANS and the tensile strength build-up in film formation. They proposed two new critical parameters in the process of film formation from latex: the location of chain ends and the geometrical packing factor. Kim^{99,100} further studied an anionically polymerized PS artificial latex, which eliminated the influence of the charged sulfate end group. The tensile strength was found to increase as a function of annealing time and then leveled off after reaching a maximum. The average interpenetration depth of the deuterated PS chains was found to depend on the one-fourth power of the annealing time up to reptation, which is in good agreement with the results obtained from a polymer interface healing study¹⁰¹.

In addition to SANS measurements, steady-state fluorescence techniques have also been used to follow polymer chain interdiffusion.¹⁰²⁻¹⁰⁵ Winnik^{102,103} et al. have studied a poly(butyl methacrylate) latex labeled with either phenanthrene or anthracene. The latex film formation process was studied by analysis of the nonradiative energy transfer from the

phenanthrene donor to the anthracene acceptor. Little energy transfer was detected at the initial stages of film formation, indicating that the particles retained their individual identifiers. With increasing annealing time, the extent of energy transfer increased, which clearly demonstrated the interdiffusion of polymer chains in adjacent particles across particle boundaries. These investigators also quantitatively investigated the effect of coalescing aids on polymer chain interdiffusion through the analysis of diffusion coefficients.

Normally, the interdiffusion of polymer chains would lead to a loss in the particle identity and would result in the formation of a completely homogeneous film. However, for particles containing incompatible polymer phases, e.g., structured particles with core/shell or multiphase morphologies, some polymer domains may retain their original shapes, although interdiffusion might also occur. These kind of composite or structured polymer latexes are of significant industrial interest due to their enhanced mechanical properties¹⁰⁶.

Okubo et al^{107,108} carried out emulsion polymerization of styrene using poly(ethyl acrylate) (PEA) after an equilibrium-swelling process. The composite latex particles exhibited a morphology where small PS domains were dispersed in the PEA phase. The ultimate tensile strengths of the latex films changed from 20 kg/cm² to 140 kg/cm² after annealing at 100C° and 150 C°, respectively. These researchers demonstrated that phase inversion occurred when the temperature was raised, i.e., the low tensile strength corresponded to the film which has a PEA continuous phase, and the high tensile strength, the PS continuous phase.

Grafting between two phases¹⁰⁹ may restrict the diffusion of polymer chains and hence hinder the deformation of latex particles during film formation as well as phase inversion. Mechanical characteristics of such systems approach those of interpenetrating polymer

networks¹¹⁰. Kast¹¹¹ has analyzed the film formation process for copolymer latexes, and in particular, heterogeneous systems with multiphase morphologies.

Molecular interdiffusion of polymer chains between adjacent latex particles during the third stage of film formation has been shown to be critically important to the cohesive strength development of a latex polymer film. However, due to the presence of surfactant and charged end groups that are distributed at the particle surfaces, an absolutely homogeneous polymer film, like that obtained from solvent-cast films, is still very difficult to obtain. In other words, the weakest parts of a latex film are still the regions where particle boundaries exist, even though these boundaries may be not obvious. This effect is more significant for crosslinked latex particles, e.g., poly(butadiene-styrene) latex, where intraparticle crosslinking is unavoidable. Zosel and Ley¹¹² prepared a series of poly(butyl methacrylate) latexes which covered the whole range from non-crosslinked to highly crosslinked particles. Using both dynamic mechanical measurements and SANS techniques, they have shown that slightly or moderately crosslinked particles behave like homogeneous networks in the linear visco-elastic range. The development of mechanical strength by interdiffusion of polymer chains across particle boundaries was observed. This effect was greatly weakened as the degree of crosslinking was increased. The films remained brittle upon annealing when the mean molecular mass between crosslinks became smaller than the entanglement length because the molecular interdiffusion and the formation of interparticle entanglements are impossible in these latex films.

2.3.3 Interfacial Crosslinking

In order to enhance the mechanical properties of latex films, functional groups are chemically incorporated into the latex particle, often at the surface of the particles, via copolymerization of a small amount of functional monomer(s) during the emulsion polymerization process. These functional groups are capable of associating with one another through such interactions as hydrogen bonding, ionic bonding, or covalent bonding to form a crosslinked network in the particle surface regions, so-called “interfacial crosslinking”, which may occur during the third stage of the film formation process.

There are a wide variety of these functional groups which can be used to form interfacial crosslinks. Depending on the characteristics of the bonds formed from the reactive moieties, functional monomers can be divided into two groups, i.e., groups capable of hydrogen/ionic bonding, and those which can undergo covalent bond formation.

Most functional monomers which can form hydrogen or ionic bonds are highly hydrophilic, such as monomers containing carboxyl groups, e.g., acrylic acid, methacrylic acid, itaconic acid, and fumaric acid; amido groups, e.g., acrylamide, and methacrylamide; or sulfonate groups, e.g., sodium styrene sulfonate. These monomers are typically used in small concentrations and are often not homogeneously incorporated throughout the polymer particles. For example, Matsumoto and Okubo¹¹³ used the soap titration method to confirm a reduction in surfactant adsorption on latex particle surfaces when polar groups were incorporated at the particle surface zone. A number of other researchers further determined that the distribution of acid-containing comonomer units between the aqueous phase, the

surface of the polymer particles and the particle interior, depended on the types of comonomer used and the reaction conditions, e.g., pH, and the mode of addition of the monomers.^{114,115} Distler¹¹⁶ and Penzel¹¹⁷ were able to show the location of the acid groups in latex directly by staining ultramicrotomed sections of latex films with uranyl acetate. It was clearly shown that the acid groups were present in a hydrophilic polymer shell around the particles and tended to form a continuous network throughout the film. Similar observations have been made in the polymerization of vinyl acetate¹¹⁸. By adjusting the polymerization conditions, poly(vinyl alcohol) can be formed at the particle surfaces by hydrolysis of poly(vinyl acetate). The absence of the further gradual coalescence of such latex particles during the film formation has been attributed to the presence of poly(vinyl alcohol) at the particle surfaces.^{119,120} Micrographs of the ultramicrotomed sections stained with OsO₄ showed that poly(vinyl alcohol) also formed a continuous network throughout the film during film formation.¹¹¹

Besides the formation of hydrogen bonds, carboxyl group-containing latexes can also be externally cured with inorganic and organic curing agents to form ionic bonds. Okubo et al.¹²¹ investigated the influence of a series of metallic chelating agents on the mechanical properties of P(EA-AA) latex films. It has been found that the mechanical properties of the latex film are dependent on the type of external crosslinkers used, e.g., in order of increasing tensile stress: $\text{Cr}^{3+} > \text{Al}^{3+} > \text{Zn}^{2+} > \text{Ca}^{2+} > \text{Mg}^{2+}$; for the crosslinkers with the same type of cation: $\text{Ca}(\text{OCOCH}_3)_2 > \text{Ca}(\text{NO}_3)_2 > \text{CaCl}_2$. Bufkin and Grawe^{122,123} also described a series of typical ionically crosslinked carboxyl-containing latexes which could be externally cured with zinc.

Latexes containing carboxyl groups are of great industrial interest for the purpose of developing room temperature-curable latex coatings¹²⁴⁻¹²⁷. Utilizing the reversibility of these kinds of bonds, the latexes can be used for removable floor wax applications. However, on the other hand, hydrogen bonds and ionic bonds may be deficient in the presence of solvent and alkaline aqueous solutions, such as detergents.

To obtain durability of latex film in harsher environments, a great deal of effort has been expended to develop latex films which are capable of covalent bond formation. Monomers that provide moieties that will spontaneously crosslink when a latex is dried to a film, usually with annealing, are valuable for making specialty coatings. Three main classes of this kind of functional monomer that can be readily incorporated into polymer latex particles are: N-methylol acrylamide/N-methyl ethers of acrylamide, methylenes, and epoxies. This last class of functional monomer, i.e., epoxies, is usually used in interstitial crosslinked systems.

Yeliseeva^{128,129} has carried out a series of emulsion polymerizations to prepare latexes comprised of copolymers of ethyl acrylate (EA) with N-methylolmethacrylamide (NMMA), and with glycidyl methacrylate (GMA). These two functional monomers, NMMA and GMA, are highly and poorly soluble in water, respectively. The difference in polarities of both monomers would lead to different distributions of the corresponding functional groups on the surfaces of the latex particles¹³⁰. The more polar NMMA monomer unit would tend to become concentrated on the particle surfaces and could form interfacial crosslinks during the annealing of the air-dried P(EA-NMMA) latex films. The tensile strength of these films increased about seven times after the concentration of NMMA monomer was increased from

2.6% to 12%. On the other hand, the less polar GMA units had a more uniform distribution within the particles and not much interfacial crosslinking took place in the latex film. The tensile strength remained low even with increased GMA concentration. By controlling the polymerization process to concentrate GMA units at the particle surface layer, interfacial crosslinking could occur in the latex films¹³¹.

Because of the toxicity and susceptibility to premature crosslinking, NMMA (and also NMA, N-methylolacrylamide) have been modified into their etherified methylol derivatives, such as N-(iso-butoxymethyl)acrylamide (IBMA)¹³². Bassett et al¹³³ investigated the kinetics of the crosslinking reactions which occur in latexes containing IBMA and carboxyl and hydroxyl functionalities. It was found that IBMA crosslinking in emulsion polymerization was strongly promoted by the presence of copolymerized carboxyl groups, but relatively unaffected by the presence of hydroxyl moieties. Some kinetic results showed that IBMA moieties located near the latex particle surfaces facilitated interfacial crosslinking. It was also found that there was a decrease in crosslinking when the carboxyl-containing latex was neutralized with a base such as triethylamine, and that acid catalysis had little effect on these neutralized latexes. Makuuchi et al.¹³⁴ studied another methylol ether derivative N-(n-butoxymethyl)acrylamide (NBM) which was incorporated into a core/shell structured latex system. The mechanical properties of the latex film, i.e., elongation and tensile strength, were found to be closely related to the relative extent of intraparticle and interparticle crosslinking.

Another group of crosslinkable monomers are the active methylenes^{135,136}, such as 2-acetoacetoxyethyl methacrylate, N-(2-acetoacetoxyethyl) acrylamide, and 2-cyanoacetoxyethyl methacrylate. These monomers are particularly stable toward hydrolysis

and will self-react as well as react with formaldehyde or multifunctional aldehydes. The films prepared from latexes containing a few percent of such monomers are insoluble. Presumably, the enol form of one unit reacts with the activated keto form of another unit to form a carbon-carbon bond¹³⁷.

The third large class of crosslinkable functional monomers is the epoxy-containing monomers. The high reactivity of the strained epoxy ring is useful for reactions with nucleophiles under mild conditions. Epoxy-containing monomers are exemplified by glycidyl acrylate (GA) and methacrylate (GMA)^{128, 137, 138}. These monomers provide sites for reactions with organic acids, amines, thiols and other nucleophiles.

Grawe and Bufkin¹³⁸ have summarized the applications of epoxy functionalities in crosslinked latex systems. Okubo and Nakamura¹³⁹ have studied the effect of epoxy groups at the surface layer of ethyl acrylate-glycidyl methacrylate copolymer latex particles on the crosslinking reactivity. Two series of epoxy-containing latexes were prepared with high and low epoxy contents on the latex particle surface. These two series of latexes were separately blended with amine functional latexes made by copolymerizing diethylaminoethyl methacrylate (DE) and ethyl acrylate (EA). Okubo et al. found that the tensile strength and modulus of films cast from the blend emulsions with high surface epoxy content were much higher than those obtained from the blends with low surface epoxy content. These results demonstrated the importance of the surface concentration of crosslinkable groups, which has also been reported by other studies using even small molecule crosslinkers, e.g., hexamethylene diamine¹⁴⁰.

In addition to these three major classes of functional monomers, there are a number

of other functional monomers which are available for preparing latex films with interfacial crosslinking by covalent bond formation.

Monomers which contain hydroxyl groups¹³⁸, e.g., hydroxyethyl acrylate, and methacrylate, can provide crosslinking sites in latex particle surfaces which are capable of reacting with curing agents such as melamine resin, polyamines, epoxy resins, and isocyanate-containing agents.

Carboxylated latexes can undergo interfacial crosslinking not only through the ionic and hydrogen bonding mechanisms, but also via reactions with several other functional groups. 2-isopropenyl-2-oxazoline (IPO)¹⁴¹ and carbodiimides¹⁴² (UCARlink[®]) are two examples of commercialized crosslinking agents for carboxyl groups. Melamine-formaldehyde (MF) resins have been used to cure carboxylated SBR latexes for non-woven applications¹⁴³.

There are also some other kinds of functional monomers that have been used in emulsion polymerization to form interfacial crosslinks in latex films. For example, the unsaturated bonds in some fatty acrylate monomers, such as linolenyl acrylate, or oleyl acrylate could act as crosslink sites through autoxidation with a lead or cobalt catalyst¹⁴⁴. Some alkoxysilanes¹⁴⁵ with substituents that protect the alkoxysilane molecules from hydrolysis can also be prepared by emulsion polymerization, and undergo self-crosslinking (forming Si-O-Si linkages) during film formation.

In addition to the emphasis on increasing the durability of latex films or binders, great efforts have also been spent on obtaining competitive durability (compared to high temperature-curing latex systems) at lower curing temperatures. Recently, the low temperature-curable latex films are of increasing commercial interest due to the inaccessibility

of energy source in lots of applications, and the current energy situation.

A monomer which contains an isocyanate group, dimethyl meta-isopropenyl benzyl isocyanate (TMI[®]), has been developed by Cytec Industries¹⁴⁶. An unusual property of TMI monomer is its ability to undergo copolymerization in emulsion polymerization with minimal hydrolysis of the isocyanate functionality. In emulsion polymerization with typical redox initiators at 40 °C, more than 98% of the isocyanate groups remained unreacted after the polymerization¹⁴⁷. In the TMI-modified latexes the isocyanate moieties can undergo crosslinking reactions during the film formation process under mild temperature conditions.¹⁴⁸

By summarizing the research work on interfacial crosslinking in the latex film formation process, several main points can be deduced, as follows:

(1) Interfacial crosslinking can greatly increase the mechanical properties and the durability of latex films.

(2) Ionic or hydrogen bonding types of interfacial crosslinking can be formed at mild temperature conditions but exhibit poor environmental resistance, e.g., low resistance to some organic solvents and alkaline aqueous solutions such as detergents.

(3) A high enough concentration of functional groups in the surface layer of latex particles is crucially important for attaining interfacial crosslinking in the latex films. The hydrophilicity of the functional monomers, polymerization process control, and preparation of structured latex particles, e.g., core/shell latex particles, result in high concentrations of the functional moieties in this region.

(4) Covalent bond formation which results in interfacial crosslinking can lead to excellent mechanical properties and high durability of films in the harsher environments. This

type of interfacial crosslinking can be divided into two groups: (i) a “one-pot” system, in which no external crosslinking agents are added and the functional monomers are reactable/crosslinkable through either self-condensation, or through some hydrolytic (by water molecules in latex film) multi-step reaction mechanism, or (ii) a “two-pot” system, in which some external curing agent is needed to accomplish the crosslinking reactions.

For most of the functional monomers used in the formation of “one-pot” latex systems, the self-reacting functional groups have to be stable at the polymerization temperature, e.g., from 20-80 °C, and crosslink at elevated temperature ($> 100^{\circ}\text{C}$) during the annealing of the films. It has been difficult to develop a “one-pot” latex system which can form films that are curable under mild temperature conditions.

It is relatively easy to obtain a lower curing temperature with the “two-pot” latex system. However, in most cases, in order to prevent premature intraparticle crosslinking, or coagulation during the storage period, the external curing agents usually have to be added right before applying the latexes.

In the present work, a model structured latex particle using TMI as the functional monomer is proposed to develop a low temperature-curable “one-pot” latex system. So far, almost all of the structured latexes for producing self-supporting elastomeric films have been prepared by acrylic polymers. In this work, polybutadiene-based structured latex has been prepared for the purpose of developing high performance elastomeric films.

References:

1. Harkins, W.D., *J. Am. Chem. Soc.*, **69**, 1428 (1947).
2. Smith, W.V. and Ewart, R.W., *J. Chem. Phys.*, **16**, 592 (1948).
3. Blackley, D.C., "Emulsion Polymerization", Appl. Sci. Pub., London, (1975).
4. Gardon, J.L., in "Emulsion Polymerization", Chapter 6, Schildknecht, C.E. Ed, Wiley-Interscience., New York (1977).
5. Fitch, R.M. Ed., "Polymer Colloids II", Plenum Press, New York (1980).
6. Poehlein, G.W., "Emulsion Polymerization" in "Encyclopedia of Polymer Sci. and Eng.", Vol 6, p.1, Wiley-Interscience., New York (1986).
7. Casey, B.S., Maxwell, I.A., Morrison, B.R., and Gilbert, R.G., *Makromol. Chem., Macromol. Symp.*, **31**, 1 (1990).
8. Odian, G., "Principles of Polymerization.", 3rd Ed. p.337, Wiley-Interscience. Pub. (1990).
9. Stockmayer, W.H., *J. Polym. Sci.*, **24**, 314 (1957).
10. O'Toole, J.T., *J. Appl. Polym. Sci.*, **9**, 1291 (1965).
11. Gardon, J.L., *J. Polym. Sci.*, A-1, **6**, 623 (1968).
12. Gardon, J.L., *J. Polym. Sci.*, A-1, **6**, 643 (1968).
13. Gardon, J.L., *J. Polym. Sci.*, A-1, **6**, 665 (1968).
14. Gardon, J.L., *J. Polym. Sci.*, A-1, **6**, 687 (1968).
15. Gardon, J.L., *J. Polym. Sci.*, A-1, **6**, 2853 (1968).
16. Gardon, J.L., *J. Polym. Sci.*, A-1, **6**, 2859 (1968).
17. Paulyuchenko, V.H. and Ivanchev, S.S., *Acta Polym.* **34**, 521 (1983).

18. Chatterjes, S.P., Banerja, M., and Konar, R.S., *J. Polym. Sci., Polym. Chem. Ed.*, **16**, 1517 (1978).
19. Medvedev, S.S., in: "Progress of the International Sym. on Macromol. Chem.", Pague, Pergamon, London, 174 (1957).
20. Medvedev, S.S., *Collect. Czech. Commun.*, **22**, 160 (1957).
21. Hansen, F.K. and Ugelstad, J., in "Emulsion Polymerization", Piirma, I. Ed., Academic Press, New York (1982).
22. Fitch, R.M. and Tsai, C.H., "Polymer Colloids", Plenum Press, New York (1971).
23. Roe, C.P., *Ind. Eng. Chem.*, **60**, 20 (1968).
24. Hansen, F.J., and Ugelstad, J., *Polym. Sci., Polym. Chem. Ed.*, **16**, 1953 (1978).
25. Feeny, P.J., Napper, D.H., and Gilbert, R.G., *Macromolecules*, **17**, 2520 (1984).
26. Song, S. and Poehlein, G.W., *J. Macromol. Sci. Chem.*, **4**, 403 (1988).
27. Houtz, R. and Adkins, H., *J. Am. Chem. Soc.*, **55**, 1609 (1973).
28. Flory, P., *J. Am. Chem. Soc.*, **59**, 241 (1937).
29. Lebras, J. and Compagnon, P., *Compt. Rend.*, **212**, 616 (1941).
30. Carlin, W. And Schakespeare, N., *J. Am. Chem. Soc.*, **68**, 876 (1940).
31. Mark, H., *Rec. Chem. Progr.*, **12(3)**, 139 (1951).
32. Battaerd, H.A. and Tregear, G.W., "Graft Copolymers", Wiley Intersci., New York (1967).
33. Brydon, A. Burnett, G.M., and Cameron, G.G., *J. Polym. Sci., Polym. Chem. Ed.*, **12**, 1011 (1974).
34. Ludwico, W.A. and Rosen, S.L., *J. Appl. Polym. Sci.*, **19**, 757 (1975).

35. Ludwico, W.A. and Rosen, S.L., *J. Polym. Sci., Polym. Chem. Ed.*, **14**, 2121 (1976).
36. Kaleem, K., Reddy, C.R., and Rajadurai, S., *Makromol. Chem.*, **180**, 851 (1979).
37. Allen, P.W., Ayrey, G., Moore, C.G., and Scanlan, J., *J. Polym. Sci.*, **36**, 55 (1959).
38. Berlin, A.A., *J. Polym. Sci.* **34**, 371 (1959).
39. Merett, F.M., *Trans. Faraday Soc.*, **50**, 759 (1954).
40. Ceresa, R.J., "Block and Graft Copolymers", Butterworths, Washington (1962).
41. Edwarks, P. *Modern Plastics Int.*, **18**, 42 (1988).
42. Rudolph, H., *Makromol. Chem. Macromol. Symp.*, **16**, 57 (1988).
43. Schellenberh, J. and Hamann, B., *J. Appl. Polym. Sci.*, **45**, 79 (1992); **45**, 1425 (1992).
44. Allen, P.W., Merret, F.M., *J. Polym. Sci.*, **22**, 193 (1956).
45. Gesner, B.D., *Rubber. Chem. and Technol.*, **38**, 655 (1966).
46. Ghosh, P. and Sengupta, P.K., *J. Appl. Polym. Sci.*, **11**, 1603 (1967).
47. Mori, Y., Minoura, Y. and Imoto, N., *Makromol. Chem.*, **25**, 1 (1958).
48. Dinges, K. and Schuster, H., *Makromol. Chem.*, **101**, 200 (1967).
49. Wetton, R.E., Moore, J.D.M., and Fox, B.E., *Makromol. Chem.*, **132**, 135 (1970).
50. Locatelli, J.L. and Riess, G., *Angew. Makromol. Chem.*, **32**, 117 (1973).
51. Chern, C.S., and Poehlein, G.W., *Chem. Eng. Comm.*, **60**, 101 (1987).
52. Beati, E. and Peguraro, M., *Die Angewandte Makromol. Chem.*, **73**, 35 (1978).
53. Grancio, M.R. and Williams, D.J., *J. Polym. Sci., A-1*, **8**, 2617 (1970).
54. Grancio, M.R. and Williams, D.J., *J. Polym. Sci., A-1*, **8**, 2733 (1970).
55. Wessling, R.A. and Gibbs, D.S., *J. Macromol. Sci., A-7*, 647 (1973).

56. Kensch, P., Prence, J. and Williams, D.J., *J. Macromol. Sci. Chem.*, **A-7**, 623 (1973).
57. Kensch, P. and Williams, D.J., *J. Polym. Sci., Chem. Ed.*, **11**, 143 (1973).
58. Gasperowicz, A., Kolendowicz, M. and Skowronski, T., *Polymer*, **23**, 839 (1982).
59. Rosen, S.L., *J. Appl. Polym. Sci.*, **17**, 1895 (1973).
60. Merkel, M.P., Dimonie, V.L., El-Aasser, M.S., and Vanderhoff, J.W., *J. Polym. Sci., Polym. Chem. Ed.*, **25**, 1219 (1987); **25**, 1755 (1987).
61. Aerdt, M.A., *Ph.D. Dissertation*, Tech. Univ. Eindhoven (1993).
62. Okubo, M. Yamada, A., and Matsumoto, T., *J. Polym. Sci., Polym. Chem. Ed.*, **15**, 3219 (1980).
63. Okubo, M., Ando, M., Yamada, A., Katsuata, Y., and Matsumoto, T., *J. Polym. Sci., Polym. Lett. Ed.*, **19**, 143 (1981).
64. Okubo, M., Katsuata, Y., and Matsumoto, T., *J. Polym. Sci., Polym. Lett., Ed.*, **18**, 481 (1980); **20**, 45 (1982).
65. Min, T.I., Klein, A., El-Aasser, M.S., and Vanderhoff, J.W., *J. Polym. Sci.*, **21**, 2845 (1983).
66. Sundberg, D.C., Arndt, J., and Tang, M.Y., *J. Dispersion Sci. Techn.*, **5**, 43 (1984).
67. Nelson, D. and Sundberg, D.C., Paper presented at the AIChE Meeting, Houston, March, 27 (1983).
68. Chern, C.S. and Poehlein, G.W., *J. Polym. Sci., Part A*, **28**, 3073 (1990).
69. Miller, G.H. and Perizzolo, A.F., *J. Polym. Sci.*, **18**, 411 (1955).
70. Miller, G.H. and Bakhtiar, A.K., *Can. J. Chem.*, **35**, 584 (1957).
71. Peng, W. and Fred, M., *J. Appl. Polym. Sci.*, **40**, 1289 (1990)

72. Voyutskii, S.S., "Autohesive and Adhesion of High Polymers", p.74, Interscience., New York (1963).
73. Bradford, E.B., *J. Appl. Phys.*, **23**, 609 (1952).
74. Dillon, R.E., Matheson, L.A., and Bradford, E.B., *J. Colloid Sci.*, **6**, 108 (1951).
75. Henson, W.A., Tabor, D.A., and Bradford, E.B., *Ind. and Eng. Chem.*, **45**, 735 (1953).
76. Frenkel, J., *J. Phys., USSR*, **9**, 385 (1945).
77. Brown, G.L., *J. Polym. Sci.*, **22**, 423 (1956).
78. Mason, G., *Brit. Polymer J.*, **5**, 101 (1973).
79. Vanderhoff, J.W., Tarkowski, H.L., Jenkins, M.C., and Bradford, E.B., *J. Macromol. Chem.*, **1**, 361 (1966).
80. Vanderhoff, J.W. and Gurnee, E.F., *TAPPI*, **39**, 71 (1956).
81. Kendall, K. and Padget, J.C., *Int. J. Adhesion and Adhesive*, **149**, 154 (1982).
82. Eckersley, S.T. and Rudin, A., *J. Coatings Techn.*, **62**, 89 (1990).
83. Eckersley, S.T. and Rudin, A., *J. Appl. Polym. Sci.*, **53**, 1139 (1994).
84. Nyugen, B., *Ph.D. Thesis*, University of Waterloo (1986).
85. Protzman, T.F. and Brown, G.L., *J. Appl. Polym. Sci.*, **4**, 81 (1960).
86. Padget, J. C. and Moreland, P.J., *J. Coatings Techn.*, **55**, 39 (1983).
87. Turner, G.P.A., "Introduction of Paint Chemistry", 3rd Ed., Chapman and Hall, London, 144 (1988).
88. Winnik, M.A., Wang, Y. and Haley, F., *J. Coatings Techn.*, **64**, 51 (1992).
89. Voyutskii, S.S., *J. Polym. Sci.*, **32**, 528 (1958).

90. Voyutskii, S.S. and Starkh D, in "Physics and Chemistry of Film Formation from High Polymer Dispersions", Gizleprom, (1954).
91. Daniels, E.S. and Klein, A., *Progr. in Organic Coating*, **19**, 359 (1991).
92. Vanderhoff, J.W., *Br. Polym. J.*, **2**, 161 (1970).
93. El-Aasser, M.S., and Robertson, A.A., *J. Paint. Techn.*, **47**, 50 (1975).
94. Hahn, K., *Ad. Study Inst. Polym. Coll.* (NATO), France (1988).
95. Hahn, K., Ley, G., Schuller, H., and Oberthur, R., *Coll. Polym. Sci.*, **264**, 1092 (1986).
96. Hahn, K., Ley, G. and Oberthur, R., *Coll. Polym. Sci.*, **266**, 631 (1988).
97. Linne, M.A., Klein, A., Miller, G. and Sperling, L.H., *J. Macromol. Sci., Phys.*, **B27**, 217 (1988).
98. Yoo, J.N., Sperling, L.H., Glinka, C.J. and Klein, A., *Macromolecules*, **23**, 3962 (1990).
99. Kim, K.D., Sperling, L.H. and Klein, A., *Macromolecules*, **26**, 4624 (1993).
100. Kim, K.D., Sperling, L.H., Klein, A. and Hammonda, B., *Macromolecules*, **27**, 6841 (1994).
101. Wool, R.P. and O'Connor, K.M., *J. Appl. Phys.*, **52**, 5194 (1981).
102. Zhao, C.L., Wang, Y., Hruska, Z., and Winnik, M.A., *Macromolecules*, **23**, 4082 (1990).
103. Wang, Y. and Winnik, M.A., *Macromolecules*, **23**, 4731 (1990).
104. Boczar, E.M., Dionne, B.C., Fu, Z., Kirk, A.A., Lesko, P.M., and Koller, A.D., *Macromolecules*, **26**, 5772 (1993).

105. Pekcan, O., Campolat, M., and Gocmen, A., *Europ. Polymer J.*, **29**, 115 (1993).
106. Lambla, M., Schlund, B., Lazarus, B., and Pith, E., *Makromol. Chem. Suppl.*, **10/11**, 463 (1985).
107. Okubo, M., Yamaguchi, S., and Matsumoto, T., *J. Appl. Polym. Sci.*, **31**, 1075 (1986).
108. Okubo, M, Seike, M.,and Matsumoto, T., *J. Appl. Polym. Sci.*, **27**, 2033 (1982).
- 109 Min, I.T., Klein, A., El-Aasser, M.S., and Vanderhoff, J.W., *J. Polym. Sci., Chem. Ed.*, **21**, 2845 (1983).
110. Sperling, L.H., "Interpenetrating Polymer Networks and Related Materials", Plenum Press, New York (1981).
111. Kast, H., *Makromol. Chem., Suppl.* **10/11**, 447 (1985).
112. Zosel, A. and Ley, G., *Macromolecules*, **26**, 2222 (1993).
113. Matsumoto, T., Okubo, M. and Suibao, S., *Kobunshi Ronbunshu*, **34**, 557 (1977).
114. Eliseeva, V.I., Petrova, S.A., and Zuikov, V., *J. Polym. Sci., Part C*, 63 (1973).
115. Bassett, D.R., in "Science and Technology of Polymer Colloids", Poehlein, G. W., Ottewill, R.H., Goodwin, J.W., Eds., Martinus Nijhoff Publishers, Vol. 1, 220, The Hague (1983).
116. Distler, D. and Kanig, G., *Colloid and Polym. Sci.*, **256**, 1052 (1978).
117. Penzel, E., Kanig, G., and Zosel, A., *Referat-Jahrestagung der Ulaamse Chemische Uereinigung*, Antwerpen, **5**, 6 (1982).
118. El-Aasser, M.S., Makgawinata, T., Vanderhoff, J.W., and Pichot, C., *J. Polym. Sci., Polym Chem. Ed.*, **21**, 2363 (1983).

119. Bradford, E.B. and Vanderhoff, J.W., *J. Macromol. Sci., Phys.*, **B6**, 671 (1972).
120. Wiest, H., *14th Fatigue Congress*, 705 (1978).
121. Okubo, M. and Matsumoto, T., *Memoirs of Faculty of Eng. Kobe Univ.*, **20**, 229 (1974).
122. Bufkin, B.G. and Grawe, J.R., *J Coatings Technol.*, **50**, 83 (1978).
123. Bufkin, B.G. and Grawe, J.R., *J Coatings Technol.*, **52**, 73 (1980).
124. Stanislawczyk, V., *U.S. Patent*, No. 4,879,364, to BF Goodrich Co. (1989).
125. Falk, C.J., *U.S. Patent*, No. 4,473,679, to Borg-Warner Chem. Inc. (1984).
126. Dickie, A.R., *U.S. Patent*, No. 3,856,883, to Ford Motor Co. (1974).
127. Fryd, M. and Leberzammer, E., *U.S. Patent*, No. 4,956,252, to E.I. duPont de Nemours and Co. (1990).
128. Yeliseeva, I.V., *Br. Polym. J.*, **7**, 33 (1975).
129. Yeliseeva, I.V., *Prog. Org. Coatings*, **13**, 195 (1985).
130. Muroi, S., *J. Appl. Polym. Sci.*, **10**, 713 (1966).
131. Kelly, D.P., and Melros, G.H., *J. Appl. Polym. Sci.*, **7**, 1991 (1963).
132. Christenson, R.M., *U.S. Patent*, No. 3,037,963 to PPG Industries. (1962).
133. Bassett, D., Sherwin, M., and Hager, S., *J. Coatings Technol.* **51**, 65 (1979).
134. Makuuchi, K., Katakai, A. and Nakayama, H., *J. Coatings Technol.*, **55**, 29 (1983).
135. Smith, A.D., *U.S. Patent*, No. 3,554,987 (1971).
136. Ponticelle, S.L., Hollister, R.K. and Tuites, C.R., *U.S. Patent*, No. 4,247,673 (1981).
137. Upson, A.D., *J. Polym. Sci., Polymer Symp.* **72**, 45 (1985).
138. Growe, R.J. and Bufkin, G.B., *J. Coat. Technol.*, **50**, 41 (1978).

- 139. Okubo, M., Nakamura, Y., and Matsumoto, T., *J. Polym. Sci., Polym. Chem. Ed.*, **18**, 2451 (1980).
- 140. Magnet, S., Guillot, J, Guyot, A., and Pichot, C., *Prog. Org. Coatings*, **20**, 73 (1992).
- 141. Nyguist, R.A. and Schuetz, J.E., *Appl. Spectroscopy*, **39**, 595 (1985).
- 142. UCARLINK Product Bulletin, UCAR Coating Resins (1993).
- 143. Schwartz, E.J. and McReynolds, B.K., *Tech. Symp. Non-woven Technol.* 64 (1979).
- 144. Chen, F. and Bufkin, B.G., *J. Appl. Polym. Sci.*, **30**, 4551 (1985).
- 145. Bourne, T., Bufkin, B., Wildman, B., and Grawe, R.J., *J. Coat. Technol.*, **54**, 69 (1982).
- 146. TMI Products Bulletin, American Cyanamid Co.
- 147. Dexter, W.R., Saxon, R. and Fiori, E.D., *J. Coating Technol.*, **58**, 43 (1986).
- 148. Inaba, Y., Daniels, E.S. and El-Aasser, M.S., *J. Coatings Technol.*, **66**, 63 (1994).

Chapter 3

Grafting Behavior of n-Butyl Acrylate onto Poly(butadiene-*co*-styrene) Latexes

Abstract: The radical-induced grafting of n-butyl acrylate (BA) onto poly(butadiene-*co*-styrene) [P(Bd-S)] latexes during seeded emulsion polymerization was studied. This P(Bd-S)/PBA rubber/rubber (core/shell) latex system exhibited unique grafting behavior as compared to other extensively studied rubber/glass (core/shell) latex systems, such as poly(butadiene-styrene)/poly(methyl methacrylate) [P(Bd-S)/PMMA], poly(butadiene-styrene)/polystyrene [P(Bd-S)/PS] and poly(butadiene-styrene)/polyacrylonitrile [P(Bd-S)/PAN]. These composite latexes were characterized by the formation of a highly grafted/crosslinked P(Bd-S)/PBA interphase zone generated during the seeded emulsion polymerization process. Although both of the individual core and shell polymers studied were “soft” themselves, the resulting P(Bd-S)/PBA composite latex particles were found to be rather “hard”. The formation of the interphase zone was studied by using techniques such as solvent extraction, differential scanning calorimetry (DSC) and transmission electron microscopy (TEM).

3.1 Introduction

Grafting in polybutadiene (PBd)-based seeded emulsion polymerization systems has been extensively studied. However, because a rubber/glass (core/shell) composite latex system is of general industrial interest, almost all of these studies used methyl methacrylate (MMA)¹, styrene (S)², styrene/acrylonitrile (S/AN)³ or S/MMA⁴ as the second stage monomers. In these applications, PBd-based latex particles are usually used as impact modifiers or toughening agents which are dispersed in a plastic matrix. The degree of grafting of the shell polymer onto the poly(butadiene-*co*-styrene) [P(Bd-S)] core latex particles has proven to be very important in obtaining the maximum benefit from the rubber phase in these applications⁵.

On the other hand, glass/rubber^{6,7} or rubber/rubber^{8,9} (core/shell) structured latexes have been found to be very useful in the production of self-supported rubbery materials. However, the rubbery polymers used in all of these studies, for either the core or the shell materials, were usually acrylic polymers. A rubber/rubber core/shell structured latex system involving PBd-based elastomers, such as a poly(butadiene-*co*-styrene)/poly(butyl acrylate) [P(Bd-S)/PBA] latex system, has rarely been reported.

P(Bd-S) (so-called SBR rubber) is a widely used elastomer. The mostly applied method used to process P(Bd-S) latex is a coagulation-vulcanization process, where the crosslinking process for the P(Bd-S) polymer is carried out during the shaping stage of the coagulated P(Bd-S) latex. This procedure requires a very low degree of crosslinking of the original P(Bd-S) latex before coagulation, and the vulcanization temperature is usually quite high. These kinds of conditions are not suitable in circumstances where P(Bd-S) is used in the

form of an elastomeric film cast directly from the latex under mild temperature conditions. In these applications, a certain degree of pre-crosslinking within the latex particles (i.e., intraparticle crosslinking) is required to form an elastomeric film. Nevertheless, crosslinking within the latex particles would hinder the interdiffusion of polymer chains between adjacent particles during the film formation process. A P(Bd-S) latex with a high degree of crosslinking in the latex particles usually can not form a strong elastomeric film by simply casting the latex. The properties of the latex film might be improved through the modification of the pre-crosslinked P(Bd-S) latex particles using another linear or lightly crosslinked rubbery polymer to form a core/shell structured latex particle. Obviously, the grafting behavior of the second-stage rubbery polymer onto the P(Bd-S) core would be important in influencing the properties of the final latex polymer film.

In this study, it was found that the grafting behavior of the second stage PBA polymer onto the P(Bd-S) seed particle turned out to be crucially important in determining the latex film properties. The resulting P(Bd-S)/PBA composite latex particles, at certain core/shell ratios, exhibited an unexpected degree of hardness, although both polymers involved are soft by themselves. A series of studies indicated that a highly grafted/crosslinked P(Bd-S)/PBA core/shell interphase zone was developed during the second stage polymerization of butyl acrylate using P(Bd-S) as the seed. The thickness of the interphase zone and/or the amount of the second stage PBA polymer used to form this interphase zone was primarily dependent on the gel fraction of the P(Bd-S) seed particles. The lower the gel fraction of the seed particles, the higher was the relative amount of PBA which would be used to form this interphase zone. It appeared that no pure PBA phase could be formed in the composite latex

particle during the formation of the interphase zone. The films cast from the latexes at this stage, i.e., before the formation of the interphase zone was completed, were non-continuous and brittle due to the tremendously increased degree of crosslinking in the core/shell interphase zone which is present at the surface layer of the latex particles. Only after this “Soft polymer + Soft polymer = Hard polymer” stage (i.e., the development of the core/shell interphase zone) was complete, could a pure PBA shell be formed on the outer surface of the composite latex particles. The latex film then became sticky and elastic.

3.2 Experimental

3.2.1 Materials

The monomers used, i.e., styrene (S), n-butyl acrylate (BA), methyl methacrylate (MMA), *iso*-butyl methacrylate (i-BMA) (all Fisher Scientific) and butadiene (Matheson Gas Products, Inc.) were treated by passing them through inhibitor-removal columns. Sodium octyl phenoxy tetra-ethoxy sulfonate (Triton X-200) and octyl phenoxy penta-ethoxy ethanol (Triton X-45) surfactants (Union Carbide) were used as received. Potassium persulfate (KPS), ammonium persulfate (APS), potassium metabisulfite (PMBS), all analytical grade (Fisher Scientific), and three azo-type initiators, 4, 4'-azobis(4-cyanopropanoic acid) (V-501), 2, 2'-azobis(2-amidinopropane) dihydrochloride (V-50) and 2, 2'-azobis(isobutyronitrile) (V-60) (all analytical grade, Waco Pure Chemical Industries, Ltd.), and normal dodecyl mercaptan (n-DDM), (commercial grade, Pennwalt Chemicals), were used as received.

Distilled-deionized (DDI) water was used in all polymerization.

3.2.2 Emulsion Polymerization

Preparation of P(Bd-S) Seed Latexes

Emulsion polymerizations to prepare P(Bd-S) seed latexes were carried out in 250 ml pressure bottles at 60, 65, and 70°C which were rotated end-over-end at 40 rpm in a bottle polymerizer unit according to the recipe shown in Table 3-1. The gel fraction of the P(Bd-S) latex was controlled by terminating the polymerization at desired conversions. The remaining monomers in the latexes were removed immediately after the termination of the polymerization by flash evaporation, which was repeated at least three times. Distilled-deionized (DDI) water was added between the evaporation processes.

P(Bd-S) Latex Seeded Emulsion Polymerization

Using P(Bd-S) as seed latex, a series of second-stage polymerizations were carried out in a four-neck 250 ml flask by using recipes Run 1 to 6 in Table 3-2. Runs 1 and 2 were carried out at 40 °C using a redox initiator system comprised of ammonium persulfate / potassium metabisulfite (APS/PMBS). Runs 3 to 6 were carried out at 70°C using the thermal initiator potassium persulfate (KPS), and three azo-type initiators, V-501, V-50, and V-60, respectively. All of the initiators used are water-soluble except for the V-60.

Table 3-1: Recipe used for the Preparation of the P(Bd-S) Seed Latex

Component	Weight (g)
Butadiene	45.0
Styrene	5.0
Triton X-200 [†]	0.1
Triton X-45 [‡]	0.3
Potassium persulfate	0.4
Potassium metabisulfite	0.5
n-Dodecyl mercaptan	0.1
Distilled-deionized (DDI) water	100.0

[†] Sodium octyl phenoxy tetra-ethoxy sulfonate; Union Carbide.

[‡] Octyl phenoxy penta-ethoxy ethanol; Union Carbide.

Table 3-2: Recipes for the Second Stage Polymerization**Using P(Bd-S) as Seed Latexes**

Component	Weight (g)					
	Run 1	Run 2 [‡]	Run 3	Run 4	Run 5	Run 6
P(Bd-S) seed (20 % solids) [†]	50.0	50.0	50.0	50.0	50.0	50.0
n-Butyl acrylate	10.0	10.0/50.0	10.0	—	—	—
iso-Butyl methacrylate	—	—	—	10.0	—	—
Methyl methacrylate	—	—	—	—	10.0	—
Styrene	—	—	—	—	—	10.0
Ammonium persulfate	0.10	0.1/0.5	—	—	—	—
Potassium metabisulfite	0.10	0.1/0.5	—	—	—	—
Thermal initiator*	—	—	0.07	0.07	0.07	0.07
Distilled deionized water	30.0	30/150	30.0	30.0	30.0	30.0

[†] Gel fractions of P(Bd-S) seed latexes: Run 1, 2% and 47%; Run 2, 6% and 87%; Run 3-6, 57%.

[‡] Second stage BA monomer: 10 g for 87% gel-fraction P(Bd-S) seed; 50 g for 6% gel-fraction seed. The same amount of initiators and DDI water were also used.

* Runs 3 to 6 were carried out at 70°C using the thermal initiators, potassium persulfate (KPS), 4, 4' - azobis(4-cyanopropanoic acid) (V-501), 2, 2' - azobis(2-amidinopropane)dihydrochloride (V-50) and 2, 2'-azobis(isobutyronitrile) (V-60), respectively.

Two modes of addition of the second stage monomers to the seed latexes were used: (1) an equilibrium swelling process was employed for all runs except Run 2, in which the monomer was allowed to swell the seed particles with tumbling for 24 hours at room temperature before the seeded emulsion polymerization was started; and (2) a semi-continuous process was utilized for Run 2, in which 5 wt% of the monomer and initiator were added at the beginning of the second stage polymerization, with the remaining monomer and initiator being added continuously to the reaction flask at a constant rate of 0.028 ml/min.

3.2.3 Measurement of the Gel Fraction and Grafting Efficiency using a Solvent Extraction Method

The gel fractions (GF) of the seed latexes were determined by a solvent extraction method. This method involved dissolving 0.2 g of latex polymer film, which was cast at room temperature and dried under vacuum for ten hours, in 25 ml toluene and mixing for 24 hours with end-over-end tumbling. The weight of dissolved polymer, W , was determined gravimetrically from the solids content in the supernatant after centrifugation at 5,000 rpm for 30 min at room temperature. The gel fraction (GF) is calculated by:

$$GF (\%) = \frac{0.2 - W}{0.2} \times 100 \quad (3-1)$$

The grafting efficiency (GE) of the second stage polymer, i.e., PBA, onto the P(Bd-S) seed latex particles represents the fraction of grafted PBA compared to the total amount of PBA in the P(Bd-S)/PBA seed particle. Specifically, for the P(Bd-S)/PBA composite latex with a 1/1 (w/w) core/shell ratio, 0.2 g of latex polymer film sample was dissolved in acetone [a good solvent for the linear part of PBA and a non-solvent for P(Bd-S)] and treated in the same manner as described previously for the determination of gel fraction. The total amount of PBA was 0.1 g in this system. The grafting efficiency (GE) is given by:

$$GE (\%) = \frac{0.1 - W_1}{0.1} \times 100 \quad (3-2)$$

where W_1 is the amount of the PBA dissolved in the supernatant. Acetone was used for the GE measurements for all of the composite latexes except for the polystyrene-based system, in which methyl ethyl ketone was used.

In order to determine the gel fraction of the P(Bd-S) seed particles after the second stage polymerization (GF'), a 0.2 g sample of 1:1 P(Bd-S)/PBA core/shell latex film was extracted with toluene (a good solvent for the linear part of both P(Bd-S) and PBA). The soluble amount (W') of both P(Bd-S) and PBA obtained from toluene extraction was used along with results obtained from the acetone extraction experiment in order to estimate GF' using the following equation:

$$GF' (\%) = \frac{(0.2 - W') - (0.1 - W_1)}{0.1} \times 100 \quad (3-3a)$$

which simplifies to:

$$GF' (\%) = \frac{0.1 - W' + W_1}{0.1} \times 100 \quad (3-3b)$$

The first bracket in equation 3-3a represents the insoluble amount after the toluene extraction (which includes both grafted PBA and crosslinked P(Bd-S)); whereas the second bracket represents the amount of PBA involved in the grafting reaction with the seed. The weights of core polymer and shell polymer in the 0.2 g sample is 0.1 g each.

3.2.4 Measurement of the Gel Fraction Using a TLC/FID Method

Thin-layer chromatography in conjunction with flame ionization detection (TLC/FID) has also been used to analyze the gel content in latex systems. The basic principle of this technique is the adsorption-desorption process of a solubilized or dispersed component at a solid-liquid interface through interaction of the various components of the polymer sample with both a stationary phase (silica) and a mobile phase (solvent used as the developer).

Depending on the solubility of each component in the developing solvent the movements of the various components differ, and hence, the traveling length and amount of the different components can be detected by flame ionization. Specifically, in determining the gel fraction of the SBR latex described in this report, the latex samples were directly dispersed into tetrahydrofuran (THF) in order to prepare a polymer solution with a concentration of about 2 mg/ml. A 2 μ l sample of this solution was then spotted on the TLC rod (10 cm long) close to the end of the rod (1 cm from the base of the rod) drop by drop with a time interval of several seconds between each drop to allow the THF of the former drop to evaporate. Three rods were spotted for each sample and the average was taken. In this way, the polymer solute can be concentrated in a small spot close to the end of the rod. The rods were then placed vertically in a development chamber containing toluene, with the toluene level between the bottom of the silica rod and the area where the polymer solution was spotted (about 0.5 cm from the end of the rod). Toluene is then allowed to diffuse from the bottom to the top of the rods, with the soluble linear polymer fraction diffusing up the rod along with the toluene. In this way, the soluble fraction and the insoluble gel part of the polymer (remaining on the rods in the region of the original spots) could be separated along the rods by repeating this development process. This development was repeated four times with a time interval of five minutes between each stage to allow the toluene on the rods to evaporate. The toluene front was allowed to travel 9 cm up the rod each time. The flame ionization measurements were then carried out after keeping the rods in an 80 °C oven for 20 min to remove any toluene residue. The soluble and insoluble fractions of the P(Bd-S) polymer on each rod corresponded to the areas of the two separate peaks as detected by FID. The gel-fraction was determined

by comparing the heights of the respective integral peaks.

3.3 Results and Discussions

3.3.1 P(Bd-S) Seed Latex

The P(Bd-S) seed latexes were prepared by emulsion polymerization. The polymerizations were carried out at 60, 65, and 70 °C using the recipe shown in Table 3-1. The gravimetric conversion vs. time curves for each reaction temperature are shown in Figure 3-1. As expected, the overall polymerization rate increased with increasing temperature. The extent of the crosslinking of the P(Bd-S) latexes was controlled by terminating the polymerization at a certain conversions.

3.3.2 Gel Fraction Measurements

In the butadiene polymerization process, polymeric radicals can form either by chain transfer between a propagating radical and a polymer chain or by the direct addition of a radical to the double bond in a polymer chain. This polymeric radical can initiate growth by adding monomer to form a grafted polymer chain. Again, this growing grafted polymeric radical can either abstract an allylic hydrogen atom from another polymer chain, by which branches are formed, or can directly attack the double bond of the polybutadiene, thereby forming crosslinks. In emulsion polymerization, the monomer to polymer ratio in a growing

latex particle continually changes during interval **III** of the polymerization. Consequently, the extent of branching and crosslinking can vary. Several methods have been used to characterize the extent of crosslinking of the P(Bd-S) latexes prepared in this study.

One of the methods used to quantify the extent of crosslinking is by measuring the gel fraction of the polymer. A standard method for the determination of the gel fraction in poly(butadiene-co-styrene) is the so-called "static" extraction method. This method defines the portion of the polymer sample which is insoluble in benzene after a 24 hour extraction period as "gel". Using this method the coagulated latex samples were dried at room temperature and then dissolved in a good solvent for the linear P(Bd-S) polymer, i.e., toluene or benzene. The polymer solution was then passed through a 100 mesh steel screen and the portion that did not pass through this screen was considered to be the gel. However, because the size of this screen was large enough to allow some crosslinked gels of small size to pass through, this method would tend to give low gel fraction values.

A similar method to measure the gel-fraction is to extract either the P(Bd-S) film or vacuum-dried latex samples using toluene for 24 h followed by centrifugation. The quantity of polymer soluble in the supernatant is determined gravimetrically, and the insoluble fraction is determined by difference. The lower curve (filled squares) shown in Figure 2 depicts the gel fractions measured by this method as a function of conversion. The drawback of this method is that at low conversions, when the amount of gel is small, an inadequate separation may result, and only a fraction of the gel can be detected. On the other hand, for the samples obtained at higher conversions, due to the high crosslinking density of the polymer chains,

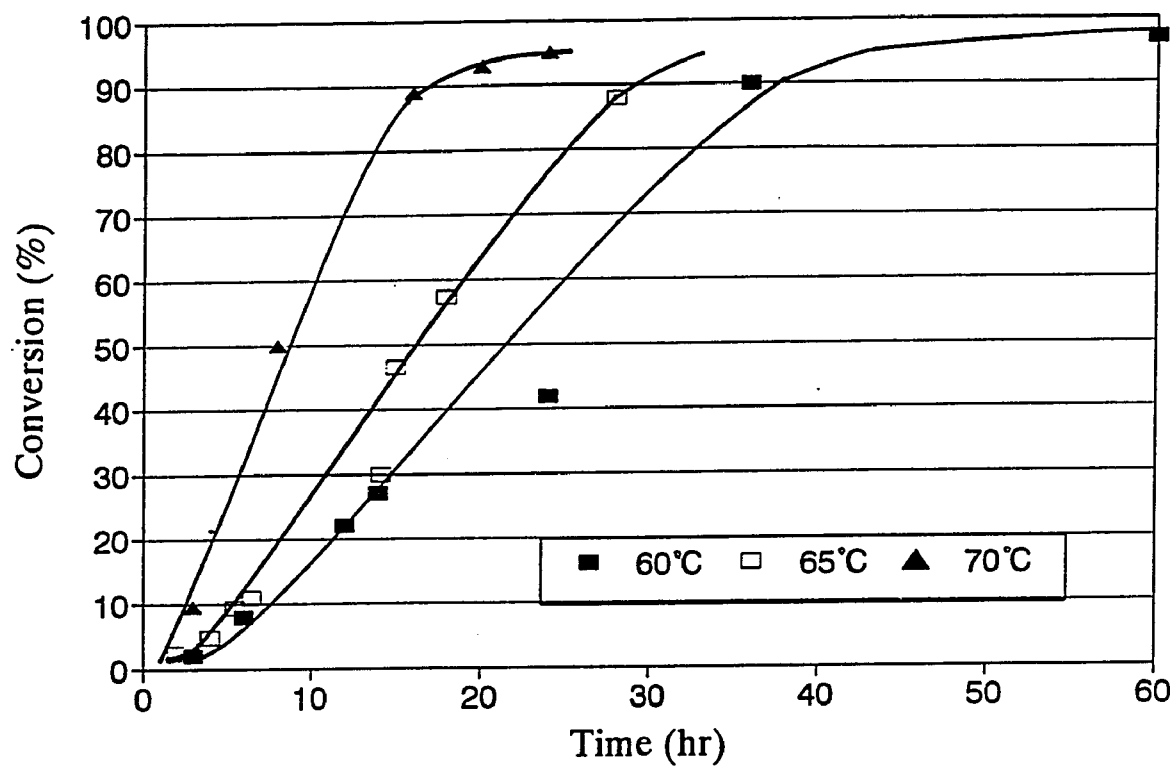


Figure 3-1: Overall percentage of monomers converted vs. reaction time for SBR latexes prepared at 60, 65, and 70 °C.

some linear or branched polymer chains might be entrapped within the highly crosslinked gels and are not extracted into the solvent. Despite the drawbacks inherent in this method, this method was used to measure the gel fraction in this work due to its simplicity.

The TLC/FID results for the gel fractions of the P(Bd-S) latexes prepared at 60 °C and stopped at different conversions are also shown by the upper curve (empty squares) in Figure 3-2. The values were larger than those determined from the solvent extraction measurements up until 80% conversion. This was especially true for conversions lower than 30% where a 5 to 10% gel fraction was detected by the TLC measurement as compared with the toluene extraction results which showed gel fraction of zero. This difference seems to reflect the amount of those microgels which were not separated by centrifugation during the extraction measurement.

One traditional way to determine the crosslinking density of a crosslinked polymer film is by comparing the size or weight changes of the film after immersion in a swelling solvent. The crosslinking density can then be determined using the Flory-Rehner equation. Considering that some interactions could possibly occur among P(Bd-S) polymer chains, such as oxidation causing further crosslinking during the process of film formation, attempts have been made to investigate the crosslinking density in the latex particles themselves, by measuring the particle size increase after swelling the latex particles with toluene. In this experiment, the first step was to add acetone slowly to a small amount of latex to prepare a dilute and stable latex dispersed in acetone. Several latex systems having different types of surfactants were investigated to prepare the acetone-dispersed latex system. The amount of water was less than 0.1 wt% with a solids content less than 0.02 wt%. It was found that the latex stabilized with

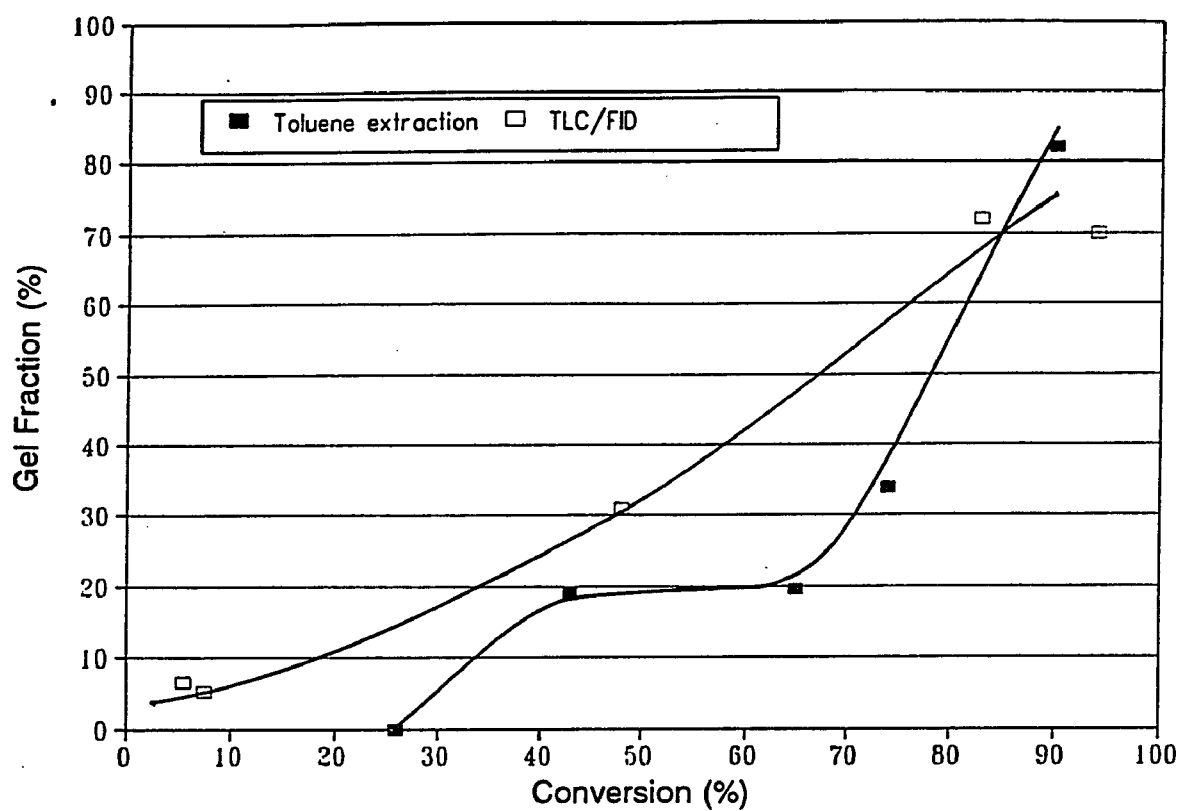


Figure 3-2. Gel fractions measured by toluene extraction (filled square) and TLC/FID (empty square) methods for the P(Bd-S) latexes at different conversions of emulsion polymerization.

the nonionic surfactant TritonX-45 (Union Carbide) could form a stable dispersion in acetone. Some coagulum was observed when the latexes which were stabilized only by the anionic surfactant sodium lauryl sulfate (SLS) or TritonX-200, were dispersed in acetone. In such cases, adding nonionic (TritonX-45) or cationic [dimethyl benzyl octadecyl ammonium chloride (Varisoft SDC, Sherex Chemical Co., Inc.)] surfactant helped to form a stable dispersion in acetone. The second step was to add a small amount of this dispersion into toluene so that the final concentration of polymer in toluene was suitable for light scattering measurements. By adding an appropriate surfactant, a small amount of latex could also be directly transferred into a large amount of 1,4-dioxane. In this way, the dominant component of the medium was toluene or 1,4-dioxane (both are good solvents for poly(butadiene-co-styrene)), and the trace amounts of water and acetone could be neglected. The viscosity of the dispersion medium could then be treated as that of pure toluene or 1,4-dioxane as long as there was not much linear polymer dissolved in the medium. The dispersion samples were kept undisturbed overnight to reach an equilibrium swelling condition before performing the light scattering measurements. However, as mentioned above, this method is only suitable for very high gel-fraction systems because only in such systems is the viscosity of the dispersion medium undisturbed by the dissolved linear polymer chains. Thus, in the P(Bd-S) latex systems prepared so far, only the 97% conversion latex, which has a gel-fraction of about 93%, exhibited reproducible results. The latex particle size increased from 308 nm before swelling to 512 nm after swelling. Since the medium is a good solvent for the P(Bd-S) latex system, the interfacial tension factor does not exist. From the Flory-Rehner equation:

$$-\ln(1-v_2) + v_2 + \chi v_2^2 = V_1 n [v_2^{1/3} - v_2/2] \quad (1)$$

where v_2 is the volume fraction of polymer in the swollen particle (which can be calculated to be 0.22 from changes in the particle volume upon swelling), V_1 is the molar volume of the solvent (this value is 106 cm³/mole for toluene), and χ is the Flory-Huggins polymer-solvent interaction parameter (this value is 0.39 for the toluene-P(Bd-S) pair). The calculated value of n , the elastically active chains per unit volume, for this latex system, is 3.4×10^{-4} mole/cm³.

3.3.3 Appearance of Latex Films

Latex films were cast on glass plates at room temperature. P(Bd-S) latexes (GF, 6% and 57%) and a PBA homopolymer control latex was able to form continuous elastomeric films. Both P(Bd-S) (GF=6%) and PBA latex films exhibited a significant degree of tackiness, as expected. Because both components, i.e., P(Bd-S) and PBA, were originally soft, a P(Bd-S)/PBA core/shell latex was also expected to be able to form a soft elastomeric film. However, contrary to this expectation, in spite of varying the conditions of the second stage polymerization of BA using P(Bd-S) seed, e.g., polymerization temperature, mode of addition of the second stage BA monomer, and the addition of chain transfer agent, the films formed from these latexes were cracked and brittle, and did not exhibit any elasticity. Obviously, the resulting composite latex particle does not have a simple P(Bd-S)/PBA core/shell structure since a continuous, soft elastomeric film should be formed otherwise. A possible reason, if not

the only one, for the hardening of an originally soft polymer by itself is the formation of a highly crosslinked network in the polymer structure. One of the methods that is usually used to evaluate the extent of crosslinking is the gel fraction measurement.

3.3.4 Gel Fraction Measurements During the Second-stage Polymerization

Figure 3-3 shows the changes in the gel fraction of the latexes obtained during the second stage polymerization along with the conversion of the BA monomer using the Run 1 recipe shown in Table 3-1. At the beginning of the reaction, the gel fractions shown in Figure 3-3 (at time = 0) are those for the P(Bd-S) seed latex. For both the low and high gel fraction P(Bd-S) seeds (i.e., LG and HG), the gel fraction increased rapidly immediately after starting the reactions, and again increased quickly after the conversion of BA reached 70 to 80%. The final gel fractions were around 90% when the reaction was finished. The increase in the gel fraction occurred during the polymerization of the second stage BA monomer. The gel fraction for PBA homopolymer obtained in a parallel experiment via the emulsion polymerization of BA under the same conditions used for the second stage polymerization was 16%. The gel obtained from the homopolymerization of butyl acrylate was a result of chain transfer reactions at the α -hydrogens in the PBA polymer chains during the polymerization. When P(Bd-S) latex was used as the seed latex, large amounts of double bonds and allylic hydrogens were present in the P(Bd-S) copolymer chains. These moieties are very active in the radical reactions which occur during the second stage polymerization of BA. Any of these reactions, e.g., chain transfer reactions to the allylic hydrogens and direct

attack on the vinyl double bonds in P(Bd-S), could lead to crosslinks or grafts on the P(Bd-S) copolymer chains. These two kinds of reactions compete with the propagation reaction of BA monomer during the entire polymerization process. In the region up to 60% conversion (time: 0 to 0.5 h), the gel fraction for both the LG and HG P(Bd-S) seed systems increased 17 and 14%, respectively. In sharp contrast, in the region from 70 to 90% conversion (time: 0.8 to 1.5 h), which represents only a 20% increase in conversion, the gel fractions increased 50 and 20% for the LG and HG P(Bd-S) seed systems, respectively. The rapid increase in gel fraction in this high conversion region was due to the much lower BA monomer concentration and/or the higher concentration of polymers, which makes the grafting/crosslinking reactions resulting from the chain transfer reactions to the existing polymer chains more competitive compared to propagation reactions.

3.3.5 Influence of the Type of the Second Stage Monomer and Initiator on the Extent of Grafting/Crosslinking

By comparing the results for the P(Bd-S)/PBA latex system obtained in this study with results from P(Bd-S)/PMMA and P(Bd-S)/PS systems in the papers published by other researchers,^{1,2,3} it was found that the BA system exhibited a higher grafting efficiency than those determined for the MMA or S systems. Furthermore, contradictory results on the influence of the type of the initiator on the grafting have been reported in some studies,^{10,11,12} i.e., whether an azo-type initiator, such as AIBN (V-60) will induce any grafting reaction or not. Since the methods used to measure the grafting efficiency and the reaction systems

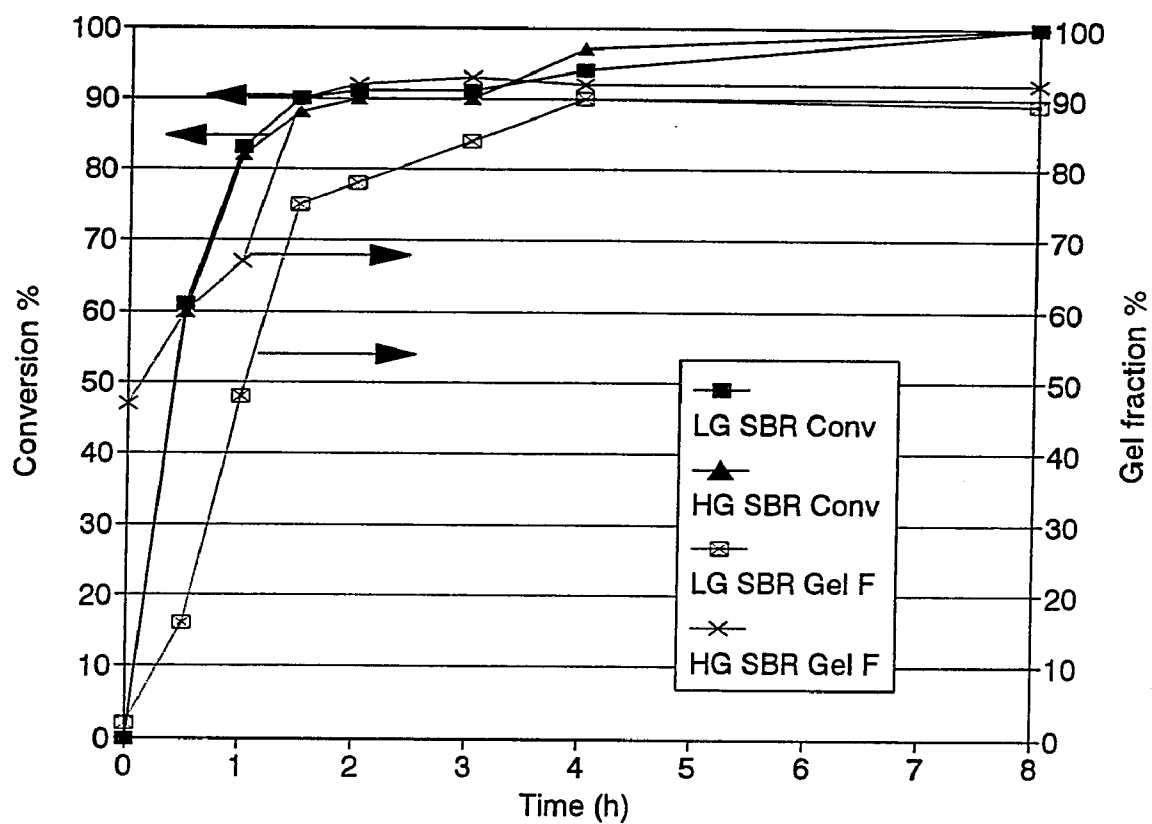


Figure 3-3: Percentage of second-stage BA monomer converted and total gel fraction of the latex vs. reaction time using the P(Bd-S) seed latex polymerized to 27% (LG SBR, 2% gel-fraction) and 57% (HG SBR, 47% gel-fraction) conversions.

employed for each of the above mentioned studies were not completely the same, it was necessary to carry out the polymerizations under the same conditions to compare these different systems.

Comparable second-stage polymerizations were carried out according to the Run 3 to 6 recipes shown in Table 3-1 using the equilibrium swelling process described in the experimental section. Figure 3-4 shows the results for the grafting efficiencies of each system obtained from acetone extraction experiments (methyl ethyl ketone for the S system since acetone is a non-solvent for PS). It is quite clear that BA does exhibit a higher GE value than any of the other systems, regardless of the type of initiator used. Three types of free radicals can be formed from S, MMA, *iso*-BMA and BA monomers and the stabilities of the radicals are in the order of ¹³: $S\bullet > MMA\bullet \sim iso-BMA\bullet > BA\bullet$. This order also reflects the reverse order of chain transfer reactions, i.e., S monomer has the highest tendency to be initiated to form a S radical, while BA radicals have the highest tendency to transfer to existing polymer chains to form grafting sites. This is understandable from the large difference in the chain transfer constants to polymer for these three types of radicals¹⁴. As mentioned before, a gel fraction of 16% was found for a PBA homopolymer system prepared by batch polymerization. In the presence of the pre-formed P(Bd-S) crosslinking network, the chain transfer reactions of BA radicals to the α -hydrogens in the PBA polymer chains could also lead to the formation of an interpenetrating polymer network (IPN), i.e., P(Bd-S)-*ipn*-PBA, a special form of grafting in which there might not be direct chemical bonding between P(Bd-S) and PBA. It is difficult to distinguish between these three structures, i.e., chemically grafted PBA, IPN PBA and an independent PBA crosslinked network, using the solvent extraction

technique because none of these structures are soluble in the solvent. Nonetheless, considering the presence of large amounts of allylic hydrogens and residual double bonds in the P(Bd-S) seed particle, the probability of forming a completely independent PBA crosslinked network should be small. This suggests that the high GE for the BA system is indeed caused by either chemical grafting or physical chain entanglements instead of an independent PBA crosslinked network.

By comparing i-BMA with the MMA monomer system, it is evident that systems including i-BMA exhibited higher GE values than those for the MMA systems, although the chain transfer tendencies for the radicals generated from both kinds of monomers are similar to each other. This suggests that the mobility of the second stage polymer chains could also play a role in influencing the grafting reaction. It has been shown in Figure 3-3 that the gel fractions of the seeded emulsion polymerization system increased rapidly in the high monomer conversion region, where the polymer concentration in the latex particles is high. In this instance, the mobility of a polymer chain is correlated to its glass transition temperatures (T_g). P(i-BMA) has a T_g of 53 °C which is lower than the polymerization temperature (70°C). On the other hand, PMMA has a T_g of about 105 °C which is much higher than the polymerization temperature. Although the actual “ T_g ” of the polymer in a monomer-swollen particle is lower than that for the pure polymer, a big difference in the mobilities of these two types of polymer chains would be expected in the high conversion region of the polymerization, where the polymer/monomer ratio in the monomer-swollen particles is high.

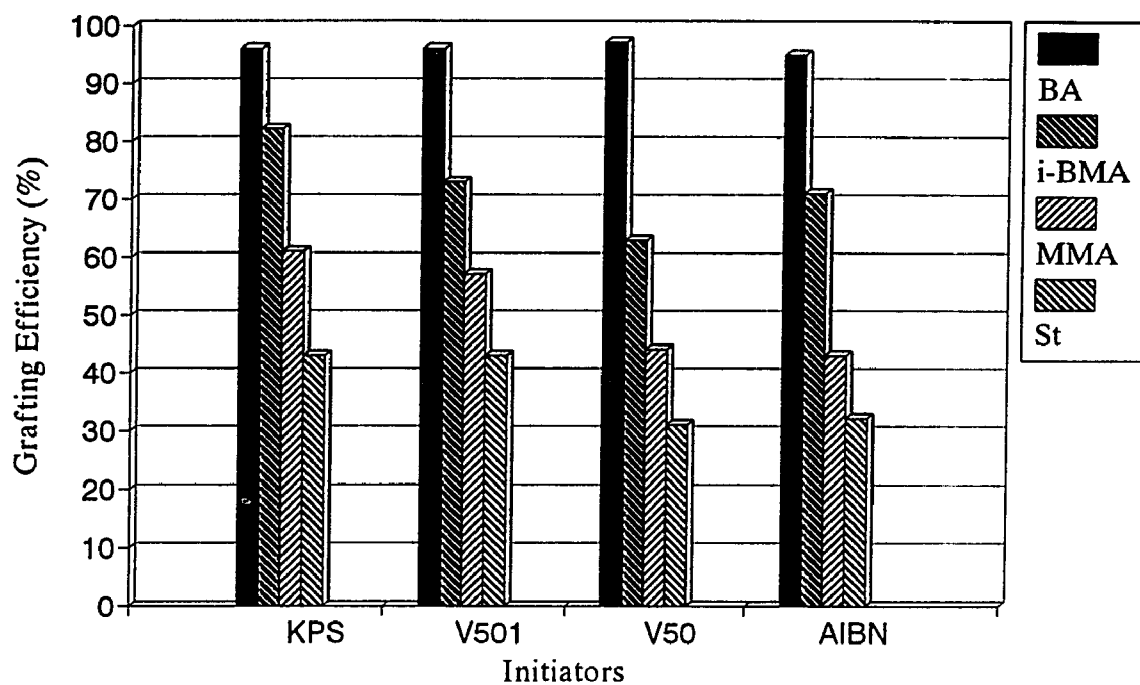


Figure 3-4: Grafting efficiency (GE) for a variety of second stage polymers onto P(Bd-S) latex seed particles after seeded latex emulsion polymerization using a variety of initiators.

Figure 3-5 shows the change in the gel fraction (GF) of the composite latex system after the second stage polymerization as determined by the toluene extraction method. The results were similar to those seen in Figure 3-4 for GE. The BA system showed the greatest increase in the GF of the composite latex system, from the original 57% GF for the P(Bd-S) seed to a value higher than 95%. The other three monomer systems also exhibited an increase in the GF of the composite latex system compared with the seed latex. Because these results obtained from the toluene extraction experiment reflect the GF for the entire composite latex particles, it would be interesting to investigate the changes in the GF for only the P(Bd-S) seed latex after the second stage polymerization for each system. In most of the previous grafting studies carried out by other researchers, high gel fraction (>90%) PBd-based seed latexes have been used. In those cases, the change in the GF of the seed latexes after the seeded emulsion polymerization could not be observed.

Figure 3-6 shows the increase in the gel fraction of the P(Bd-S) seed latex itself (GF') after the seeded emulsion polymerization was complete, calculated from the results obtained from both acetone (methyl ethyl ketone for S system) and toluene extraction experiments according to equation (3-3b) shown in the experimental section. The gel fraction of the P(Bd-S) seed latexes increased from the original 57% to higher than 97% for the BA monomer system regardless of the type of initiator used. The other two acrylate monomer (i-BMA and MMA) systems exhibited increases in the gel fraction of the P(Bd-S) seed latex to around 85% to 93%. S monomer also showed significant increases to higher than 95%.

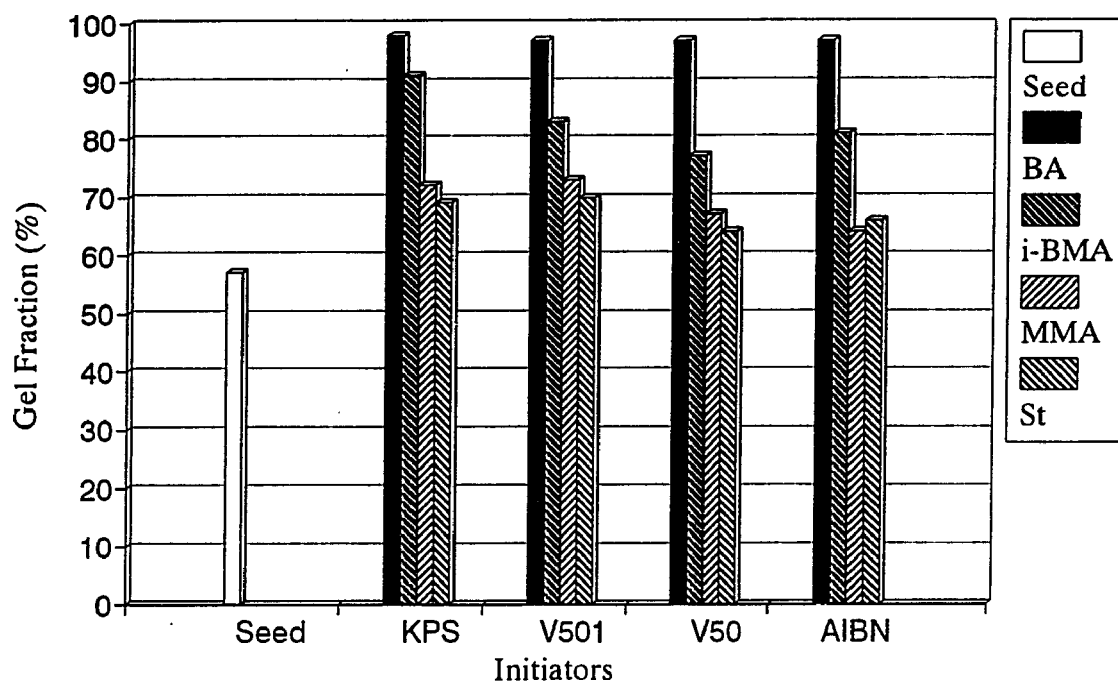


Figure 3-5: Gel fraction (GF) of composite latex particles prepared via a P(Bd-S) seeded emulsion polymerization with different second stage monomers.

As mentioned previously, controversial results concerning the influence of the type of the initiator on grafting has been described in the literature. It was claimed that azo-type initiator e.g., AIBN, could not initiate any grafting reactions in solution polymerization systems. The results shown in Figures 3-4 and 3-5 demonstrate that the P(Bd-S)/PBA system exhibited almost the same high value of GE and GF, regardless of the initiator type. For the other three polymer pairs, the persulfate (KPS) initiator did show notably higher values of GE and GF than did the other three azo-type initiators. Nonetheless, there were significant increases in either GE or GF for all of the azo-type initiators. These results suggested that the grafting/crosslinking reactions could be initiated not only by the primary radicals, but also by chain transfer or direct attack from the propagating polymer radicals to those allylic hydrogens and vinyl double bonds present in the P(Bd-S) seed latex. In the case of the BA second-stage monomer system, the high chain transfer to polymer concealed the influence of the types of initiators. For the other three systems with lower chain transfer tendencies, the influence of the type of initiator could be observed.

Figure 3-7 shows the relationship between GE and the PBA/P(Bd-S) shell/core ratio. Two types of P(Bd-S) seed latexes with high and low gel fractions, i.e., HG SBR with 87% GF and LG SBR with 6% GF, were used. In both cases, the GE remained at values between 80% to 90% before the shell/core ratio reached approximately 1.0 for the HG SBR seed series, and 1.5 for the LG SBR seed series. Note that in this figure, the units for the X-axis are expressed as a shell/core ratio (not a core/shell ratio as is normally used) for convenience. The GE values decreased after these two values of the shell/core ratio are reached, i.e., 1.0 and 1.5 for the HG and LG SBR series, respectively. These two ranges could indicate the

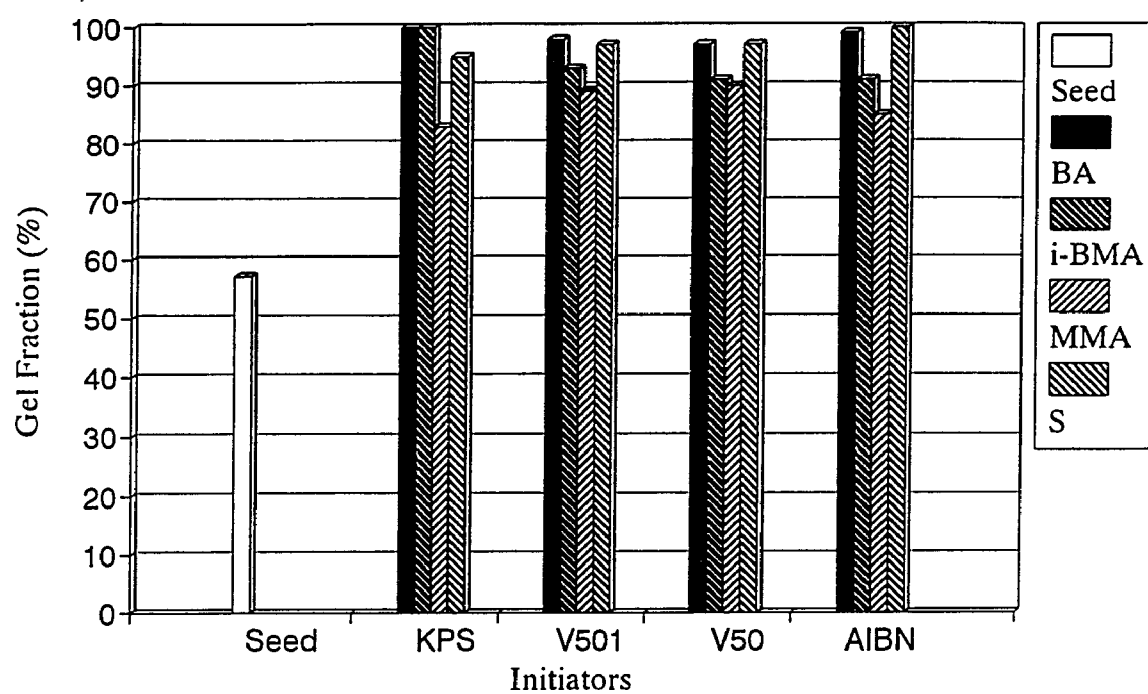


Figure 3-6: Changes in the gel fraction (GF) of P(Bd-S) seed latexes after the second stage seeded emulsion polymerization was complete for different monomer and initiator systems.

beginning of the formation of separate PBA phases in the composite particles. In these PBA phases, the post-formed PBA chains were not grafted to any great extent to the P(Bd-S) chains.

3.3.6 Morphological Observations of the Development of the Grafting/Crosslinking Interphase Zone using Transmission Electron Microscopy (TEM)

In order to investigate the development of the core/shell interphase zones, the second stage polymerizations of BA using P(Bd-S) as seed were carried out according to the Run 2 recipe shown in Table 3-1. The addition rate of BA monomer was controlled to maintain monomer-starved conditions, i.e., the instantaneous conversion of BA monomer as detected by gas chromatography (GC) reached 100% during the entire addition period. In order to investigate the influence of the gel fraction of the P(Bd-S) seed latex particles on the development of the core/shell interphase zone, two series of second stage polymerizations were carried out with different gel fractions (6% and 87%) of the P(Bd-S) seed latexes which are referred to as LG SBR and HG SBR, respectively. Latex samples were taken from the reactor at various times (i.e., varying P(Bd-S) /PBA ratios) during the addition process of BA monomer.

Figure 3-8 shows transmission electron micrographs obtained for both the LG (left) and HG (right) series. These particles were stained with osmium tetroxide (OsO_4). Phosphotungstic acid (PTA) was used as a background stain in some cases. From the LG SBR series shown in the left half of Figure 3-8, it was noted that as the second stage

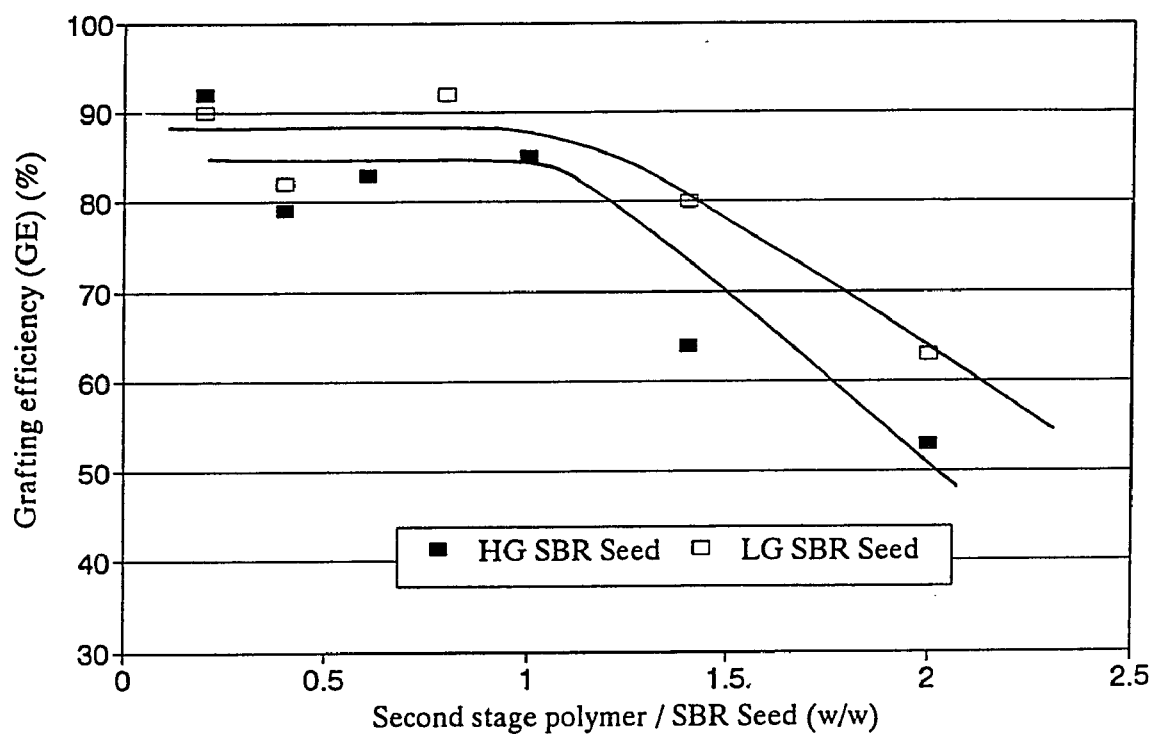


Figure 3-7: The grafting efficiency (GE) of butyl acrylate grafted on P(Bd-S) seed latexes (HG or LG SBR seed) vs. shell/core ratios as determined by solvent extraction measurements.

polymerization progressed, some non-uniform domains with different contrast (Figure 3-8B-L) were developed around the original spherical seed particles (Figure 3-8A-L). Because OsO_4 can only stain the polybutadiene regions through reactions with the residual double bonds present in polybutadiene (shown as the dark regions within the particles), the presence of lighter domains suggests that there were lower concentrations of double bonds in these regions. With the further progression of the second stage polymerization, as shown in Figure 3-8C-L, a third light domain could be observed. These domains are believed to represent pure PBA phases. Through these observations, it is believed that the gray domains shown in Figures 3-8B-L and 3-8C-L actually represent the core/shell interphase zones. These interphase zones are comprised of PBA grafted onto crosslinked P(Bd-S) networks. Because the double bonds in these domains were "diluted" by the incorporated PBA, the color in these regions was found to be gray instead of dark black, as was seen in the center regions of the particles. The image of the 1/0.8 core/shell ratio latex particles shown in Figure 3-8B-L, where the pure PBA phase can not be observed yet, indicates that the amount of PBA consumed to form these core/shell PBA-graft-P(Bd-S) interphase zones could represent almost the same weight as the LG-SBR seed particles. It seems that only after the formation of these highly grafted interphase zones could it be possible to form some separated PBA domains, as shown in Figure 3-8C-L in which the core/shell ratio was 1/1.5. Figure 3-8D-L shows complete coverage of the P(Bd-S) seed by the PBA shell. Here, the core/shell ratio was 1/3 and the shell is so thick that the P(Bd-S) core could not be stained by OsO_4 within the treatment period (6 hours).

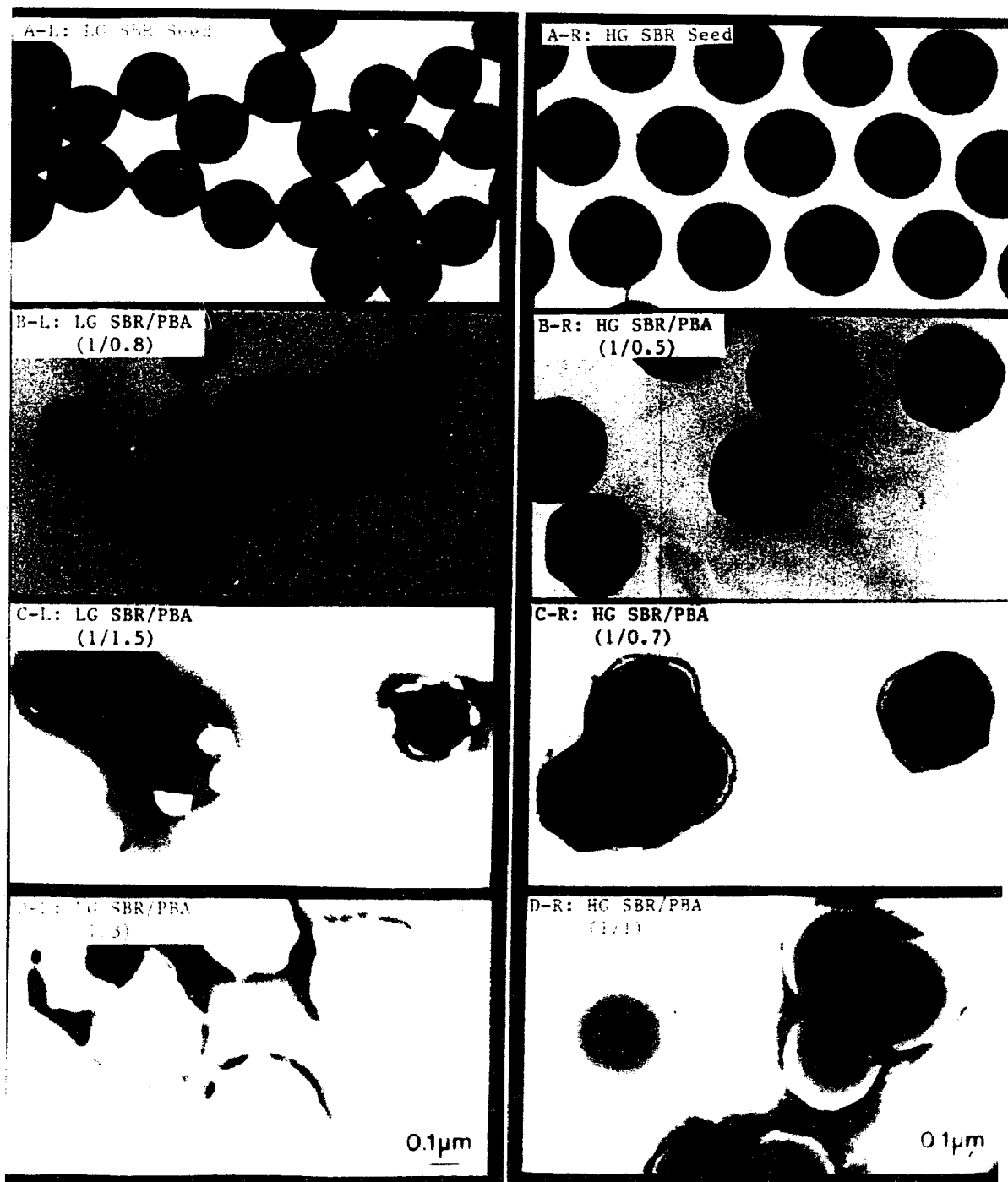


Figure 3-8: TEM micrographs (cold stage) of LG-SBR/PBA (left) and HG-SBR/PBA (right) composite particles with different core/shell ratios obtained during the second stage semi-continuous polymerization.

A similar situation could also be observed in the case of the HG SBR seed latex (Figure 8A-R). Compared to the LG SBR latex shown in Figure 8B-L, the deformation of the HG SBR latex particles shown in Figure 8B-R, caused by the formation of the interphase zones, was not that obvious. In this case, only a thin gray ring around the seed particles could be observed. Another difference was that the core/shell ratio (Figure 8C-R) at which the visible PBA phases started to form was lower than that for the case shown in Figure 8C-L. The core/shell values shown in Figure 8B-R (1/0.5) and Figure 8C-R (1/0.7) indicate that the amount of PBA consumed in forming the interphase zones for this higher gel fraction seed was about half the weight of the HG SBR seed latex particles.

The results shown in Figure 3-8 suggested that the extent of the formation of the core/shell interphase zone was very much influenced by the gel fraction of the P(Bd-S) seed particles. The lower was the gel fraction of the seed particles, the higher was the mobility of both the P(Bd-S) and the PBA chains, and the higher was the probability for both types of chains to interact with each other, which led to the formation of a relatively thicker interphase zone. It is also observed that the interphase zone is developed non-uniformly, especially in the low gel fraction P(Bd-S) seed system. This observation suggests that the entering oligomeric free radicals, and hence the grafting sites, do not distribute uniformly within the particle¹⁵.

3.3.7 P(Bd-S)/PBA Core/Shell Interphase Zone Hardening Process

— Comparison with P(Bd-S)/PMMA Core/Shell Systems via Platinum Shadowing TEM Studies

The high degree of crosslinking in the interphase zone could greatly harden the particle surfaces, which makes film formation from these particles very difficult. Platinum (Pt)-shadowing TEM studies are useful in evaluating the hardness of individual latex particles. In this technique, latex samples were first dried on a carbon-coated TEM grid. A very thin layer of Pt was then coated onto these particles in a vacuum chamber at a certain angle, as shown schematically in Figure 3-9. The shadows of the particles that are coated by the Pt would appear as a white shadow in a TEM photograph. In this way, soft particles that would collapse during the sample preparation drying process would display a small shadow as shown in Figure 3-9A. In contrast, a hard particle would retain its spherical shape during drying and would exhibit a large shadow, as shown in Figure 3-9B. The distance between the bottom of the particle and the intersection of the particle center line with the shadow line (H), can be calculated by the shadow length (L) and the Pt coating angle (θ), which was 27° in this experiment. At this small shadowing angle, the difference between the H value and the real particle height is very small (H is slightly larger than the real particle height); thus, H is used to represent the particle height in this study. The diameter of the particle (R) on the grid can be measured directly from the micrograph. The H/R ratio can be used to represent the hardness of the particle. A hard particle would give a H/R value of one (or slightly higher than one for a hard spherical particle), while a soft particle would exhibit a small H/R value. For

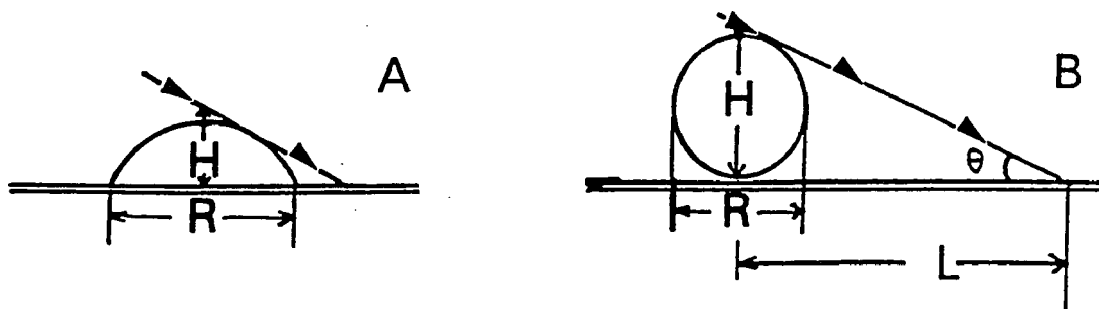


Figure 3-9: Schematic illustration of Pt-shadowed transmission electron micrograph (TEM) for: (A) soft and (B) hard latex particles.

comparison, two series of latex samples were investigated in parallel by the semi-continuous emulsion polymerization of BA or MMA monomers onto a low GF (27%) P(Bd-S) seed latex. Because the polymerizations were carried out under monomer-starved conditions, latex samples with different core/shell ratios could be obtained by taking latex samples from the reactor during the second stage polymerization.

As shown at the top of Figure 3-10, the soft P(Bd-S) seed latex particle exhibits a very small shadow that can barely be seen. The H/R ratio is only 0.33. Starting from this soft seed particle, the left half of Figure 3-10 shows an increase in the shadow length with increasing amounts of the second-stage PMMA polymer. H/R reaches 1 at a P(Bd-S)/PMMA ratio of 1/0.6. This phenomenon had been demonstrated in some previous studies by other researchers and was considered to be caused by the complete coverage by a hard PMMA shell around the soft P(Bd-S) core. Following this reasoning, a soft PBA shell, if formed on the soft P(Bd-S) core, should not lead to an increase in H/R because both polymers are soft. However, the results shown in the right half of Figure 3-10 for the P(Bd-S)/PBA system were quite similar to those of the P(Bd-S)/PMMA system. H/R reached 0.95 at a P(Bd-S)/PBA ratio of 1/0.8. This tendency could be seen more clearly by plotting the H/R ratio as a function of the shell/core ratio (the shell/core ratio, instead of the core/shell ratio, was used for convenience), as shown in Figure 3-11. It was observed that the H/R ratio increased with an increasing shell/core ratio for both systems. The increase in the H/R values for the P(Bd-S)/PBA system was only slightly slower than that found for the P(Bd-S)/PMMA system before the shell/core ratio reached 1/1. For the P(Bd-S)/PMMA system, the H/R ratios remained at 1.1 after the

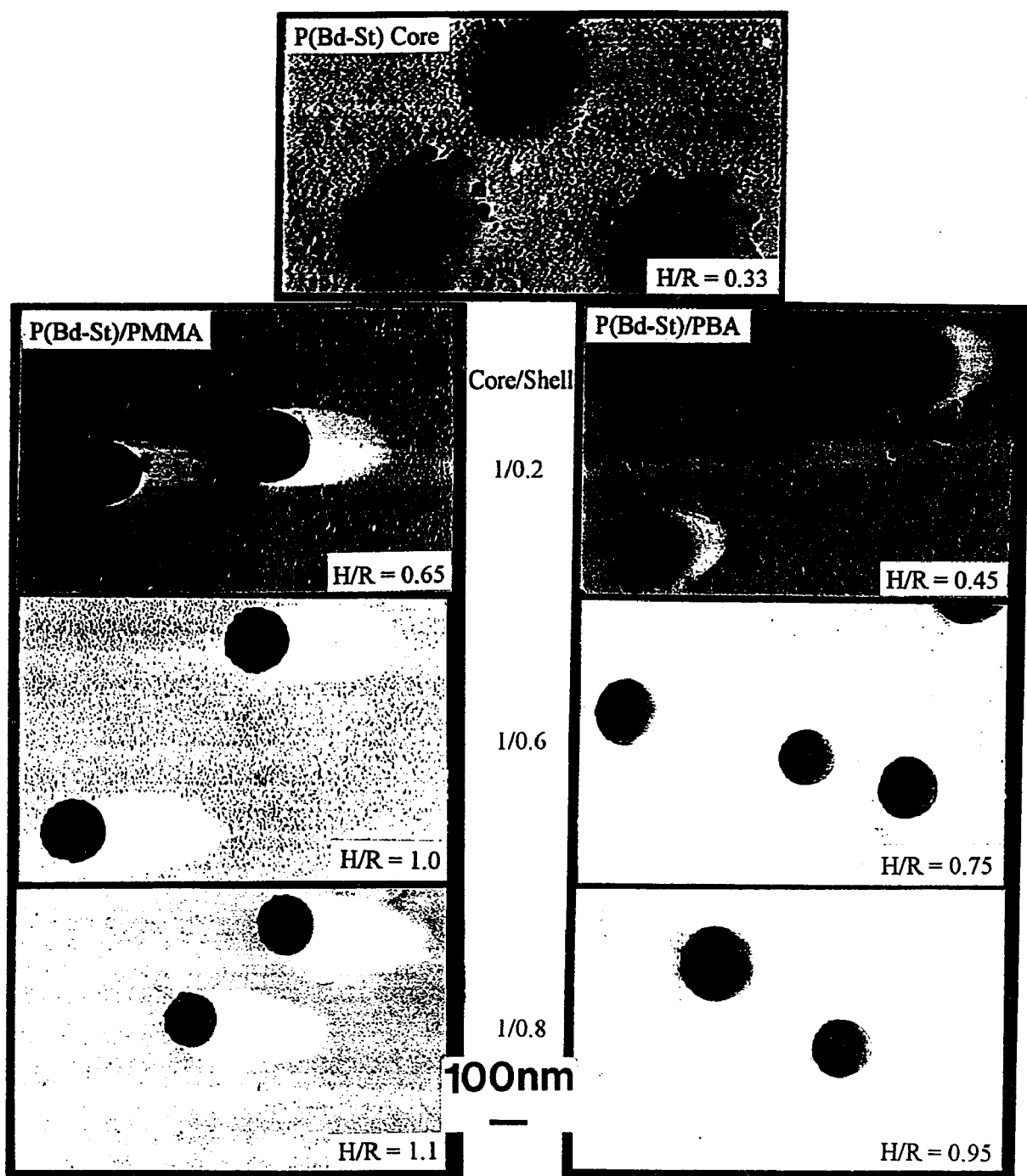


Figure 3-10: Hardening process for the original soft P(Bd-S) seed latex particle (top) during the seeded emulsion polymerization of MMA (left) and BA (right) as observed by Pt-shadowed TEM micrographs.

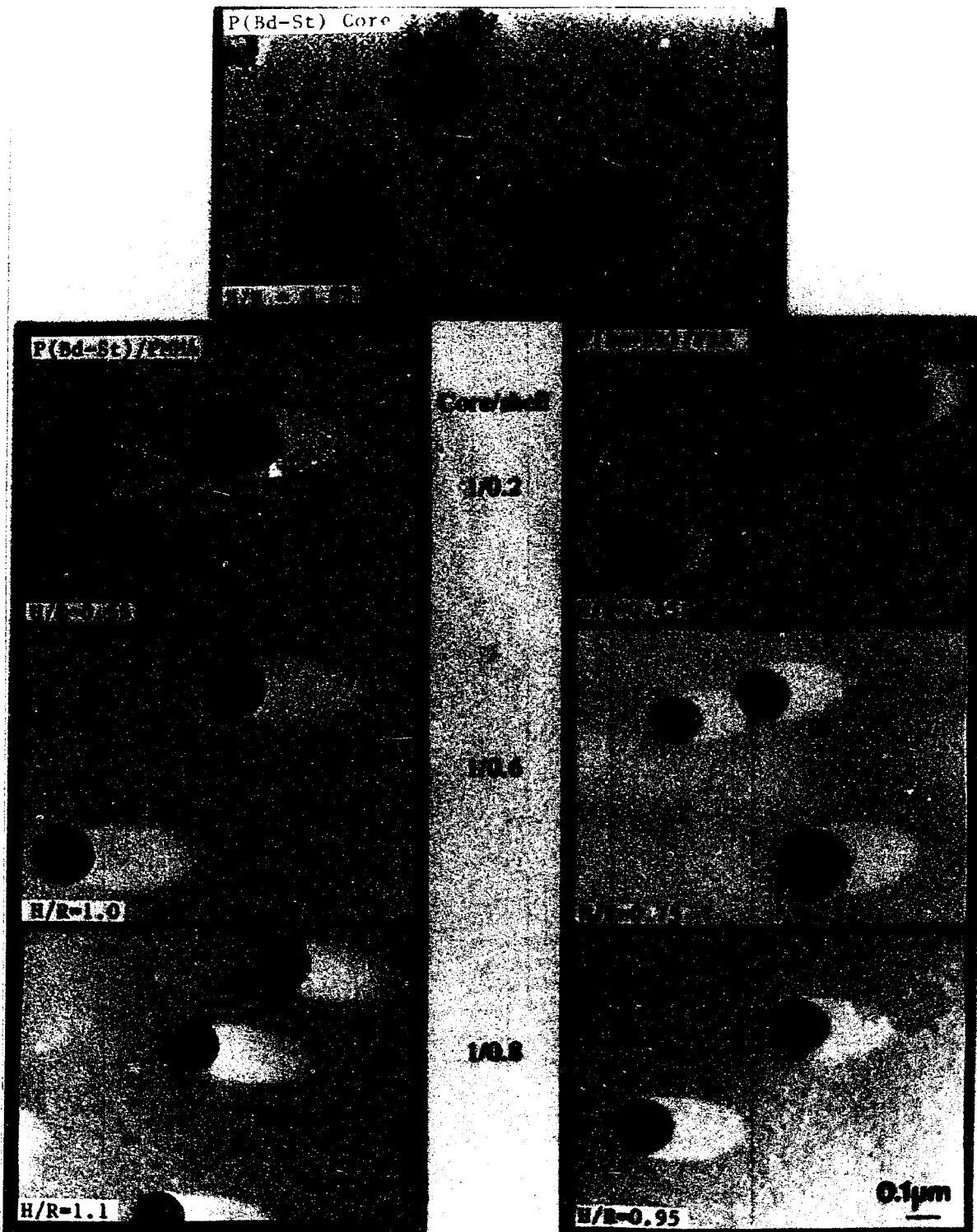


Figure 3-11: Changes in the H/R ratio of composite latex particles as determined by Pt-shadowing TEM studies with different shell/core ratios prepared by the P(Bd-S) seeded emulsion polymerization with MMA or BA.

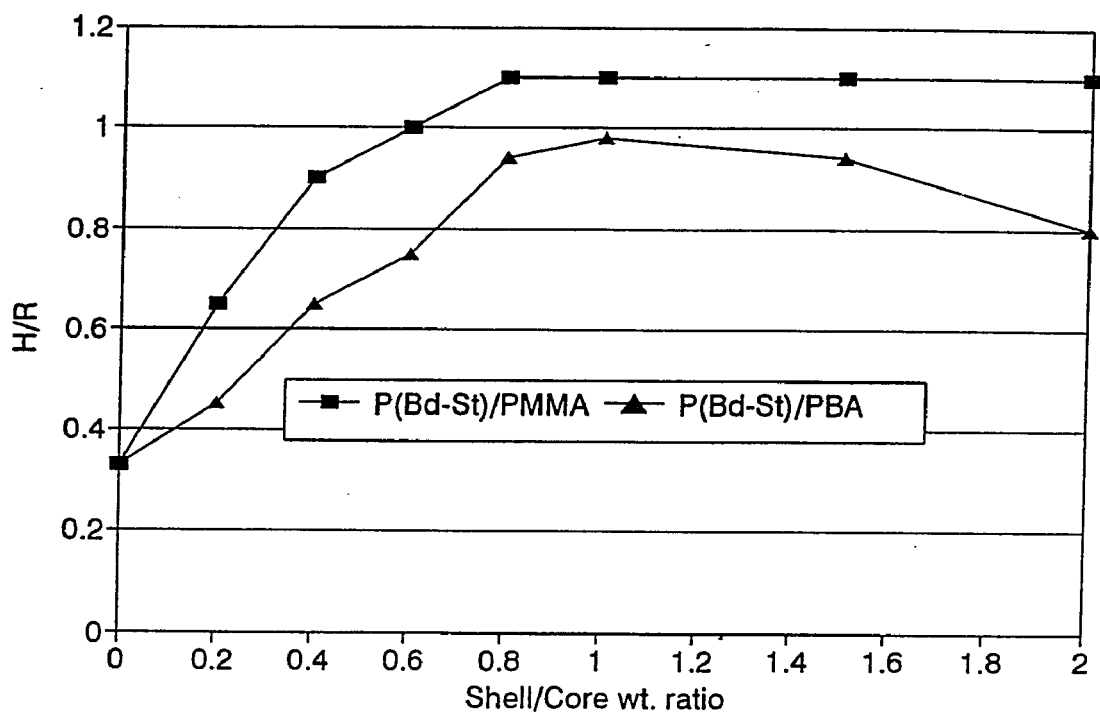


Figure 3-11: Changes in the H/R ratio of composite latex particles as determined by Pt-shadowing TEM studies with different shell/core ratios prepared by the P(Bd-S) seeded emulsion polymerization with MMA or BA.

shell/core ratio reached 0.6/1. Interestingly, for the P(Bd-S)/PBA system, the H/R ratio approached 1 at a 1/1 shell/core ratio, and then dropped down at higher shell/core ratios. This indicates that the increase in H/R before reaching a 1/1 shell/core ratio was due to the formation of the highly grafted/crosslinked core/shell interphase zone. The increase in the crosslinking density in the interphase zone resulted in a hardening of the originally soft P(Bd-S) particle. A PBA phase with much less grafting/crosslinking began to form as polymerization was continued to higher shell/core ratios. The PBA phase formed at this stage was soft and would collapse during the drying process when the TEM sample was prepared, which consequently led to a decrease in the H/R ratio. The onset of this decrease in H/R at about a 1/1 shell/core ratio indicates that the formation of the interphase zone was almost complete, after which a pure PBA shell will start to form. This result is in good agreement with the results obtained by the morphological observations shown in Figure 3-10. Comparing these results with those shown in Figure 3-9 for the LG SBR seed system, it can be found that the GE is still very high in the shell/core ratio range of 1/1, where pure PBA phases start to be seen from TEM observations. This comparison suggests that the GE is still very high at the point where the pure PBA phase start to form.

3.3.8 DSC Study of the Development of the Core/Shell Interphase Zone

It is clear that a highly crosslinked P(Bd-S)/PBA interphase zone is formed during the emulsion polymerization of BA using P(Bd-S) as seed. Notable deformation in the shapes of the particle surface layer could also be observed in Figure 8. This indicates that a non-uniform

structure for the crosslinking networks might be present in the P(Bd-S) seed particle, which caused a non-uniform development of the core/shell interphase zone during the second stage polymerization. Electron microscopy has proven to be a powerful tool to investigate the appearance of the morphology of these particles. However, it could not provide much information related to the configuration of the polymer chains, i.e., the extent and distribution of grafting and crosslinking in the composite particles. To investigate the evolution of grafting and crosslinking in the composite P(Bd-S)/PBA particle, differential scanning calorimetry (DSC) was used to study the development of crosslinking and the phase separation process during the second stage polymerization according to the recipe and procedure shown as Run 2 in Table 3-2. The 6% gel-fraction P(Bd-S) seed was used in this study.

Figure 3-12 presents the DSC results. Curve 1 represents the transition for the P(Bd-S) seed latex; Curves 2 to 6 show the transitions for the P(Bd-S)/PBA composite latexes with core/shell ratios from 1/0.2 to 1/1.5, respectively. It could be noted that when moving from Curve 1 to Curve 4, which corresponds to the samples with core/shell ratios from 1/0.0 to 1/0.4, the starting temperatures for the DSC transition did not change significantly, while the ending temperature rose from -66.5 to -55.1 °C, a change of 11.4 °C. According to the glass transition theory based on the free-volume model,^{16,17} the starting temperature in a DSC transition curve reflects polymer chains with lower molecular weights for linear chains, or lower degrees of crosslinking for crosslinked chains. The ending temperature, on the other hand, reflects polymer chains with higher molecular weights or higher degrees of crosslinking. The small shift in the starting temperatures from Curve 1 for the P(Bd-S) seed latex polymer to Curve 4 for the P(Bd-S)/PBA composite latex polymer with a core/shell ratio of 1/0.4

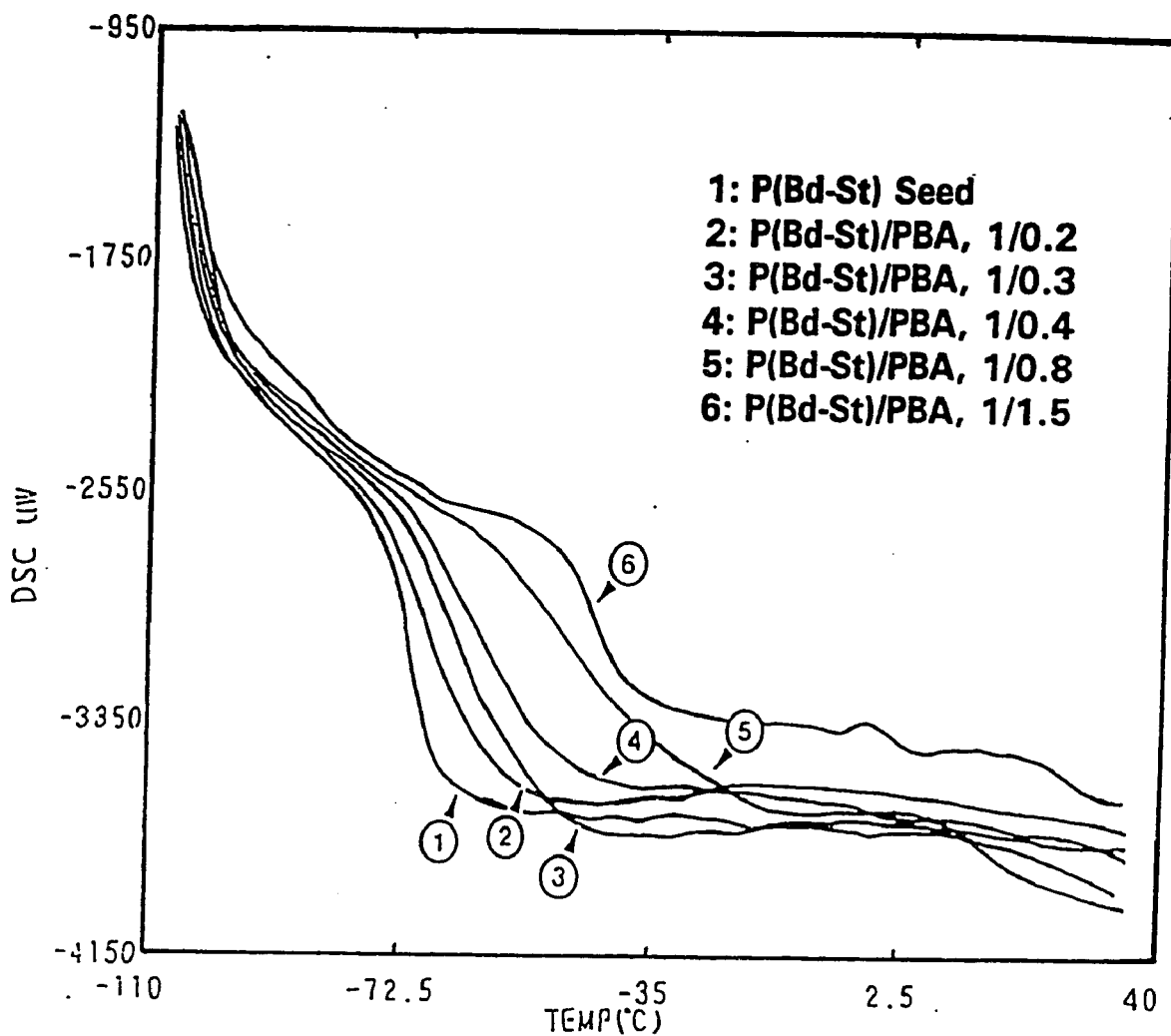


Figure 3-12: DSC curves for the core/shell LG-SBR/PBA latexes prepared with different core/shell ratios; the arrows show the end points of the transitions.

indicates that some domains of P(Bd-S) polymer are not in contact with the second stage PBA polymer and still remain in their original state, i.e., they maintain their original compositions and crosslinking level. The large shift in the ending temperatures corresponds to the domains which consist of the grafted/crosslinked P(Bd-S)/PBA interphase zone. As the second stage polymerization proceeds, and the core/shell ratio reaches 1/0.8 as shown in Curve 5, both the starting and ending temperatures shifted significantly to higher temperatures and the curve becomes much broader. This suggests that the degree of crosslinking has increased throughout the entire composite particles while a gradient of composition and crosslinking level may be present, i.e., higher PBA composition and crosslinking levels in the outer surface and lower crosslinking levels within the particles. However, the transition for the PBA polymer, which is supposed to appear around -45°C , still cannot be detected until a core/shell ratio of 1/0.8 was reached. In other words, the composite latex particle formed at this stage still consists of P(Bd-S) mixed with PBA polymer through crosslinking and grafting, instead of a P(Bd-S)/PBA core/shell structure with a sharp core/shell interface. When the core/shell ratio reached 1/1.5 (Curve 6), only one transition at about -45°C which corresponded to the PBA phase could be seen. The disappearance of the transitions at lower temperatures indicates that the degree of crosslinking in the mixed P(Bd-S)-PBA domains was too high to exhibit any DSC thermal transition. The high degree of crosslinking would greatly restrict the diffusion of newly-formed PBA polymer chains as well as pre-formed P(Bd-S) and P(Bd-S)-PBA composite polymer chains. At the same time, the number of grafting sites in the surface layer of this composite particle has also decreased as a result of the formation of the highly crosslinked/grafted interphase zone. Only at this stage can a PBA

phase be formed on the composite particles. These results are in good agreement with those discussed previously in describing the morphological observations obtained by using TEM.

3.4 Summary

A schematic illustration of the phase development in these systems is given in Figure 3-13 which sums up the results on the grafting/crosslinking behavior for a P(Bd-S)/PBA core/shell system. The structures of polymers in the interphase zone, considering the nature of both kinds of polymer species, could consist of P(Bd-S)-*graft*-PBA, P(Bd-S)-*cross*-PBA, P(Bd-S)-*ipn*-PBA, and a very small amount of linear PBA. A pure PBA phase would be formed only after the completion of the formation of the interphase zone. The formation of a gradient in the grafting and crosslinking density, i.e., high to low grafting/crosslinking level from the surface to the center of the P(Bd-S)/PBA composite particles could be hypothesized. The development of these grafted composite particles would be followed by the formation of a much lower grafted PBA phase with further polymerization of BA.

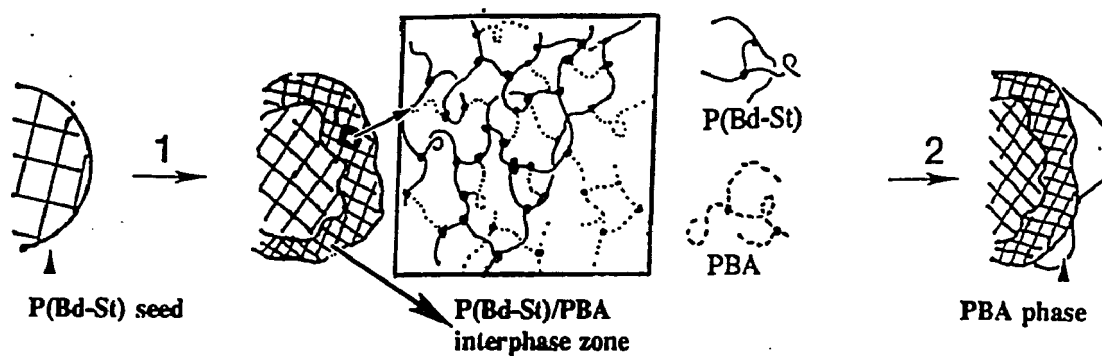


Figure 3-13: Schematic illustration of the development of the core/shell SBR/PBA interphase zone and the formation of PBA phase during the second stage semi-continuous polymerization.

References

1. Merkel, M.P., Dimonie, V.L., El-Aasser, M.S., and Vanderhoff, J.W., *J. Polym. Sci., Polym. Chem. Ed.*, **25**, 1219 (1987).
2. Sundberg, D. C., Arndt, J., and Tang, M. Y., *J. Dispers. Sci. Techn.*, **5**, 433(1984).
3. Schellenberg, J., and Hamann, B., *J. App. Polymer Sci.*, **45**, 1425 (1992).
4. Aerdts, M. A., *Ph.D. Dissertation, Techn. Univ. Eindhoven* (1993).
5. Rosen, S.L., *Polymer. Eng. Sci.*, **7**(2), 115 (1967).
6. Hoffmann, H. G., U.S. Patent No. 4180529 to E.I. duPont Co. (1979).
7. Falk, C. J., Mylonakis, S., and Beek, V., U.S. Patent No. 4473679 to Borg-Warner Chem. Inc. (1984).
8. Stanislawczyk, V., U.S. Patent No. 4879364 to The BF Goodrich Co. (1989).
9. Fryd, M., U.S. Patent No. 4956252 to E.I. duPont Co. (1990).
10. Ayrey, G., and Moore, C. G., *J. Polym. Sci.*, **36**, 41 (1959).
11. Honrston, D. J., and Romaine, J., *J. Appl. Polymer Sci.*, **43**, 1207 (1991).
12. Sacak, M., Bastug, N., and Talu, M., *J. Appl. Polymer Sci.*, **50**, 1123 (1993).
13. Elias, H.G., "*Macromolecules II*", **4(19)**, Plenum Press Inc. (1977).
14. Berger, K. C., and Meyerhoff, G. in *Polymer Handbook*, **3rd Edition**, by Brandrup, J. and Immergut, E. H.(John Wiley & Sons.) (1989).
15. Chern, C.S., and Poehlein, G.W., *J. Polym. Sci., Part A*, **28**, 3073 (1990).
16. Fox, T. G., and Flory, P. J., *J. Polymer Sci.*, **14**, 315(1954).
17. Kaelble, D. H., in *Rheology - Theory and Applications*, by Frederick, R., **5(5)**, Academic Press (1969)

Chapter 4

Hydrogenation of Poly(butadiene-*co*-styrene) in Latex Form

Abstract: The mechanism and the optimum conditions for the reduction of residual double bonds in poly(butadiene-*co*-styrene) latex by hydrogenating the polydiene in the latex form have been studied. The hydrogenation involves a copper ion (II)-catalyzed procedure in which diimide hydrogenation agent is generated *in situ* at the surfaces of latex particles by a hydrazine/hydrogen peroxide redox system.

The surface density of the copper ion in particle surfaces has been found to be a crucially important parameter in controlling the degree of hydrogenation. The distribution of the double bonds in the latex particles after the hydrogenation was found to be dependent on the particle size and the extent of crosslinking in the particles.

4.1 Introduction

Polydiene-based polymers are widely used as rubbers, binders, and adhesives because of their high strength and good elastic properties. However, a disadvantage of these materials is their aging behavior which is caused by the oxidation of the residual double bonds in the polydienes which could deteriorate the properties of the polymers.

Conventional processes to hydrogenate the residual double bonds present in polydiene-based polymers, such as BR (butadiene rubber), SBR (styrene-butadiene rubber), and NBR (acrylonitrile-butadiene rubber), are carried out in the polymer solutions, either by transition catalytic hydrogenation using pressurized hydrogen¹⁻⁵, or through a noncatalytic diimide reduction process^{6,7}. There are some obvious problems for these kinds of hydrogenation processes. Besides the high cost of hydrogenation equipment and catalyst, and low efficiencies resulting from the limited solubility and solvent-induced environmental concerns, this method can only be used for linear polydiene polymers because of the requirement for a polymer solution. Moreover, these methods are not feasible when a hydrogenated polydiene is needed in the latex form.

A breakthrough process was developed by Wideman⁸ in 1984 to directly convert BR, SBR and NBR latexes into their saturated forms. He described a procedure which involved a system containing hydrazine hydrate, an oxidant, and a metal-ion catalyst. A hydrazine/hydrogen peroxide redox system was typically used with copper ion as the catalyst, and an 80% degree of hydrogenation for NBR latex was attained. Recently, a

series of studies on the mechanism for the hydrogenation process in latex polymers was reported by Parker⁹ and coworkers. Based on early studies¹⁰⁻¹² on the reductions of the multiple bonds in olefins with metal-catalyzed hydrazine/oxidant systems, Parker et al. proposed a diimide reduction mechanism for the latex in which the diimide hydrogenating agent was generated at the surfaces of particles from a hydrazine/hydrogen peroxide redox system. Carboxylated surfactants adsorbed at the latex particle surfaces play an important role in this procedure by forming hydrozinium carboxylates with hydrazine, and a dicopper fatty acid complex¹³ with copper ions. Diimide intermediates which are primarily generated at the adsorbed surfactant layer at the latex particle surfaces would then diffuse into the particles to effectively reduce the residual carbon-carbon double bonds within the limited lifetime of the diimide intermediate. Hydrogenated polydiene-based polymers did not only exhibit excellent ozone and oxidation resistance as expected⁹, but also showed improved mechanical properties in some circumstances^{14,15}.

The present work was focused on determining the optimal conditions for the hydrogenation process of latex polymer in terms of factors such as the loci and concentration of the copper ion catalyst, latex particle size, and the gel fraction of poly(butadiene-*co*-styrene) [P(Bd-S)] latexes. The structure of the hydrogenated P(Bd-S) latex particles with regards to the distribution of the double bonds in the latex particles during the hydrogenation process has been investigated through the analysis of the degree of hydrogenation for the different types of double bonds, i.e., trans, cis, or vinyl. Morphological observations of the hydrogenated latex particles by transmission electron microscopy (TEM) have also been carried out to confirm the structures.

4.2 Experimental

4.2.1 Materials

The monomers used, butadiene (Bd) (Matheson Gas Products, Inc.) and styrene (S) (Fisher Scientific) were treated by passing them through inhibitor-removal columns. Purified stearic acid, lithium hydroxide (Fisher Scientific), and cupric sulfate ($\text{CuSO}_4 \cdot 5\text{H}_2\text{O}$; J. T. Baker Chem. Co.) were used as received. Hydrazine hydrate ($\text{H}_2\text{NNH}_2 \cdot \text{H}_2\text{O}$) and hydrogen peroxide (H_2O_2 , 50%), reagent grade (Fluka), Dowfax 2A1 (a sodium dodecyl diphenylether disulfate surfactant, Dow Chemical) and Dow Corning Antifoam 1430 were used as received. SBR-1502 P(Bd-S) latex (Goodyear Rubber & Tire Co.) was used as received.

4.2.2 Preparation of P(Bd-S) Latexes

P(Bd-S) latexes with various particle sizes and gel fractions were prepared by emulsion polymerization techniques in 250 ml pressure bottles at 65 and 70 °C by end-over-end rotation in a thermostated bottle polymerization unit at 40 rpm according to the recipes shown in Table 4-1. To obtain the latex particles with desired particle sizes and gel fractions, the surfactant concentrations, polymerization time, and temperature were varied. For latexes obtained at conversions lower than 100%, the remaining monomers in the

Table 4-1: Recipes for The Preparation of P(Bd-S) Latexes

Component (g)	P(Bd-S)-S -LG	P(Bd-S)-S -HG	P(Bd-S)-L -LG	P(Bd-S)-L -HG
Butadiene	45.00	45.00	45.00	45.00
Styrene	5.00	4.50	5.00	4.50
Divinylbenzene	---	1.00	---	1.00
n-Dodecyl mercaptan	0.10	---	0.10	---
Potassium persulfate	0.25	0.25	0.25	0.25
Stearic acid	0.50	1.80	0.50	0.70
Lithium hydroxide	---	---	0.040	0.056
Sodium hydroxide	0.067	0.24	---	---
Distilled-deionized (DDI) water	90.00	90.00	90.00	90.00
Conversion (%)	64	100	57	100
Particle size (nm)	80	60	230	240
Gel fraction (%)	41	100	34	100
Polym. temp. (°C)	70	70	65	65

latexes were removed immediately after the termination of the polymerization by flash evaporation, which was repeated at least three times. DDI water was added between the evaporation processes. The particle sizes of the latexes were determined by using light scattering (Nicomp) and transmission electron microscopy (TEM), and the gel fractions were determined by a solvent (toluene) extraction technique which has been described in Chapter 3.

4.2.3 Hydrogenation of P(Bd-S) latexes

The recipes used in the hydrogenation study are shown in Table 4-2. An aqueous solution of $\text{CuSO}_4 \cdot 5\text{H}_2\text{O}$ and Dowfax 2A1 was added to P(Bd-S) latex in a 250 ml flask. The $\text{H}_2\text{NNH}_2 \cdot \text{H}_2\text{O}$ was then charged into the flask. The mixture was warmed to 50 °C with stirring. H_2O_2 (50%) was then added dropwise over a seven hour period. Small amounts of antifoam agent (Dow Corning Antifoam 1430) were periodically added during the reaction as required.

4.2.4 IR Analysis for Determination of the Degree of Hydrogenation

The final conversion of the double bonds to single bonds in the hydrogenated P(Bd-S) [H-P(Bd-S)] latex was determined by infrared spectroscopy (FTIR). The latex film formed from diluted latex was cast on a Zn-Sn plate at atmospheric pressure and then dried in a desiccator at room temperature and used for the IR measurement. The thickness of the

**Table 4-2: Recipe Used for The Hydrogenation of P(Bd-S) Latexes
with Different Copper Ion Concentrations**

Component	Weight (g)
P(Bd-St) latex (20 % solids)	100 (0.378 mol double bond)
Hydrazine hydrate ($\text{H}_2\text{NNH}_2 \cdot \text{H}_2\text{O}$)	18.9 (0.378 mol)
Hydrogen peroxide (H_2O_2 , 50 wt%)	25.5 (0.378 mol)
Cupric sulfate pentahydrate ($\text{CuSO}_4 \cdot 5\text{H}_2\text{O}$)	Varying amount (g) (1×10^{-3} to 4×10^{-2} for SP [†] ; 4×10^{-5} to 1×10^{-3} for LP [‡] latex)
Dowfax 2A-1	Varying amount (g) (0.02 to 0.08)

[†] SP: "Small Particle", 50 nm in diameter.

[‡] LP: "Large Particle", 230 nm in diameter.

latex films for the IR measurements was controlled such that the IR absorbances were in the range of 0.3 to 0.7 cm^{-1} .

4.3 Results and Discussion

4.3.1 IR Analysis

Figure 4-1 shows the IR spectra of both non-hydrogenated P(Bd-S) and partially hydrogenated P(Bd-S) latex. The P(Bd-S) spectrum shows distinct peaks for trans, cis, and vinyl double bonds at 966, 722, and 910 cm^{-1} wavenumbers, respectively; the percentages of these three types of double bonds as determined from their absorbance intensities are 62, 18, and 20%, respectively. The peak at wavenumber 700 cm^{-1} representing the phenyl ring in the styrene unit was used as an internal standard to determine the relative concentrations of trans and vinyl double bonds. It can be noted that the absorbance peak for the cis double bond at a wavenumber of 722 cm^{-1} slightly increased after the hydrogenation, instead of decreasing as was expected. This increase is caused by the overlap from the absorbance of polyethylene formed after the hydrogenation. After the hydrogenation, the 1,4-polybutadiene segments were converted to polyethylene, which has two absorbance peaks around 720 and 730 cm^{-1} wavenumbers for amorphous and crystalline state polymer chains, respectively. The 720 cm^{-1} peak would overlap with the 722 cm^{-1} peak for the cis double bond and cause the increase for this peak in this range. It had been reported^{16,17} that the reactivity for cis double bonds is about the same as that for the trans double bonds for the hydrazine/oxidant-induced

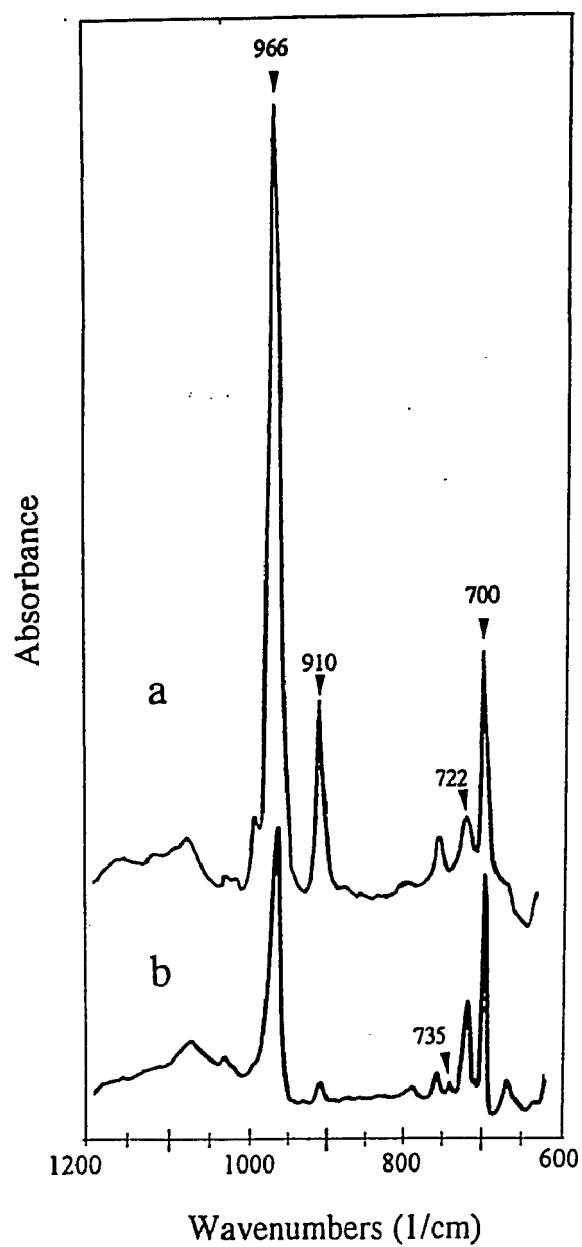
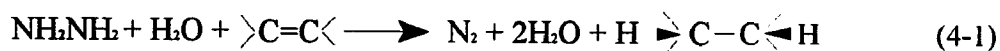


Figure 4-1: IR spectra of: (a) non-hydrogenated P(Bd-St), and (b) partially hydrogenated P((Bd-St) latexes.

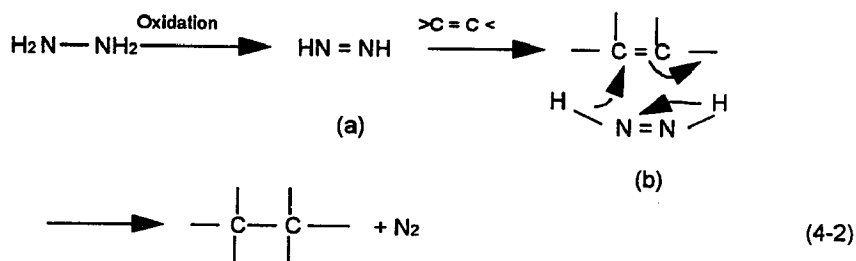
diimide hydrogenation reaction. Since the concentration of cis double bonds was lower than that of the trans double bonds in the latex particles, a lower percentage of hydrogenation for the cis double bonds is expected. In this study, the degree of hydrogenation for the cis double bonds is assumed to be 10% less than that for the trans double bonds which could be determined directly from the phenyl ring internal standard. It can also be noted that a new peak appears at 735 cm^{-1} after the hydrogenation. This peak could represent the crystalline polyethylene segments formed after the hydrogenation of 1,4-polybutadiene segments.

4.3.2 Location and Concentration of Copper Ion

The overall hydrogenation reaction using hydrazine/oxidant is shown below:



The reduction mechanism of this $\text{H}_2\text{N-NH}_2/\text{H}_2\text{O}_2$ redox system has been extensively studied in homogeneous reaction systems for small molecules^{10-12,19,20}. These studies indicated that this reduction procedure involved an intermediate diimide structure (a) according to the following scheme:



In this procedure, the diimide formed in the first step is a mixture of cis and trans isomers. The reduction of carbon-carbon double bonds with diimide can only be carried out by the cis-diimide involving a stereospecific cis addition of hydrogen with a cyclic diimide transition state (b). At the same time, diimide is very unstable, and is capable of reacting with itself to form the disproportionation products, hydrazine and nitrogen:



The copper ion is able to greatly accelerate the formation of diimide from the $\text{H}_2\text{N}-\text{NH}_2/\text{H}_2\text{O}_2$ redox system. A simple experiment was done by adding H_2O_2 (50%) to a 20% $\text{H}_2\text{N}-\text{NH}_2$ aqueous solution with and without the presence of copper ion. It was found that the system with copper ions reacted remarkably fast while the system without the copper ions present reacted much more slowly. This indicates that for the heterogeneous latex system used in this study, the location and concentration of the copper ions are extremely important.

Location of Copper Ions

Copper ions can be present at three locations in a polymer latex: in the water medium, at the polymer particle surfaces, and inside of the particles. Obviously, localizing copper ions in the water phase will only lead to reaction (4-3) because there are no carbon-carbon double bonds to be reduced. This has been proven in Parker's work⁹ by complexing copper ions in water with aqueous ethylenediamine tetraacetic acid tetrasodium salt (Na_4EDTA). Their results showed that no double bonds could be reduced in this case. To localize the copper ions inside of the latex particles, a small amount of oil-soluble 2-(acetoacetoxy)ethyl methacrylate (AAEM) was used. The results, however, were negative, i.e., a much lower degree of hydrogenation (HD) was attained compared to the system without AAEM. This was due to the low diffusivity of the highly water-soluble species, $\text{H}_2\text{N-NH}_2$ and H_2O_2 , into the polymer particles. In order to reach a higher degree of hydrogenation, the copper ions should reside only at the surfaces of the latex particles, which can be accomplished by ionically associating them with acidic groups present in the surfactants (e.g., carboxylated surfactants such as sodium stearate) adsorbed at the latex particle surfaces. In practice, coagulum would form instantly in a latex stabilized with a carboxylated surfactant when a copper ion solution is added because Cu^{2+} would bridge carboxylates in the surfactants. A small amount of surfactant that is stable to copper ions has to be added together with the copper ions to stabilize the system. Dowfax 2A-1 was used for this purpose. Another important function of a carboxylated surfactant is to form hydrazinium carboxylate⁹ by which the hydrozinium ion could also be present on the

particle surface. A schematic illustration of the hydrogenation process is shown in Figure 4-2.

Concentration of Copper Ions at the Particle Surface

Considering the competitive reactions shown in reactions (4-2) and (4-3), a high concentration of carbon-carbon double bonds is preferred for the reduction reaction which competes with the disproportionation reactions of diimide with itself. At the particle surface, the concentration of double bonds is fixed by the composition of the polymer latex itself. In another words, a controllable factor related to reactions (4-2) and (4-3) is the concentration of diimide. The concentration of diimide formed should be controlled at a level where it is high enough for the reduction of double bonds to occur, and yet low enough to minimize the extent of the disproportionation reaction of the diimide. Thus, the concentration of copper ions at the particle surfaces is the key factor which needs to be controlled. Table 4-2 shows a recipe for the hydrogenation of P(Bd-S) latex. One of the P(Bd-S) latexes used in this recipe was the carboxyl surfactant-stabilized SBR-1502 latex. The particle size is 50 nm as measured by dynamic light scattering (Nicomp) and labeled as SP (i.e., "Small Particle"). Another P(Bd-S) latex used was the P(Bd-S)-L-LG latex described in Table 4-1 which is labeled as LP (i.e., 230 nm, "Large Particle"). Various amounts of $\text{CuSO}_4 \cdot 5\text{H}_2\text{O}$ were added to the latex to investigate the influence of the copper

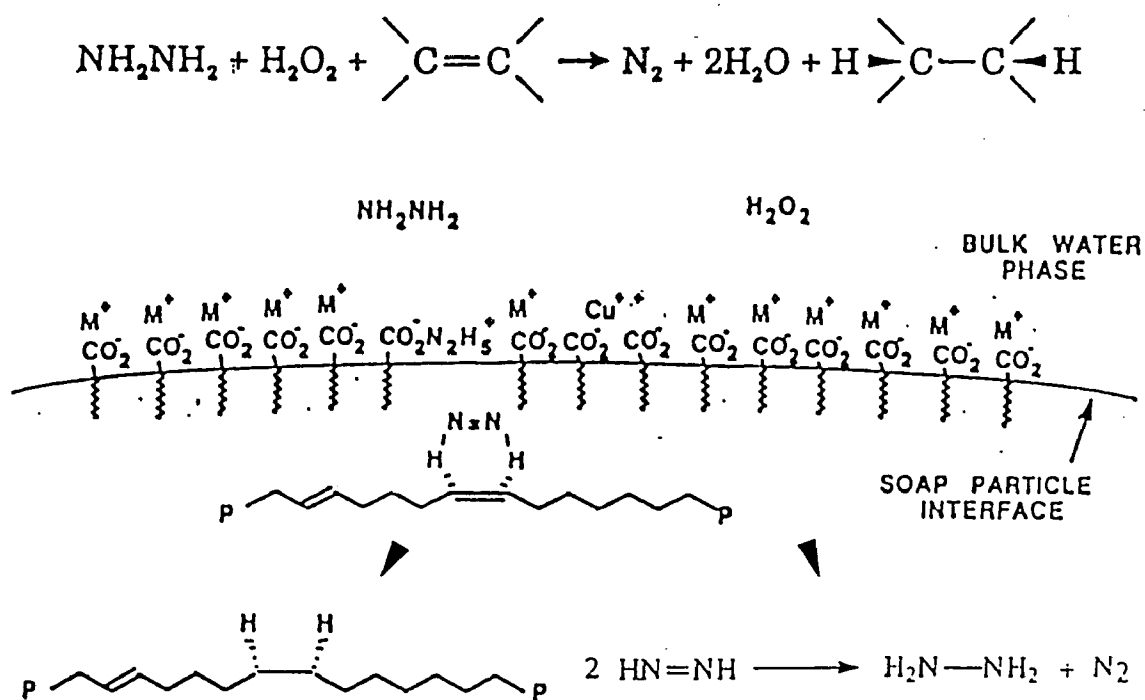


Figure 4-2: A schematic illustration of the hydrogenation of P(Bd-S) latex particle by the Cu^{2+} catalyzed $\text{H}_2\text{N}-\text{NH}_2/\text{H}_2\text{O}_2$ redox system.

ion concentration on the degree of hydrogenation. The influence of the particle size of the P(Bd-S) latexes will be discussed by comparing the SP and LP latex systems. It should be mentioned that the purpose of this experiment was to investigate the optimum copper ion concentration needed for the hydrogenation reaction to occur, and not to determine the overall conditions necessary to achieve the highest degree of hydrogenation. Actually, there will be some hydrazine remaining in the system after the hydrogenation following this recipe. The degree of hydrogenation can be increased by adding some additional hydrogen peroxide.

Figure 4-3 shows the degree of hydrogenation (HD) with different copper ion concentrations in the SP latex system. It is clearly shown that HD is very sensitive to the overall copper ion concentration. A maximum HD could be reached at very low copper ion concentrations ranging between 0.05 to 0.2 mM (based on total latex system). A higher copper ion concentration would decrease the HD to a very low level. For the LP system, as shown in Figure 4-4, a similar tendency is shown, except that the concentration of copper ions for the peak HD appears over a range of about 0.005 to 0.015 mM (based on total latex system) which is about one tenth of that found in the SP system. By converting the copper ion concentration to the number of copper ions per 100 nm² of particle surface, with the known particle sizes for both the SP and LP systems, it is interesting to note that, as shown in Figure 4-5, the HD peaks appear over the same range of about two copper ions per 100 nm² of particle surface for both the SP and LP systems. This result indicated that under these conditions the amount of copper ions at the particle surfaces is appropriate to enhance the extent of the diimide/double bond reduction as

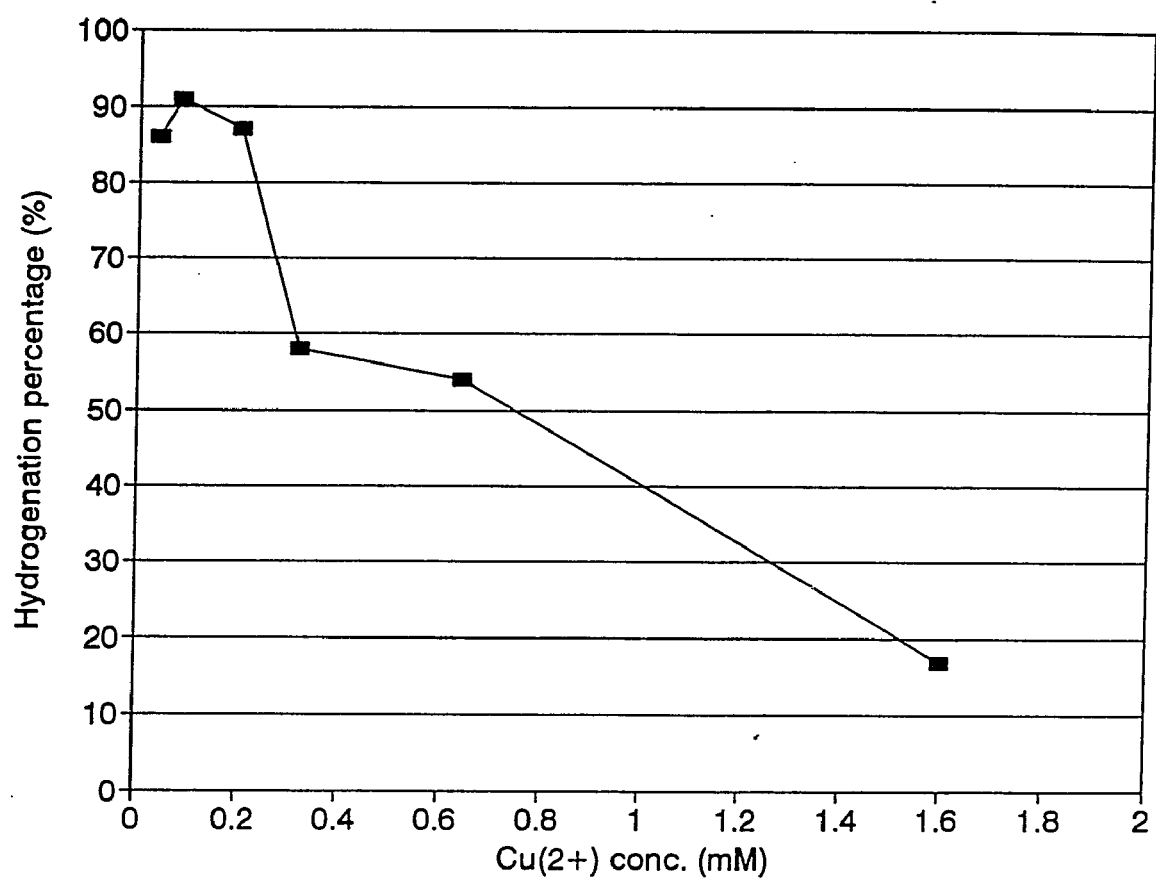


Figure 4-3: Hydrogenation percentage with different molar concentrations of copper ion in the SP latex system (50 nm).

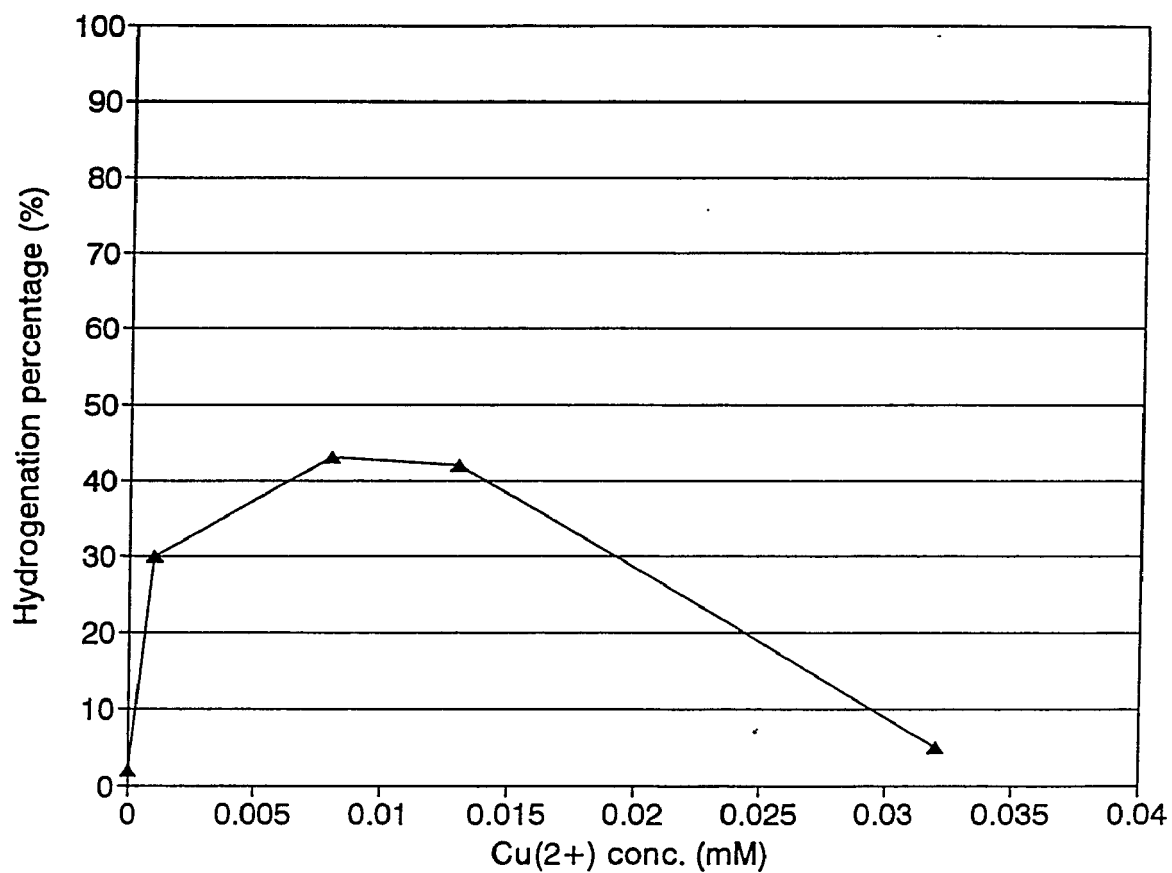


Figure 4-4: Hydrogenation percentage with different molar concentrations of copper ion in the LP latex system (230 nm).

compared to the diimide disproportionation reaction. However, at higher copper ion concentrations the rate of diimide formation would be faster; this would enhance the diimide disproportionation reaction compared to the reduction reaction. At even higher copper ion concentrations, some free copper ions may also be present in the water medium; this would make the $\text{H}_2\text{N-NH}_2/\text{H}_2\text{O}_2$ reaction occur mostly in water. As a result, the double bond reduction would be decreased to a very low level.

Figure 4-5 also shows that the overall HD for the LP system is about two-fold lower than that obtained for the SP system around the peak region. As mentioned above, the reactions between $\text{H}_2\text{N-NH}_2$ and H_2O_2 could occur in either the water phase or at the particle surface, regardless of the presence of copper ions. With appropriate amounts of copper ions localized only at the particle surface, the rate of formation of diimide at the particle surfaces would be much higher than in the water medium. However, this competition reaction always exists during the entire hydrogenation process. As shown in Figure 4-5, the condition needed for reaching the maximum HD is determined by the surface area density of copper ions at the particle surface for either the SP or LP system. Thus, the total number of copper ions at the particle surface is limited by the surface area of the total latex particles. In other words, the total catalyzed reaction sites for the formation of diimide are limited by the total surface area. This limit would certainly be reflected by the overall rate of double bond reduction competing with the reaction in water. At the optimum surface area density of copper ions, which is about the same for either the SP or LP system, i.e., $2 \text{ Cu}^{2+}/1000 \text{ nm}^2$ surface, the total number of copper ions in the LP latex system is much less than that for the SP latex system because of the much

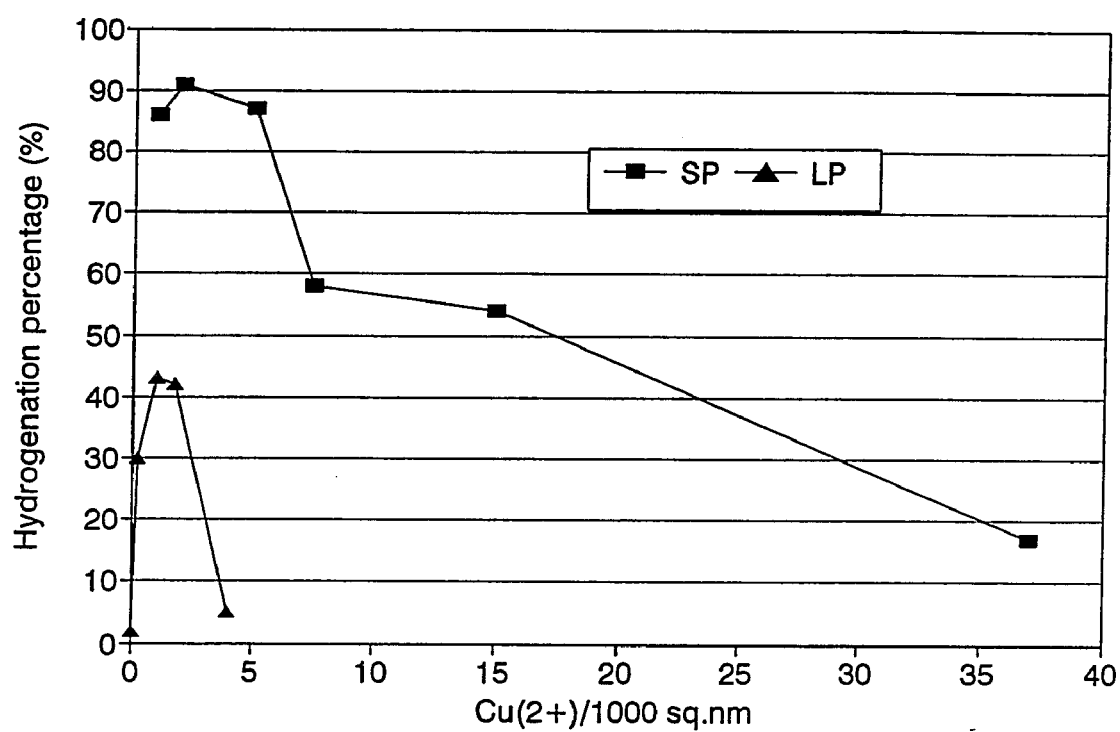


Figure 4-5: The relationship between the hydrogenation percentage and the surface area density of copper ions at the particle surface ($\text{Cu}^{2+} / 1000 \text{ nm}^2$) for the SP and LP latex systems.

smaller total surface area for the latexes with the same solids content (20%). This could be one of the reasons that led to the decreased overall HD for the LP system. Another possible factor that could influence the HD for the LP system is the increased distance for the diffusion of the diimide molecules from the surface to react with double bonds residing in the inner side of the particles due to the larger particle size. The longer the diffusion distance, the longer the lifetime needed for the diimide before reaching a double-bond and the greater the probability for the disproportionation reaction of diimide itself to occur during the diffusion process. Obviously, the relative extents of these two competitive reactions are decided by the local concentrations of double bonds and diimide molecules, which are dependent on the rates of diffusion of both polymer chains and diimides. To further investigate the mechanism of this hydrogenation process, a series of P(Bd-S) latexes with different gel fractions and particle sizes were used in subsequent hydrogenation reactions.

4.3.3 Distribution of Double Bonds in the Latex Particles after Hydrogenation

First of all, parallel hydrogenation reactions were carried out on two latex systems with high and low gel fractions (HG, 95% and LG, 23%); the average particle sizes for both latexes were 60 and 50 nm, respectively. High degrees of hydrogenation were attained in both systems, i.e., 91% and 93% for the HG and LG system, respectively. Although the mobilities of polymer chains in the latex particles for these two systems are expected to be quite different, it seems that the high gel fraction does not exert much influence on the diffusion of the small diimide molecules generated at the particle surfaces. In other words, the particle size

is small enough for the diimide molecules to diffuse from the surface to the center of the particle.

For latexes with larger particle sizes, as shown in Figure 4-4, a low degree of hydrogenation of only 42% was reached at the optimum hydrogenation condition after a 1/1 molar ratio of $\text{H}_2\text{NNH}_2/\text{H}_2\text{O}_2$ redox system to residual double bonds during hydrogenation was employed. In this type of partially hydrogenated P(Bd-S) latex, two possible structures could be present. Since the hydrogenation reactions take place during the process in which the diimide hydrogenation agent which is formed at the particle surfaces diffuses into the interior of the particles, a relatively highly hydrogenated layer could form close to the particle surface. However, diffusion of the soft P(Bd-S) chains inside of the particles occurs at all times, especially at the hydrogenation temperature of 50 °C. This diffusion of polymer chains would tend to diminish the formation of the hydrogenated layers and would instead lead to a structure in which the double bonds are uniformly distributed. We can define these two kinds of model structures, as shown in Figure 4-6, as either a layer model (a) or a uniform model (b). To verify these two possible models, repeat hydrogenation reactions were carried out in another series of P(Bd-S) latexes with high and low gel fractions using P(Bd-S)-L-LG and P(Bd-S)-L-HG latexes as described in Table 4-1.

Figure 4-7 shows the degree of hydrogenation after each hydrogenation process. The numbers 1, 2, and 3 on the X-axis represent the molar ratio of the hydrogenation redox components ($\text{H}_2\text{NNH}_2/\text{H}_2\text{O}_2$) to the residual double bonds in the P(Bd-S) latex corresponding to three repeat hydrogenation reactions. A time interval of 8 h was allowed between hydrogenation reactions. Figure 4-7 shows that the degree of hydrogenation increased

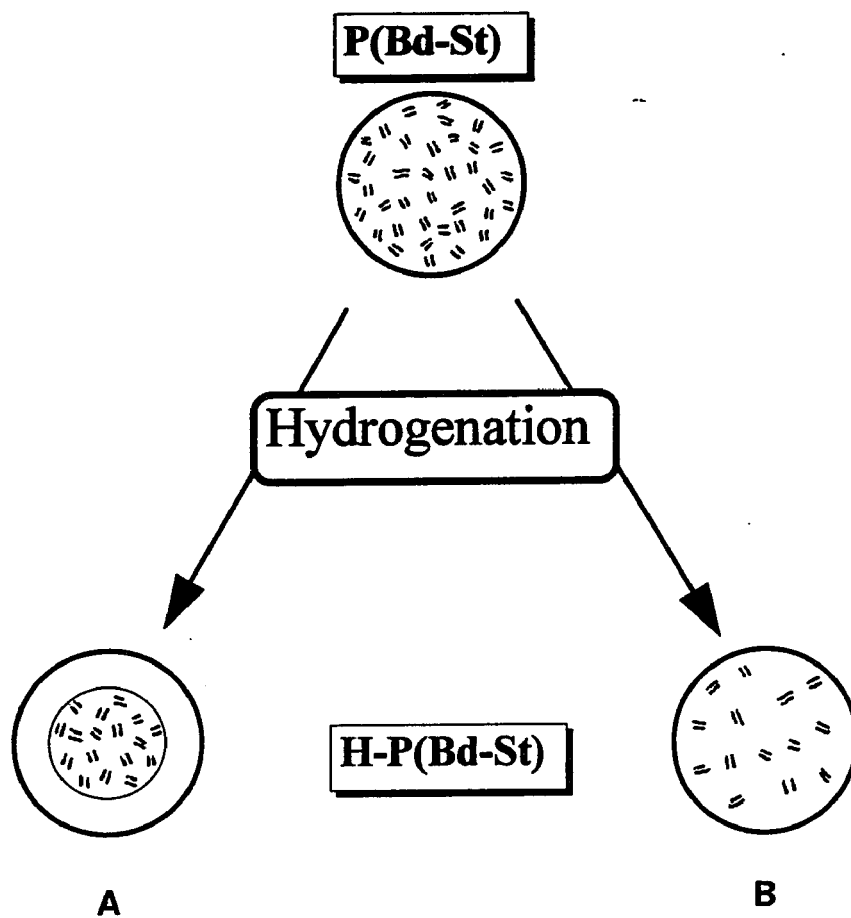


Figure 4-6: Two models for the distribution of double bonds in hydrogenated P(Bd-S) latex particles: (A) layer model, and (B) uniform model.

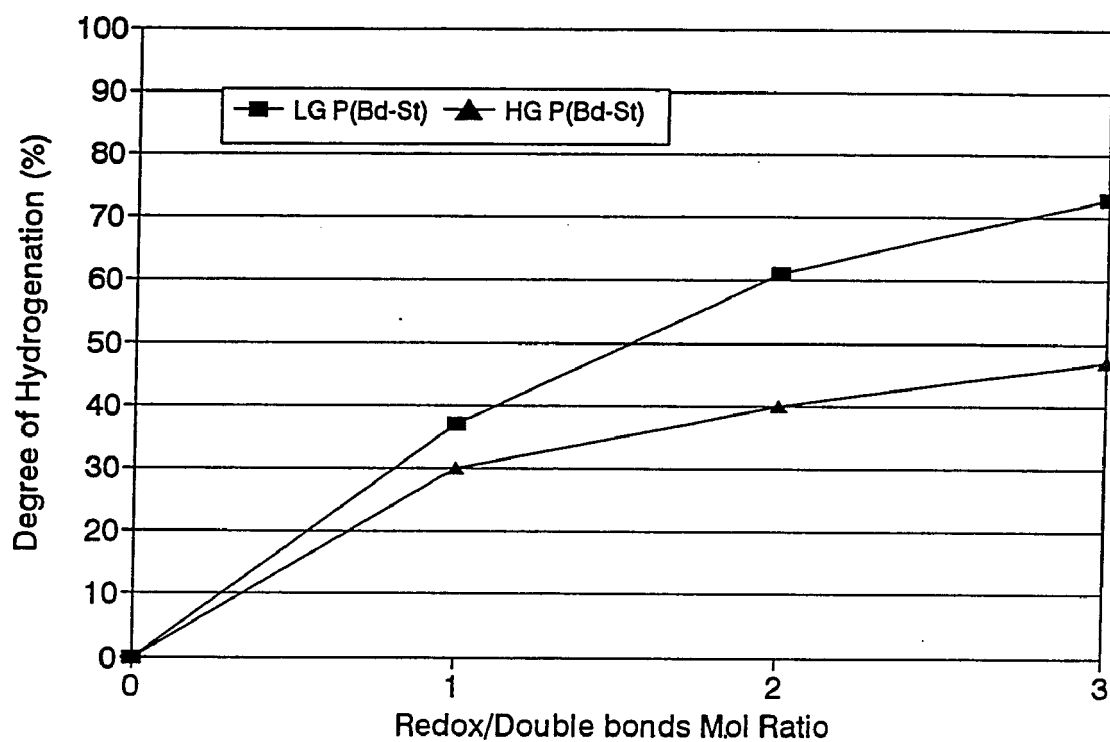


Figure 4-7: Degree of hydrogenation after each run for three successive 1/1 molar ratio hydrogenations of the high gel (HG) and low gel (LG) P(Bd-S) latex systems (particle sizes: HG=240 nm; LG=230 nm)

gradually for the LG system after each hydrogenation. The differences in the hydrogenation levels between runs were 37%, 22% and 12%. These numbers support the uniform model, i.e., double bonds in the latex particles are uniformly distributed at all times due to the diffusion of polymer chains. If 37% of the double bonds in the particles would be hydrogenated after each hydrogenation process, it can be easily calculated that the increased percentages of the hydrogenation between the first and the second, the second and the third hydrogenation should be 23% and 11.5%, respectively. The experimental results obtained, i.e., 22% and 12% (differences between the first and the second, the second and the third hydrogenations), are very close to these values. The extent of the hydrogenation zone (i.e., thickness) inwards from the surface of the particles, which should be about 37% of the total volume of the particle, is estimated to be about 20 nm. However, this model obviously does not fit the HG latex system. The increase in hydrogenation after each run for the HG system is much lower than that of the LG system, especially after the first run. The increase in the degree of hydrogenation after each run was shown to be 30%, 10%, and 7%, respectively. This result suggests that a layer close to the surface of the particles which has a relatively higher degree of hydrogenation due to the low mobility of those highly crosslinked polymer chains may exist. The concentration of double bonds in this layer is lower than the inner portion of the particle after the first run. As a result, the disproportionation reaction among diimide molecules becomes more competitive in this layer, and consequently results in a low degree of hydrogenation after the second and third runs.

This explanation can be further confirmed by investigating the degree of

hydrogenation for different types of double bonds in the P(Bd-S) latex systems. The percentages of the three types of double bonds, i.e., trans, cis, and vinyl, in the P(Bd-S) latex system are 62, 18, and 20%, respectively. Kinetic studies¹⁷ on the rate of reaction of diimide with olefins showed that the hydrogenation rate for vinyl double bonds is almost ten times faster than those for trans and cis double bonds. Figure 4-8 shows the degree of hydrogenation for each type of double bond in the LG latex system. After the first run, more than 50% of the vinyl double bonds were hydrogenated, while the degrees of hydrogenation for the trans and cis double bonds were about 30%. More significantly, almost all of the vinyl double bonds were hydrogenated after the third run, while there were still 30% of the trans and cis double bonds remaining in the system. For the uniform model, all of the double bonds are highly mobile, and the possibility that any type of double bond is present in the hydrogenation zone depends only on the concentrations of the bonds instead of their initial loci. Thus, vinyl double bonds, which have a much higher reaction rate with diimide, should certainly be consumed faster. This is not the case for the HG latex system. Figure 4-9 shows the analysis for the HG latex under the same conditions as that shown in Figure 4-8. The differences between the percentage of hydrogenation for each type of double bond are very small compared with the LG latex system. After the third run, the vinyl double bond does not exhibit a significantly higher percentage of hydrogenation. As mentioned above, the mobility of polymer chains in these HG latex particles is greatly restricted and all of the double bonds are fixed at a specific location after the latex particle is formed. Consequently, only those double bonds that are initially located in the hydrogenation zone could be hydrogenated. In this way, the

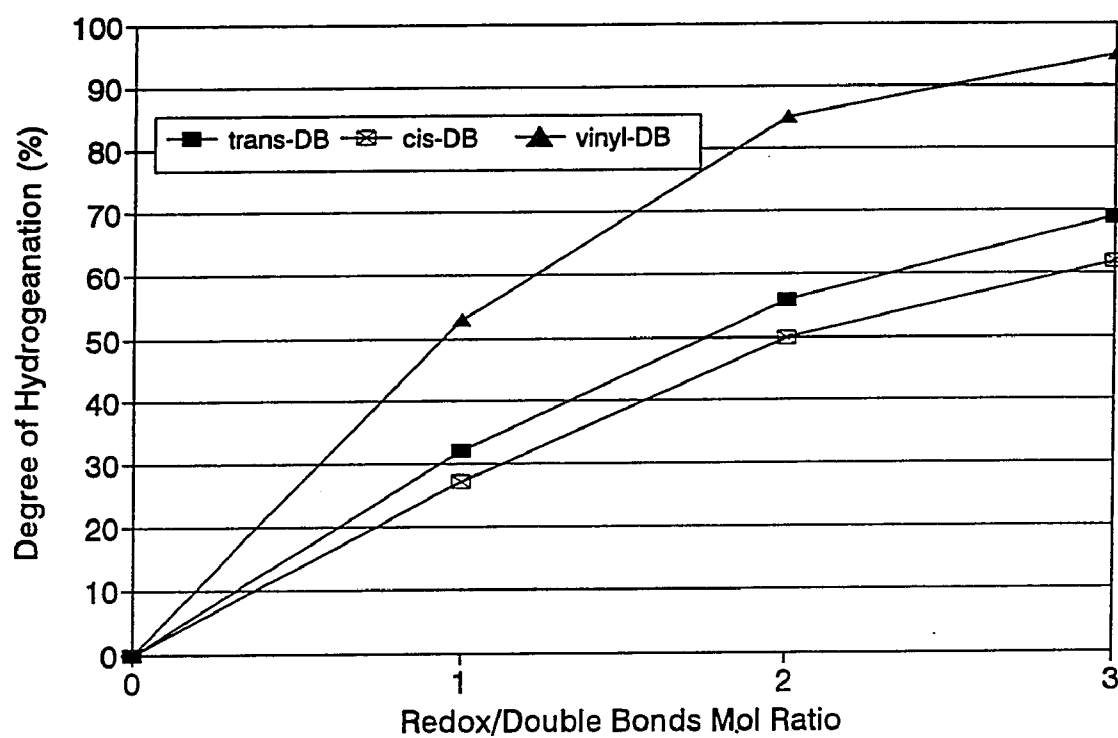


Figure 4-8: Degree of hydrogenation for each type of double bond in the LG P(Bd-S) latex system; particle size = 230 nm.

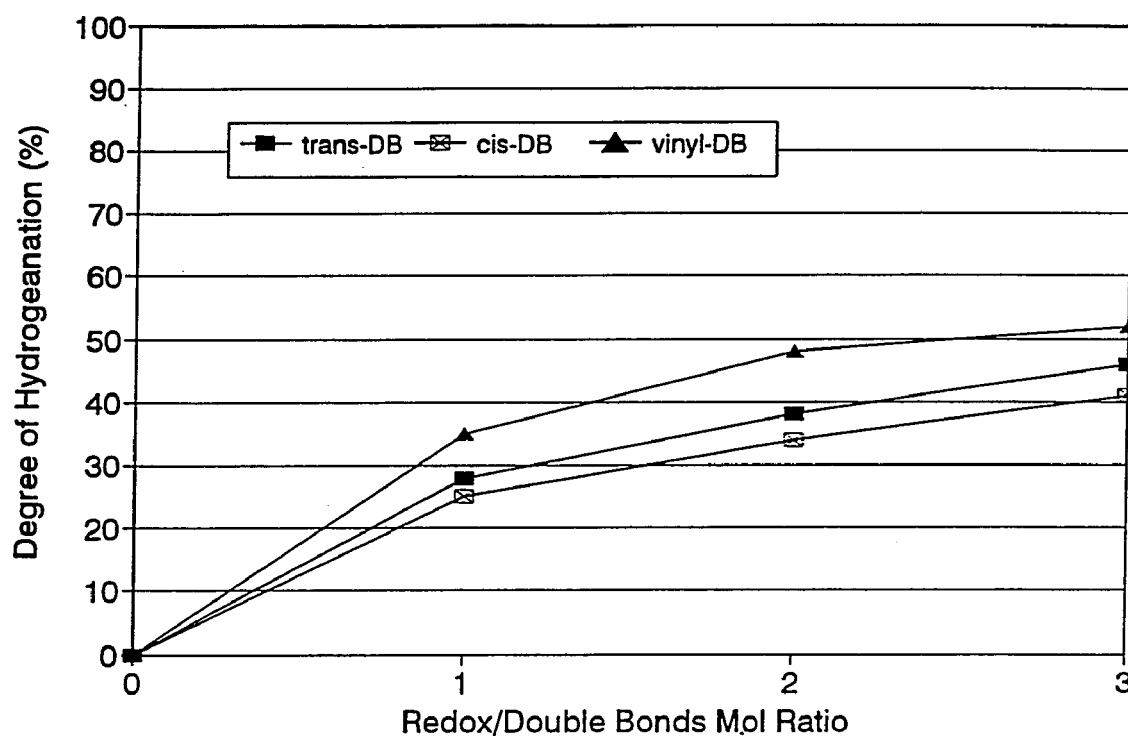


Figure 4-9: Degree of hydrogenation for each type of double bond in the HG P(Bd-S) latex system; particle size = 240 nm.

percentage of hydrogenation for each type of double bond should be about the same.

Figure 4-10 shows TEM micrographs of the LG (C) and HG (D) latex particles after the third hydrogenation step. Since the OsO_4 staining agent can only stain double bonds, lightly colored domains should indicate lower double bond concentrations. For comparison, a control P(Bd-S) latex (with no hydrogenation; particle size=80 nm) (A) and the P(Bd-S) latex with a degree of hydrogenation of 90 % (B) are also shown. The non-hydrogenated P(Bd-S) (A) shows relatively sharp particle edges because the concentration of the OsO_4 inside the particle is high. On the other hand, the 95 % hydrogenated latex (B) exhibits a much lighter color due to the small amount of the double bonds available for OsO_4 staining. For the partially hydrogenated cases, (C) (particle size=230 nm) and (D) (particle size=240 nm), the contrast between the center and the surface of the hydrogenated LG particles (C) is quite vague compared with that of HG particles (D), where a sharp contrast can be observed. The contrast shown in Figure 4-10(C) could simply be the contrast due to thickness differences. The sharp contrast shown in Figure 4-10(D), on the other hand, could represent contrast due to a concentration difference in addition to thickness. It is interesting to note that there is a lightly colored small particle appearing in Figure 4-10(D). The light color indicates that this particle is highly hydrogenated throughout the particle because of its small particle size, even though it has a high gel fraction.

Finally, it should be mentioned that the gel fractions of P(Bd-St) latexes were found to increase after the hydrogenation. The gel fractions for P(Bd-S)-S-LG and P(Bd-S)-L-LG latexes used in this study increased from 41 and 34 % to 52 and 38%, respectively, after

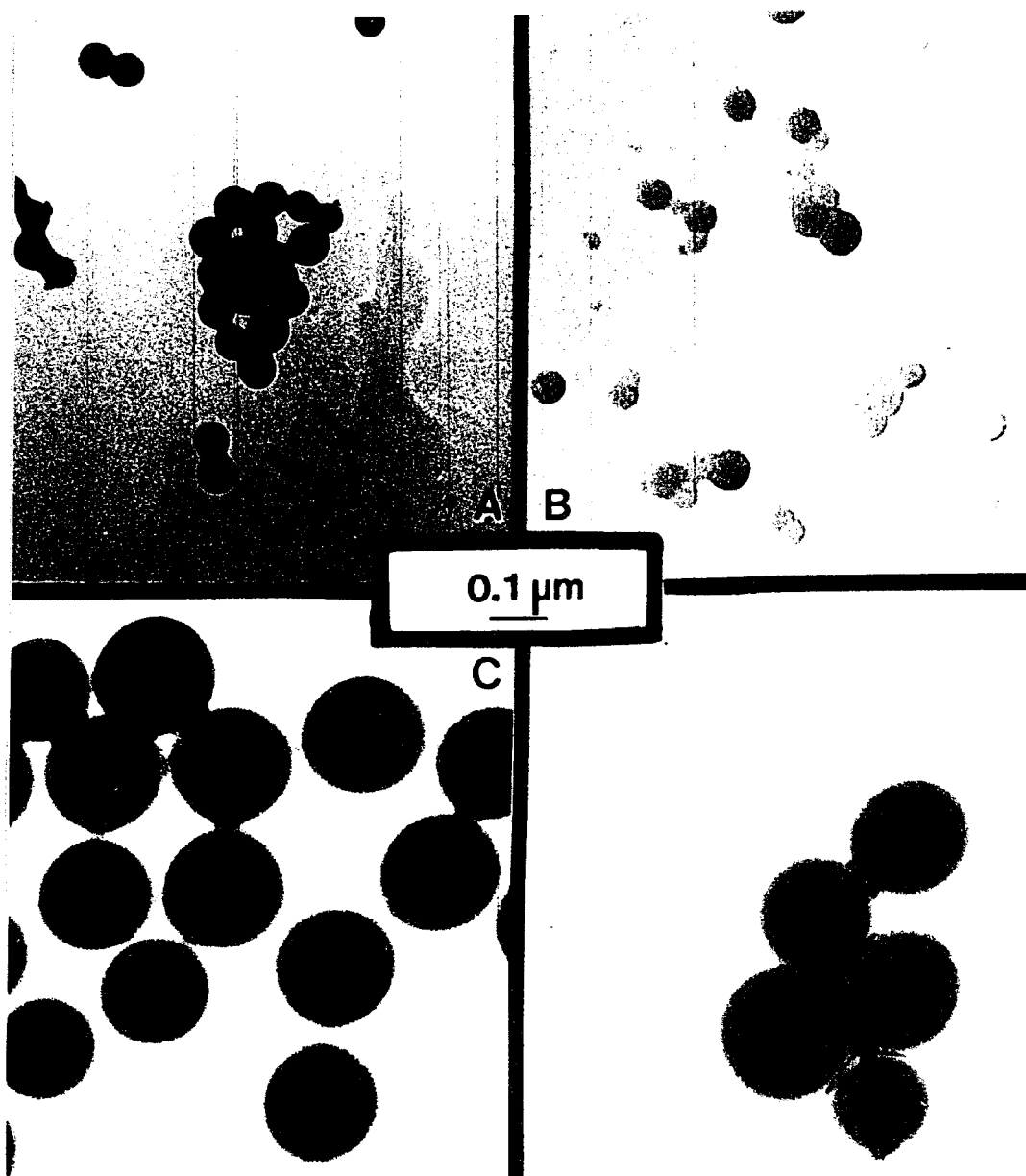


Figure 4-10: TEM micrographs of: (A) non-hydrogenated P(Bd-S) latex, 80 nm in diameter; (B) completely hydrogenated P(Bd-S) latexes, 80 nm in diameter; (C) and (D) partially hydrogenated P(Bd-S) latex, 230 and 240 nm, respectively, for LG (C) and HG (D) latexes.

the equimolar hydrogenation process (i.e., molar ratio of the $\text{H}_2\text{NNH}_2/\text{H}_2\text{O}_2$ redox system to residual double bond = 1/1). The redox system used for the hydrogenation could have generated radicals which induced the formation of crosslinks among residual double bonds in the P(Bd-S) latex particles.

4.4 Summary

From the results shown above, it can be concluded that in addition to other parameters, such as temperature, pH, and the addition rate of the hydrogen peroxide, the surface area density of copper ions at the latex particle surface is a key factor which influences the optimum conditions for hydrogenation. The optimum surface area density is estimated as $2 \text{ Cu}^{2+}/1000 \text{ nm}^2$. The hydrogenation reaction does occur radially from the particle surface inward. The gel fraction in the latex particles does not influence the diffusion of diimide molecules very much, but greatly influences the mobility of polymer chains within the particles. Therefore, the LG latex system fits the uniform model describing the hydrogenation reaction, while the HG latex is closer to the layer model. The hydrogenation zone (thickness) from the particle surface inward where diimide molecules can diffuse before disproportionation reactions occur among themselves is about 20 nm.

References:

1. Wicklatz, J., in *Chemical Reactions of Polymers*, E. M. Fettes. ed. Wiley-Interscience, New York, Chapt. 2F, 1964.
2. Krause, R.L., (to Dow Chem. Co.) *U. S. Pat.* 3,898,206 (1975).
3. Inomata, J., Michijima, S., Kasahara, K., Hino, S., Igarashi, S., Takamiya, N and Tano, T., (to Mitsubishi Chem. Co.) *Jpn, Kokai Tokkyo Koho, JP* 76,661,593 (1976).
4. Camberlin, Y., Gole, J., Pascault, J.P., Durand, J.P. and Dawans, F., *Makromol. Chem.*, **180**, 2309 (1979).
5. Schulz, D.N., Turner, S.B. and Golub, M.A., *Rubber Chem. Technol.* **55**, 809 (1982).
6. Harwood, H.J., Russell, D.B., Verthe J.J. and Zymous.J., *Makromol. Chem.* **163**, 1 (1973).
7. Sanui, K., Macknight, W.J. and Lenz, R.W., *J. Polym. Sci, Polym. Lett. Ed.* **11**, 427 (1973).
8. Wideman, L.G., (to The Goodyear Tire & Rubber Company) *U. S. Pat.* 4,452,950 (1984).
9. Parker, D.K. and Roberts, R.F, *Rubber Chemistry & Techn.* **65**, 245 (1992).
10. Van, E., Dewey, R., Lease, M and Pirkle, W., *J. Am, Chem Soc.*, **83**, 4302 (1961).
11. Corey, E., Mock, W. and Pasto, D., *J. Am, Chem Soc.*, **83**, 347 (1961).
12. Hüller, S. and Their, W., *Angew. Chem. intern. Ed. Engl.*, **4**, 271 (1965).

13. Parker, D.K., personal communication.
14. Halasa, A.F., *Rubber Chem. Technol.* **154**, 627 (1981).
15. Riess, G., *Makromol, Chem. Angew*, **60/61**, 21 (1977)
16. Chapter 3.
17. Garbisch, E.W., Schildcrout, Jr. S.M., Patterson, D.B. and Sprechen, C.M., *J. Am. Chem. Soc.*, **87**, 2932(1965).
18. Ast, W., Zott C. and Kerber, R., *Makromol. Chem.*, **180**, 315(1979).
19. Hunig, S., Muller, H.R and Their, W., *Angew. Chem. Intern. Ed. Engl.*, **4**, 271(1965).
20. Miller, C.E., *J. Chem. Ed.*, **42**, 254(1965).

Chapter 5

Study of the Consumption of TMI in Latex

Using Attenuated Total Reflectance FTIR (ATR-FTIR)

Abstract: Attenuated Total Reflectance-Fourier Transform Infra-Red (ATR-FTIR) spectroscopy was used to study the mechanism for consumption of isocyanate groups from dimethyl meta-isopropenyl benzyl isocyanate (TMI[®]) monomer. A series of polystyrene/poly(butyl acrylate-TMI) [PS/P(BA-TMI)] core/shell structured latexes with different core/shell ratios were prepared by seeded emulsion polymerization techniques. These latexes were air-dried on ATR-FTIR Germanium (Ge) discs while the FTIR spectra were taken during the film formation process. The amounts of isocyanate moieties which were reacted during polymerization and the film formation process were determined quantitatively using the FTIR data combined with titration calibration of the isocyanate groups. The thickness of the shell in which the TMI monomer was incorporated was found to be very important in determining the extent of consumption (hydrolysis) of the isocyanate groups during either polymerization or film formation.

5.1 Introduction

Among a number of functional monomers that can undergo crosslinking reactions during the latex film formation process, the dimethyl meta-isopropenyl benzyl isocyanate (TMI®; Cytec Industries) monomer is of considerable commercial interest. The two reactive moieties in the TMI monomer, i.e., via the vinyl double bond and the aliphatic isocyanate group, can be reacted independently, i.e., copolymerization with other vinyl monomers through the vinyl group or reaction of the isocyanate groups with some active hydrogen-containing compounds^{1,2}. An unusual property of the TMI monomer is its ability to undergo emulsion copolymerization in an aqueous medium with only a small fraction of the isocyanate groups being hydrolyzed. The isocyanate moieties which remain inside the latex particles (or on the particle surfaces) could then undergo crosslinking reactions during the film formation process. Obviously, it is very important to quantify the fractions of isocyanate groups reacted during polymerization and film formation. Any premature crosslinking of the isocyanate groups inside the latex particles during the emulsion polymerization process would hinder the molecular interdiffusion of polymer chains during the film formation process^{3,4} and would usually degrade the mechanical properties of the latex film. On the other hand, the reactions of the isocyanate groups during the film formation process, especially during the cohesive strength development stage, would tend to form interfacial crosslinks between adjacent latex particles, which could greatly enhance the mechanical properties of the latex film⁵⁻⁸.

The ATR-FTIR spectroscopy technique has been successfully applied to the study of polyurethane foam systems by monitoring isocyanate absorption near 2250 cm⁻¹

wavenumber^{9,12}. ATR techniques have also been used to study surfactant migration behavior during latex film formation¹³, and determining suspended material in polymer latexes¹⁴.

The amount of isocyanate groups remaining in a latex film has been determined by FTIR in our laboratory for some time¹⁵. However, since the FTIR spectra were determined on latex film samples, the information obtained described the amount of isocyanate groups remaining in the final latex film. It has been hard to distinguish the consumption of the isocyanate groups in latex particles themselves and in the latex film. The ATR technique is a rather new tool for monitoring the consumption of the isocyanate groups during the entire latex film formation process.

In the present work, we report studies which show that ATR-FTIR spectroscopy is an appropriate method for studying the latex film formation process. A series of polystyrene/poly(n-butyl acrylate-TMI) [PS/P(BA-TMI)] core/shell structured latexes with different core/shell ratios were prepared by seeded emulsion polymerization techniques. The freshly prepared latexes were cast on a Germanium (Ge) ATR-FTIR disc while the FTIR spectra were taken during the entire film formation process. A decreased pattern of water absorption clearly showed the different stages of film formation. Combined with titration calibration of the isocyanate groups, the amount of isocyanate moieties in the latex particles before film formation occurred, which could reflect the consumption of the isocyanate groups during the emulsion polymerization process, and the amount consumed after the final stage of film formation, i.e., the cohesive strength development stage, were determined quantitatively.

5.2 Experimental

5.2.1 Materials

n-Butyl acrylate (BA) monomer (Fisher Scientific) was treated by passing it through an inhibitor-removal column. TMI[®] monomer (Cytec Industries) was used as received. Ammonium persulfate (APS) and potassium metabisulfite (PMBS), all analytical grade (Fisher Scientific), and sodium dihexyl sulfosuccinate surfactant (Aerosol MA 80; Cytec Industries) were used as received. Polystyrene (PS) seed latex (LS-1039-E, Dow Chemicals; particle size = 93 nm, PDI = 1.004) was used as received. Distilled-deionized (DDI) water was used in all polymerizations.

5.2.2 Emulsion Polymerization

Emulsion polymerizations of BA and TMI were carried out in a four-neck 250 ml flask at 40 °C, according to the recipes shown in Table 5-1. Runs 1 to 3 were carried out in the presence of PS seed latex, while Run 4 was conducted without PS seed latex. In Run 4, 10 % of the total monomers and initiator, all of the surfactant, and 80% of the DDI water were initially charged in the flask and allowed to react for 1 hr. A semi-continuous process was utilized for the addition of the second-stage monomers and initiator for Runs 1 to 3, and the remaining monomers and initiator for Run 4, at a constant rate of 0.028 ml/min using a syringe pump.

Table 5-1. Emulsion Polymerization Recipes Used to Prepare Latex Samples Used in the ATR-FTIR Film Formation Study

Component (g)	Run 1	Run 2	Run 3	Run 4
Polystyrene Seed [†]	50.0	50.0	50.0	---
n-Butyl acrylate	5.0	10.0	20.0	20.0
TMI [®]	0.15	0.3	0.6	0.6
Ammonium persulfate	0.06	0.12	0.24	0.24
Potassium metabisulfite	0.06	0.12	0.24	0.24
Aerosol MA 80 [‡]	---	---	---	0.80
Distilled-deionized (DDI) water	10.0	20.0	40.0	80.0

[†] 20 % solids content; particle size = 93 nm, PDI = 1.004.

[‡] Sodium dihexyl sulfosuccinate, 78-80 % solution in a mixture of isopropanol and water.

5.2.3 ATR-FTIR Spectroscopy

The IR spectra were obtained on a React IR-2000 Fourier transform spectrometer (Applied System Inc.), by averaging 64 scans with a resolution of 4 cm^{-1} . One spectrum was recorded every 30 min during the entire latex film formation process over a 24 hr period.

5.2.4 Titration of Isocyanate Groups in P(BA-TMI)

A series of P(BA-TMI) latexes were prepared following the same procedure described for Run 4 of Table 5-1. The concentrations of TMI monomer used in the copolymers varied from 0.4 to 3.2 wt% of the total copolymer. Latex films were cast at room temperature, dried for four days, and then dried in a vacuum oven for 24 hr. The titration was carried out as follows: (1) approximately 8.0 g of latex film samples were dissolved in 150 ml THF and mixed with tumbling for 48 h; (2) solutions were filtered to remove large insoluble gels (for systems with high TMI contents); (3) the solids contents for each filtered solution sample was determined gravimetrically; 100.00 g of each solution was then transferred to an Erlenmeyer flask; (4) appropriate amounts of dibutylamine (DBA) (0.05N in THF) were added into each solution and stirred for 3 min before each titration; three drops of bromothymol blue indicator were added and the solution exhibited a light blue color; (5) 40 ml isopropanol was added into the solution to ensure the solubility of HCl in the system; (6) the solution was titrated with HCl (0.02N); some additional isopropanol was added when the system exhibited any cloudiness; an end point was shown by the sharp transition of the light blue to light yellow

color when the titration was completed. In step (4), to make the final amount of HCl (0.02N) consumed during the titration to be around 10 to 20 ml, the amount of DBA used should be about 0.2 to 0.4 mMoles in excess, which corresponded to the amount of isocyanate from the recipe in each solution sample.

5.3 Results and Discussions

A schematic representation of the ATR-FTIR is shown in Figure 5-1. The latex sample is deposited on the Germanium (Ge) disc, the IR beam undergoes a series of total reflections at the Ge/sample interface, which would then pass to the detector. The depth that the IR beam can probe into the sample is about 100 nm. In other words, the thickness of the sample detected by the IR beam would be fixed and would remain close to the Ge/sample interface. Since the IR spectrum was recorded during the whole film formation process, the change in the concentration for each functional group in the system can be followed.

Figure 5-2 shows typical ATR-FTIR spectra obtained during a 24 h period of time in which a film is being formed from a PS/P(BA-TMI) core/shell (1/1, w/w) latex system. An individual IR spectrum was determined every 30 min. Three peaks of interest at wavenumbers of 1640, 1750 and 2259 cm^{-1} represent water, carbonyl (-CO-), and isocyanate (-NCO) groups, respectively. From this series of spectra, profiles of the absorbance with time for each of these three peaks can be plotted.

Figure 5-3 shows the profiles for these three peaks for this specific system. At the beginning of the film formation process ($t = 0$), the high absorbance intensity of water reflects

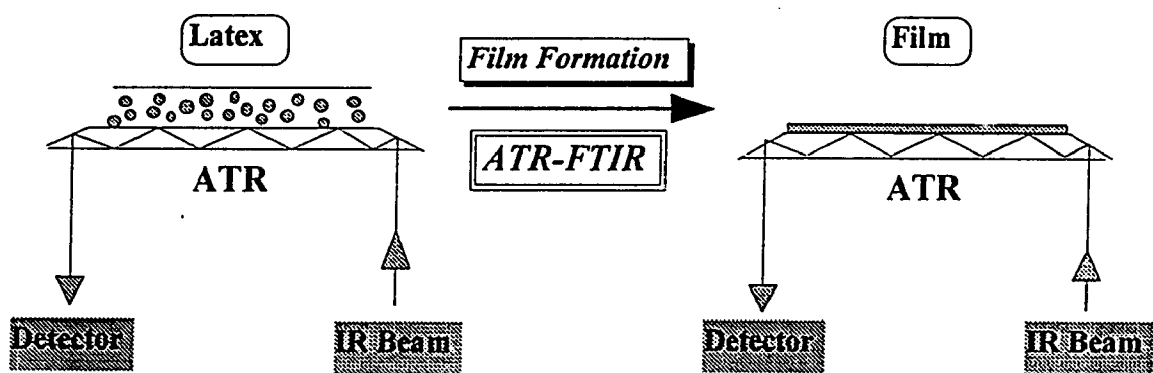


Figure 5-1: A schematic illustration for attenuated total reflectance FTIR (ATR-FTIR) for the *in situ* study of the latex film formation process.

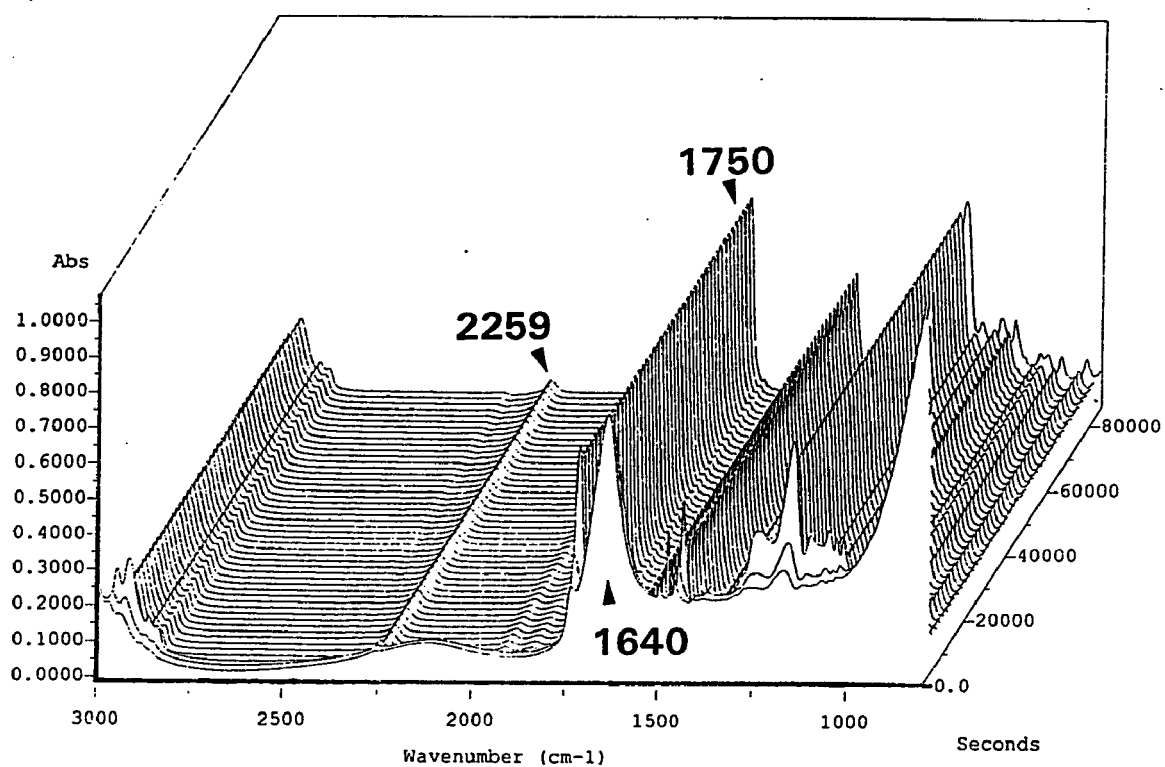


Figure 5-2: Time-dependent ATR-FTIR spectra recorded during the film formation process for 1/1 (w/w) PS/P(BA-TMI) core/shell latex over a 24 h period.

the high concentration of water in the polymer dispersion, while both organic peaks (-CO- and -NCO) exhibit relatively low absorbance values due to their low concentration at this stage. With the evaporation of water from the latex during film formation, the absorbance for the water peak decreases rapidly to a minimum value, while the absorbances for both organic peaks increase to their respective maximum values. The film formation process could be roughly divided into two stages by monitoring the different decreasing rates of water absorbance during the drying process. The rapid decrease in water peak absorbance in the first stage of film formation from time 0 to 60 min, indicates that water, as the continuous phase of the system, evaporates quickly. When the latex system becomes highly concentrated and massive coalescence is occurring among latex particles, the continuous phase changes from a water phase to a polymer phase. At the same time, the absorbance for the carbonyl (-CO-) groups, which should not be consumed by any reaction during the film formation process, reaches its maximum absorbance value, and remains at this value thereafter. Thus, it is reasonable to define this time as the point at which an extremely concentrated latex changes into a latex film. In other words, the maximum absorbance of the carbonyl group could be used to represent the carbonyl concentration in the latex right before the formation of the latex film. The absorbance for the isocyanate group, on the other hand, reaches its maximum value at the same time (about 60 min) as the carbonyl group, decreases rapidly in a short time period, and then decreases gradually thereafter. This decrease suggests that the isocyanate moieties are consumed by chemical reactions, i.e., hydrolysis and addition reactions between the isocyanate groups and newly formed amine groups from the hydrolysis, during this stage. By setting up the analysis method shown above, the relative consumption of the isocyanate

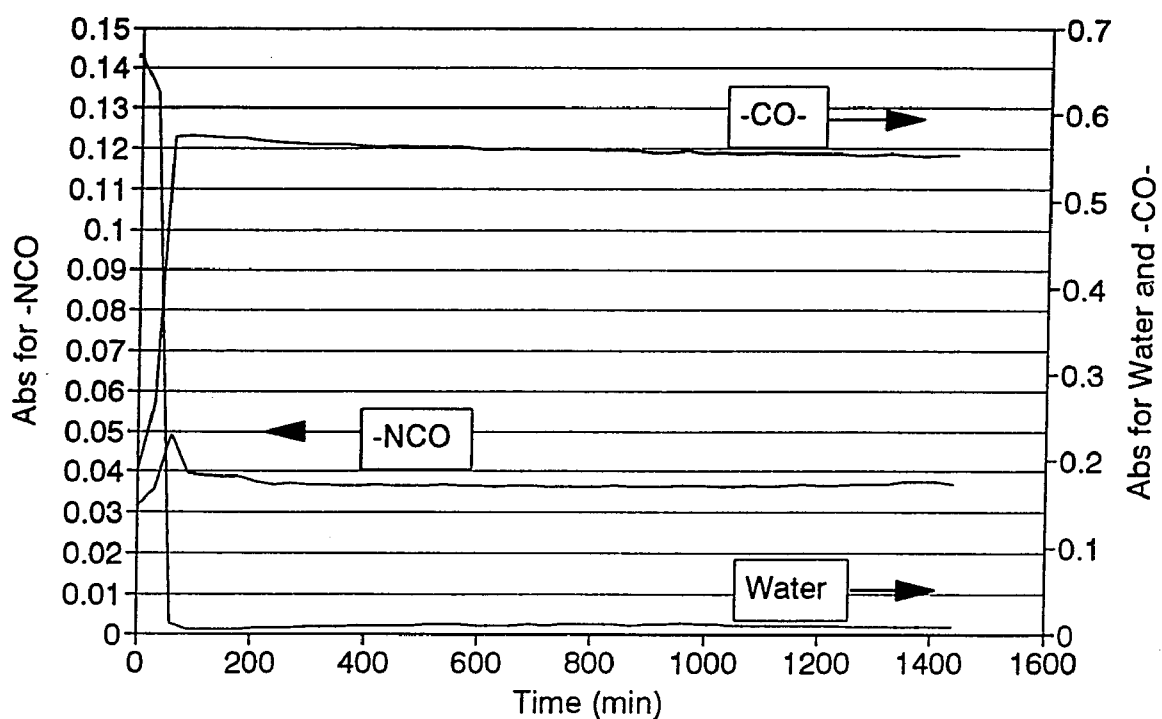


Figure 5-3: Profiles for the intensities of water, carbonyl (-CO-) and isocyanate (-NCO) functional groups at wavenumbers of 1640, 1750, and 2259 cm^{-1} , respectively, from ATR-FTIR measurements during a 24h film formation process.

groups during the film formation process can be monitored. However, to understand quantitatively the consumption mechanism for the isocyanate groups during both the polymerization and film formation processes, a calibration between the ATR-FTIR absorbance and absolute concentration of isocyanate groups is needed.

Figure 5-4 shows the ATR-FTIR absorbance calibration curve and the absolute concentration of isocyanate groups as obtained by titration. A well-fitted linear calibration relationship was obtained.

To investigate the influence of the structure of the latex particles on the consumption of isocyanate groups during the polymerization and film formation process, a series of latexes with shells of varying thickness (in which isocyanate groups were incorporated) were prepared according to recipes shown in Runs 1 to 3 in Table 5-1. To avoid the formation of any core/shell interphase zone and obtain a relatively sharp core/shell interface, a polystyrene seed latex with a narrowly distributed particle diameter of 93 nm ($PDI = 1.004$) was used to carry out the second stage polymerization of BA/TMI (97.1/2.9, w/w). In this way, the theoretical shell thickness could be controlled and calculated in various PS/P(BA-TMI) latexes with different core/shell ratios. A P(BA-TMI) latex (Run 4 of Table 5-1) with a particle diameter of 180 nm was also used to represent the largest “shell” thickness of 90 nm (= particle radius). Figure 5-5 shows the results. The calculated shell thickness for the PS/P(BA-TMI) latexes with core/shell ratios of 1/2, 1/1, and 1/0.5 (w/w) are 20, 12, and 7 nm, respectively.

The percentages of NCO groups remaining at the maximum of each curve were obtained from values determined by the calibration curve shown in Figure 5-4 divided by the

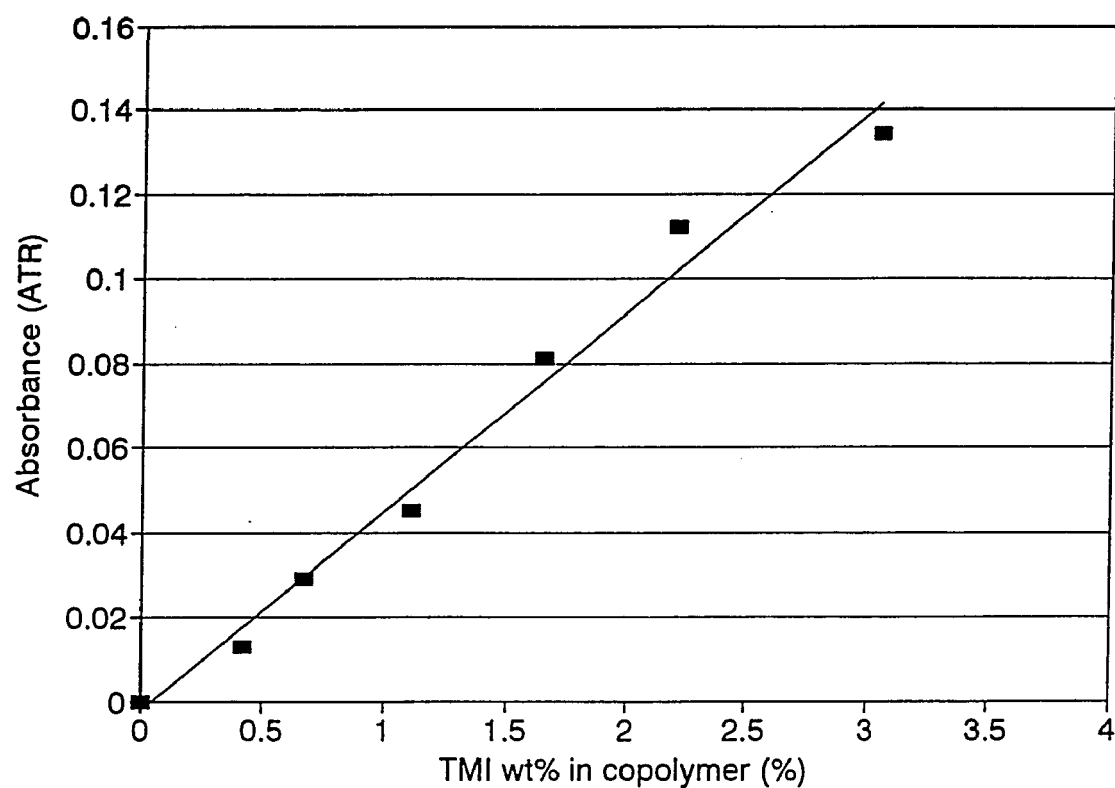


Figure 5-4: ATR-FTIR absorbance calibration curve for the isocyanate groups in P(BA-TMI) copolymer and its corresponding weight concentration as determined by titration.

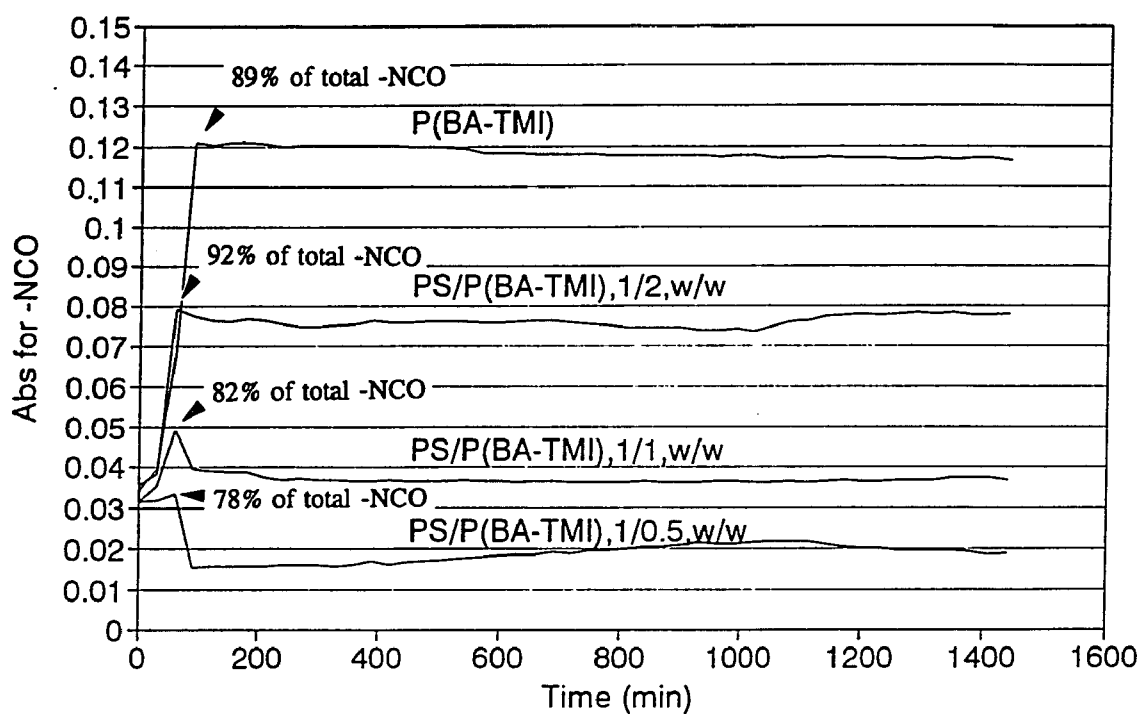


Figure 5-5: ATR-FTIR absorbance profiles of the isocyanate group in P(BA-TMI) (180 nm) latex and a series of PS/P(BA-TMI) core/shell latexes with shell thicknesses of 20, 12, and 7 nm obtained during a 24 h film formation process.

total amount of TMI which was initially added. First of all, from the percentage values shown at the maximum points for each curve, it is seen that the isocyanate groups present in the latex did undergo some degree of hydrolysis before the latex films were formed. Since these experiments were carried out a short time (less than one day) after the latexes were prepared, these values should indicate the percentage of isocyanate moieties remaining right after the emulsion polymerization was complete. Obvious differences in these values were seen for each system. It seems that the larger the domain size or the shell thickness in which the isocyanate moieties are incorporated, the lower the percentage of the isocyanate groups which were hydrolyzed, and the greater number of isocyanate groups which remained in the latex particles after the polymerization. The hydrolysis percentage of the isocyanate groups after an emulsion polymerization is also dependant on some other polymerization parameters, such as temperature, pH value and the mode of addition of the monomers, i.e., batch or semi-continuous. It has been found that the average percentage of hydrolysis of isocyanate groups from the TMI monomer after a 10 h batch emulsion polymerization of BA/TMI (3 wt% TMI) at 40 °C is around 5%. The reaction rate (K) of the isocyanate groups during the emulsion polymerization can be estimated as $1.3 \times 10^{-5} \text{ M}^{-1} \text{ sec}^{-1}$, with the assumption that the equilibrium concentration of water in the polymer latex particle is around 0.2 wt% (0.11 M).

Compared to the percentage of hydrolysis (5%) after a batch emulsion polymerizations, greater degree of hydrolysis were found after emulsion polymerizations using semi-continuous mode of addition of monomers, as shown in Figure 5-5. In a batch polymerization system, due to the hydrophobicity and the relative high reactive rate (compared to BA monomer) of the TMI monomer, isocyanate moieties from the TMI units

would tend to more likely be distributed more likely in the inner side of the monomer-swollen polymer particles throughout the process of batch emulsion polymerization. On the other hand, during an emulsion polymerization using a semi-continuous mode of addition of monomers under monomer-starved conditions, the TMI units distribute uniformly in the latex particle and have longer time to expose to the particle/water interfaces where the water concentration is much higher than the inner side of the latex particle. The dependence of the extent of hydrolysis on the shell thickness indicates that the isocyanate moieties in a "thick shell" would tend to stay far from the highly polar particle/water interface due to the relatively high hydrophobicity of the TMI unit, which could decrease the chance of exposure to water. In contrast, in a "thin shell", there is not much space for the isocyanate groups to stay away from the interface, and as a result, a greater degree of hydrolysis of the isocyanate groups would take place. However, despite the lower percentage values of hydrolysis for the case of the thicker shell system, i.e., 1/2 core/shell ratio, the absolute amount of isocyanate groups which is hydrolyzed is still greater than that found for the thin shell system, i.e., 1/0.5 core/shell ratio, due to the larger amount of the total isocyanate groups. This is understandable because the thick shell had to grow gradually. During this shell growth process, more hydrolysis occurred at the beginning stages when the shell was still thin. A decreasing amount of hydrolysis would take place as the shell become thicker.

After the maximum absorbance values for each curve shown in Figure 5-5 were attained, latex systems entered the film stage where polymer started to become the continuous phase. In this stage, although the bulky water phase has disappeared, large numbers of water molecules are still present in the film and are most likely present in the interfaces of the

coalesced particles where surfactant molecules are localized. These water molecules would undergo diffusion in the latex film. This diffusion is restricted by the high viscosity of the polymer phase and the high polarity of surfactant, which should have a low tendency to diffuse. For this reason, if an isocyanate moiety is present at this interface, it would have much longer period of time to contact with water molecules since the mobilities for both of these species are relatively low. It is noted that relatively large amounts of isocyanate groups consumed in a short period of time (~ 60 min) after the maxima of the curves for both of the “thin shell” latexes. The absorbances of isocyanate groups for PS/P(BA-TMI) latexes with core/shell ratios of 1/1 and 1/0.5 decreased 20% and 50%, respectively. The obvious higher reaction rates (compared with the rate during the emulsion polymerization) indicate that the water concentration in the interface regions between those coalesced particles is considerably high during this short time period, i.e., the beginning of the second stage of latex film formation. Taking the latex system with the PS/P(BA-TMI) ratio of 1/1 as an example, the 20% decrease in isocyanate groups (i.e., absorbance of -NCO reduced from 0.05 to 0.04) can be assumed to be resulted from the reactions of those isocyanate moieties that distribute in a surface layer of the particle which takes up 20% of the entire volume of the shell. It can be easily calculated that the thickness of the surface layer is about 2 nm. Since the thickness of this “high water zone” is independent on particle size or shell thickness, the same 2 nm layer would take higher volume fraction for a “thin shell” than a “thick shell”, and results in higher percentage of hydrolysis at this stage of the film formation. Since the hydrolysis at this stage occurs primarily at the interfaces of the latex particles, interfacial crosslinks would be formed via crosslinking reactions between isocyanate groups and amine groups resulted from those

hydrolysis reactions. For the same reason, if the isocyanate moieties are not close to these layers, which is the cases for the non-structured latex particles with large particle size or “thick shell” particles, hydrolysis and interfacial crosslinking could not occur in a short time. Obvious differences are observed for each system shown in Figure 5-5. For the P(BA-TMI) latex system, the amount of isocyanate groups decreased only slightly when the film was formed. For the other three core/shell latex systems, the percentages of isocyanate groups hydrolyzed after the film formation, based on the amounts showed at the maximum absorbance values, are about 5%, 20% and 50% for 20 nm, 12 nm and 7 nm shell thickness, respectively.

5.4 Summary

In summary, the consumption of isocyanate groups could occur either during polymerization and/or the film formation process. In most of the systems studied, the percentage of isocyanate groups consumed during the polymerization stage is less than 5% for batch emulsion polymerization, and about 10 to 20%, depending on the particle size or the shell thickness in which the isocyanate groups are incorporated, for semi-continuous emulsion polymerizations under monomer starved conditions. During the process of film formation, higher percentage of isocyanate moieties could be consumed for a thin shell layer latex system, some of which form interfacial crosslinks. When the particle size is larger than 60 nm, or the shell layer is thicker than 30 nm, interfacial crosslinking from the reactions of isocyanate groups would not take place in a short period of time.

References

1. Dexter, R. W., Saxon, R., and Fiori, R. E., *J. Coatings Technol.*, **58**, 43 (1986).
2. TMI Unsaturated Aliphatic Isocyanate Products Bulletin, American Cyanamid Co.
3. Hahn, K., Ley, G., Schuler, H., and Oberthur, R., *Colloid Polym. Sci.*, **266**, 631 (1988).
4. Zosel, A., and Ley, G., *Macromolecules*, **26**, 2222 (1993).
5. Yeliseeva, V. I., *Br. Polym. J.*, **7**, 33 (1975).
6. Okubo, M., Yamaguchi, S., and Matsumoto, T., *J. Appl. Polym. Sci.*, **31**, 1075 (1986).
7. Bufkin, B. G., and Grawe, J. R., *J. Coat. Technol.*, **52**, 73 (1980).
8. Bassett, D., Sherwin, W., and Hager, S., *J. Coat. Technol.*, **51**, 65 (1979).
9. Cole, K. C., and Van Cheluwe, P., *J. Appl. Polymer Sci.*, **34**, 395 (1987).
10. Carlson, G. M., Neag, C. M., Kuo, C., and Provder, T., *Adv. Urethane Sci. Technol.*, **9**, 47 (1984).
11. Margalit, E., Dodiuk, H., Kosower, E. M., and Katzir, A., *Surface and Interface Analysis*, **15**, 473 (1990).
12. Priester, R. D., McClusky, J. V., O'Neill, R. E., Turner, R. B., Horthcock, M. A., and Davis, B. L., *J. Cellular Plast.*, **26**, 346 (1990).
13. Thorstenson, T. A., Tebelius, L. K., Urban, M. W., *Pro. American, Chem. Soc. Div., Polym. Mat.*, Denver, Co., USA (1993).
14. Tickanen, L. D., Tejedor-Tejedor, M. I., and Anderson, M. A., *Langmuir*, **7**, 451 (1991).
15. Inaba Y., Daniels, E. S., and El-Aasser, M. S., *J. Coat. Technol.*, **66**, 63 (1994).

Chapter 6

ELASTOMERIC FILMS FROM STRUCTURED LATEXES

Abstract: A model structured latex that is capable of forming a self-curable elastomeric film under mild temperature conditions was developed. In this model latex system, a small amount of dimethyl meta-isopropenyl benzyl isocyanate (TMI[®]) was copolymerized with n-butyl acrylate (BA) onto poly(butadiene-*co*-styrene) (P(Bd-S)) seed latex particles. In the final stage of the film formation process, the latex particles coalesce with each other, and interdiffusion of PBA-based polymer chains in the shell layers of adjacent structured particles occurs. At this stage, the isocyanate groups in the P(BA-TMI) shell layer would begin to crosslink by either a moisture-cure reaction via trace amounts of water remaining in the latex film or by a post-added crosslinker that contains amine groups. Improved elastomeric properties of the latex film are expected from this kind of "interphase" crosslinking structure.

However, latex films prepared from the model P(Bd-S)/P(BA-TMI) core/shell latexes were cracked and brittle which was explained by the formation of a highly crosslinked/grafted core/shell interphase zone, as discussed in Chapter 3. Saturation of the residual double bonds in the P(Bd-S) seed latex particles by hydrogenation was found to

be an effective way to reduce the development of the interphase zone and the degree of crosslinking during the second-stage polymerization. An elastomeric film with satisfactory mechanical and anti-aging properties was formed from this hydrogenated-P(Bd-S)/P(BA-TMI) structured latex.

6.1 Introduction

The applications for film-forming latexes are of great interest in industry. The mechanism of film formation from latexes has been studied extensively¹⁻⁴. A great deal of attention has been focused on the final stage of the film formation process, i.e., the development of cohesive strength in the film. In this stage, latex particles begin to coalesce with each other through either molecular interdiffusion^{3,5,6} or interfacial crosslinking⁷⁻¹³ (if appropriate crosslinking groups are available), or both. The molecular interdiffusion of polymer chains between adjacent latex particles has been shown to be of critical importance to the development of the final mechanical properties of latex polymer films. However, the extent of the polymer chain interdiffusion greatly depends on the mobility of the polymer chains, i.e., the rigidity of the polymer chains themselves, their molecular weight, the degree of crosslinking and the conditions of film formation, such as temperature and the presence of external additives. For example, a relatively high degree of crosslinking of the polymer chains inside the latex particle, e.g., rubber particles, would greatly hinder interdiffusion between adjacent particles¹⁴. Interfacial crosslinking, as compared with molecular interdiffusion, can be a more effective method to strengthen the latex film, and at the same time allows for more process control by varying the type, concentration, and the distribution of the crosslinkable functional groups within the latex particles. With the increasing demand for aqueous-based latex polymer systems in such applications as paints, coatings, and elastomers, interfacially crosslinkable latex films are

of great commercial interest.

One of the most extensively employed methods to attain interfacial crosslinking is to modify the latex particles by incorporating a small amount of functional groups via copolymerization into the latex particles. These functional groups are capable of associating with one another through ionic, hydrogen, or covalent bond mechanisms. It has been demonstrated by numerous studies^{11,12,15,16} that a high concentration of functional groups in the particle surface layer is a key parameter to attain interfacial crosslinking. It is relatively easy to concentrate hydrophilic functional groups at the particle surfaces via emulsion polymerization. A typical functional group which is capable of ionic or hydrogen bonding is the carboxyl moiety, which can be incorporated into the particle structure by copolymerizing a small fraction of functional monomer, such as acrylic acid, methacrylic acid, or itaconic acid.⁶⁻⁸ In these cases, however, because of the presence of the highly hydrophilic carboxyl groups, the films formed from these latexes do not exhibit strong resistance to alkaline aqueous solutions, such as detergents.

Compared with ionic and hydrogen bonding interparticle associations, interfacial crosslinking through covalent bonding could greatly improve both the mechanical and environmental resistance properties of the latex film. Some of the commonly used functional monomers are N-methylolacrylamide (NMA), glycidyl methacrylate (GMA), and N-(isobutoxymethyl)acrylamide (IBMA).¹¹⁻¹³ The functional monomers are either self-condensable or may react with some other groups. The main disadvantage for these types of functional monomers is that a relatively high temperature thermal curing period (usually higher than 100 °C and longer than 20 min) is required, which is energy-intensive, and

may not be feasible in many applications, such as architectural paints.

The synthesis of interfacially crosslinkable latex films under mild curing conditions has been of great interest. One example for this type of latex is an isopropenyloxazoline-based copolymer latex¹⁷ developed by Dow Chemical Company. Oxazoline groups are readily reacted with acid groups at room temperature. By blending latexes containing oxazoline groups with carboxylated latexes, an interfacially crosslinked latex film could be formed at room temperature. However, since two types of latexes are utilized in this blending/curing process, i.e., a so-called “two-pot” system, and crosslinking can only occur between different types of latex particles, it would be difficult to achieve uniform interfacial crosslinking.

In order to develop a “one-pot” low-temperature self-curable latex film, a model structured latex was developed in this study. In a core/shell structured latex particle, the crosslinkable functional groups are effectively distributed in the shell layer via the core/shell polymer phase separation. This approach is specially significant for those highly hydrophobic functional monomers which tend to be distributed throughout the latex particle. As shown in Figure 6-1, two types of crosslinkable functional groups (I and II) are separately distributed in the inner side of the shell and the outer surface of the core/shell particle. Functional group I can be incorporated in the shell layer by copolymerizing functional monomer with a second stage monomer. A surfactant which contains multiple hydrophilic functional groups (II) such as carboxyl, hydroxyl, or amine groups, is post-added. This surfactant (which acts in the role of a crosslinking agent) would then tend to adsorb onto the particle surfaces with their functional groups facing

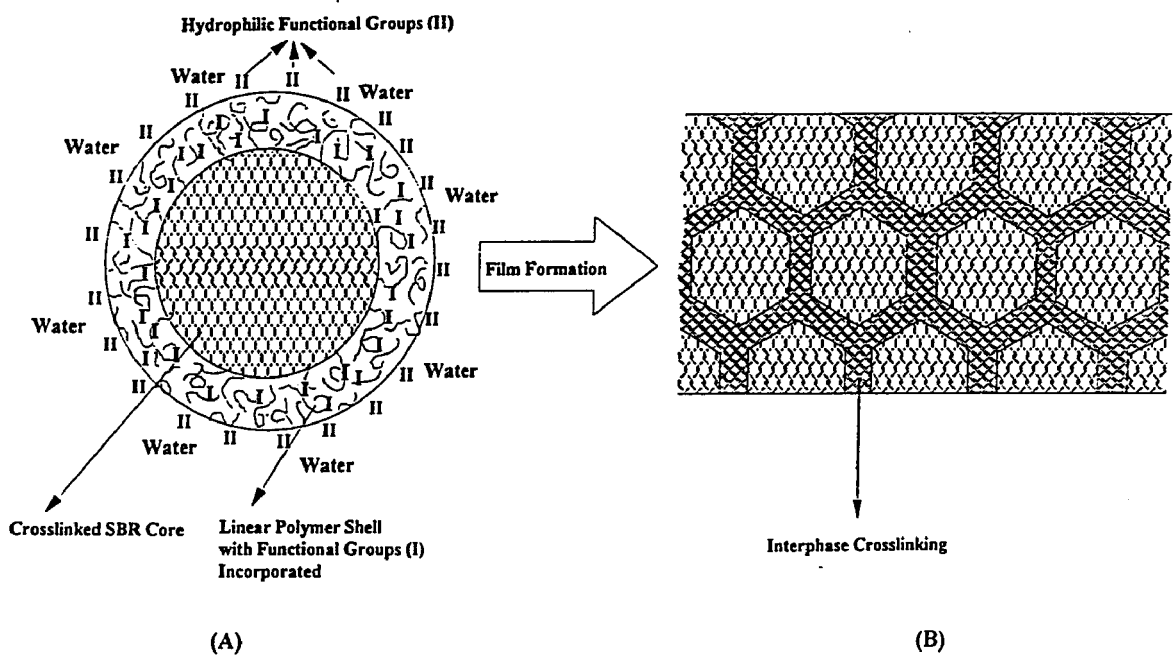


Figure 6-1: Schematic representation of : (A) the structured latex particle; and (B) the elastomeric film formed from the particles.

towards the water phase due to their hydrophilicity. In this way, through the control of the addition sequence, and the large difference in the hydrophilicity (or hydrophobicity) of the two types of functional groups, these I and II functional groups are separated from one another in the shell layer of the structured particles as long as the particles remain surrounded by a water medium, as shown in Figure 6-1(A). In the final stage of the film formation process, water, as the bulk phase, disappears, and the latex particles start to interact by coalescing with each other. The two types of functional groups would then approach one another and react via molecular interdiffusion, as shown in Figure 6-1(B). By controlling the distribution of functional groups, an “interphase” crosslinked network separating the core particles could be formed.

To the best of our knowledge, most of the polymers used to prepare core/shell structured latexes for the production of elastomers have been acrylic polymers. Considering the excellent elastomeric properties of polybutadiene (PBd)-based materials, and more important, from the economic point of view (i.e., the price of butadiene is about one-ninth of that for most of the acrylic monomers), it is very meaningful to modify PBd-based latexes to develop high performance elastomeric materials.

Poly(butadiene-*co*-styrene) [P(Bd-S)] (known as SBR for certain copolymer compositions) is a widely used elastomer. The most widely applied method to process P(Bd-S) is through a coagulation-vulcanization process, where the crosslinking process for the P(Bd-S) polymer has to be carried out during or after the shaping of the coagulated P(Bd-S) crumb. This procedure requires a very low degree of crosslinking of the original P(Bd-S) latex before the coagulation, and the vulcanization temperature is usually higher

than 150 °C¹⁸. These kinds of conditions are not suitable when P(Bd-S) is processed as an elastomeric film formed by direct casting of the latex under mild temperature conditions. In these applications, a certain degree of pre-crosslinking in the latex particles is required to form an elastomeric film. Nevertheless, crosslinking inside the latex particles would hinder the interdiffusion of polymer chains between adjacent particles during film formation¹⁴. Actually, an elastomeric film cannot be formed by simply casting the P(Bd-S) latex which is highly crosslinked. Through the modification of the pre-crosslinked P(Bd-S) latex particles by using another linear or lightly crosslinked rubbery polymer to form a core/shell latex particle by utilizing the model structured latex particle approach, the properties of the latex film might be improved. However, an unavoidable problem that occurs when a PBd-based seed latex is used is that the large number of residual double bonds in the P(Bd-S) seed particles are highly active to radical reactions, and are able to continue reacting among themselves, and with the second stage monomers during second stage polymerization. In Chapter 3, the authors reported that the composite latex particles became greatly hardened from the development of a highly crosslinked/grafted core/shell interphase zone in a P(Bd-S)/PBA latex system. Very little fusion of these particles occurred during the film formation process in air at either room temperature or elevated temperature (e.g., 70 °C), and the resulting films were cracked and brittle, although both types of the polymers were originally soft (i.e., possessed low glass transition temperature).

Saturation of the residual double bonds in P(Bd-S) seed latex particles by hydrogenation^{19,20} has been found to be an effective way to reduce the formation of the

interphase zone, and at the same time reduce the effect of aging (i.e., oxidation of residual double bonds) that usually deteriorates PBd-based polymer materials. Elastomeric films were produced from modified hydrogenated P(Bd-S) [H-P(Bd-S)] latex using the model structured particle concept.

6.2 Model Structured Latexes Used for the Study

A small amount of dimethyl meta-isopropenyl benzyl isocyanate (TMI[®], Cytec Industries) was copolymerized with n-butyl acrylate (BA) onto poly(butadiene-*co*-styrene) [P(Bd-S)] seed latex particles to prepare the model structured latexes. Since the isocyanate groups from the TMI monomer are relatively stable to hydrolysis during emulsion polymerization²¹ under certain conditions, and because of the relatively high hydrophobicity of the TMI monomer unit, it is possible to control the loci of the isocyanate groups (functional group I) so that they are distributed in the interior portion of the PBA-based shell layer nearest to the core P(Bd-S) polymer. Several types of functional groups with active hydrogens can possibly be used as the second functional group. Generally, the order of the reactivity of these functional groups to the isocyanate group is: amine > hydroxide > carboxylate²². The amine group rapidly reacts with the isocyanate group, while some metal catalyst is usually needed for the other two types of functional groups. Surfactants or water-soluble polymers that contain such functional groups can be post-added as the surfactant (crosslinker). In Chapter 5, the crosslinking

mechanism of the structured latex particles containing isocyanate groups was studied using the ATR-FTIR technique. It was shown that most of the isocyanate groups, e.g., 80 to 90 % for some systems, will remain intact during the emulsion polymerization process and will become incorporated inside the latex particles. The shell thickness in which the isocyanate groups are incorporated was found to be an important parameter influencing the hydrolysis of the isocyanate groups during the polymerization and the film formation process. For this specific structured latex system, in the final stage of film formation, trace amounts of water molecules remaining in the latex film could effectively react with the isocyanate groups to form amines and hence, to cure the film through the isocyanate-amine reactions, i.e., a two-step water molecule-curing mechanism. The focus of this study is on the preparation of the structured latexes and the mechanical properties of the latex films formed through the moisture-curing mechanism.

6.3 Experimental

6.3.1 Materials

n-Butyl acrylate (BA) (Fisher Scientific) was treated by passing it through an inhibitor removal column, while dimethyl meta-isopropenyl benzyl isocyanate (TMI*, Cytec Industries) was used as received. Ammonium persulfate (APS), and potassium metabisulfite (PMBS), both analytical grade (Fisher Scientific) were used as received.

Three kinds of hydrogenated P(Bd-St) latexes were used; H-P(Bd-S)-1 and H-P(Bd-S)-2 were prepared by hydrogenating P(Bd-S)-S prepared in this laboratory, while Chemisat HSBR LPH-7382X (abbreviated as HSBR hereafter) was kindly supplied by The Goodyear Tire & Rubber Company.

6.3.2 Treatments of Hydrogenated P(Bd-S) Seed Latexes

Both non-hydrogenated and hydrogenated P(Bd-S) [H-P(Bd-S)] latexes were used as seeds in the second stage polymerization. The particle sizes, gel fractions, and degrees of hydrogenation of these latexes are listed in Table 6-1. The preparation, hydrogenation of P(Bd-S)-S latex, and characterization of these latexes were described in Chapter 3 and 4.

After the hydrogenation of P(Bd-S) latexes using the hydrazine/hydrogen peroxide redox system was complete, a small amount of either hydrazine reductant or hydrogen peroxide oxidant, depending on the ratio of both components used for the hydrogenation, would still remain in the latex system. Since any trace amount of either component would greatly inhibit the second-stage polymerization employing a redox initiator system, excesses of hydrazine or hydrogen peroxide must be removed from the system. Usually, the hydrazine/hydrogen peroxide ratio used in the hydrogenation was controlled in such a way that a slight excess amount of hydrazine remained in the system after the hydrogenation was complete. The remaining hydrazine in the HSBR latex had been removed by treating with ozone gas. The method used in this lab to treat the H-P(Bd-St)

Table 6-1: Characteristics of Seed Latexes

	P(Bd-St)-S	H-P(Bd-St)-1	H-P(Bd-St)-2	LPH-7382
Particle size (nm)	80	80	80	50
Gel fraction before Hydrogenation (%) [†]	41	41	41	13
Gel fraction after Hydrogenation (%) [†]	---	53	60	52
Hydrogenation (%)	0	74	93	95

[†] measured by toluene extraction at 23 °C.

latexes is described as follows: (1) 5 ml of the latex sample was diluted to 20 ml with distilled-deionized water and a few drops of a 10% aqueous solution of CuSO_4 /Dowfax 2A-1 surfactant (1/10, w/w) was added; (2) ferrothiocyanate indicator was added to the system (ferrothiocyanate can detect hydrogen peroxide down to 0.001% which involves conversion of colorless ferrothiocyanate to red ferrithiocyanates); and (3) the diluted latex was titrated with hydrogen peroxide (50% solution) until reaching the equivalent point, at which point the color of the latex became red. The addition of the copper ion in step (1) can greatly increase the reaction rate between hydrazine and hydrogen peroxide to obtain a sharp equivalent point. Since iron and copper ions introduced into the system could influence the stability of the latex, Dowfax 2A-1 surfactant (sodium dodecylphenylether disulfonate, Dow Chemical) was used to stabilize the latex system during the titration process. The amount of hydrogen peroxide used right before the equivalent point is considered to be suitable to minimize the amount of hydrazine remaining in this latex. To further remove trace amounts of the remaining hydrazine, the latex was bubbled with air with stirring for 24 hour.

For the HSBR latex, although remaining hydrazine had been removed during the manufacturing process, some unknown additives, i.e., inhibitor and antioxidants, may possibly be present in this industrial latex sample. Very low conversions were obtained when using this latex directly as the seed latex in the second-stage polymerization, especially when redox initiator was used. To remove any polymerization retarding agents from the system, the HSBR latex was treated as follows before the second stage polymerization: (1) 0.5 g of the second stage BA monomer was added to the HSBR latex

and stirred for 8 h at 15 °C; (2) the temperature of the system was then raised to 80 °C and 0.1 g of potassium persulfate (KPS) was added; and (3) the system was kept at this temperature for 24 h.

6.3.3 Seeded Emulsion Polymerization

A series of second-stage emulsion polymerizations using different seed latexes were carried out at 40 °C with a redox initiator system according to the recipe shown in Table 6-2.

Two modes of addition of the second stage monomers to the seed latex particles were utilized: (1) an equilibrium-swelling process was used for Run 1 only, in which the monomer was allowed to swell the seed particles for 24 hours at room temperature before the seeded emulsion polymerization was started; and (2) a semi-continuous process for all of the other runs, in which 5 wt% of the monomer and the initiator were added at the beginning of the second stage polymerization, and the remaining monomer and initiator were added continuously to the reaction flask with a syringe pump at a constant rate of 0.028 ml/min.

6.3.4 Preparation of Latex Films

Latex films were cast on a clean glass plate and dried in an oven. The film formation temperatures used in this study were 25, 45, and 65 °C. The thickness of the

Table 6-2: Recipe for the Second-Stage Polymerization at 40 °C

Component	Wt (g)
Seed latex (20.0 % solids content) [†]	50
n-Butyl acrylate	10
Dimethyl meta-isopropenyl benzyl isocyanate (TMI [*])	None, 0.1 and 0.3
Redox initiator [‡]	0.15
DDI water	20

[†] Seed latexes used for Runs 1- 4 are P(Bd-S)-S, H-P(Bd-S)-1, H-P(Bd-S)-2, and LPH-7382, respectively. (see Table 6-1 for their characteristics).

[‡] Redox system: potassium metabisulfite (PMBS) and ammonium persulfate (APS) (Fisher Scientific), 1/1, w/w.

latex films used in this work ranged from 0.50 to 0.65 mm. The film was considered to be completely dried when its weight did not change appreciably (drying usually took 1-3 days depending on the oven temperature).

6.3.5 Gel Fraction, and Swelling Ratio Measurements

Gel fraction measurements were carried out using a solvent extraction technique, the details of which had been described in Chapter 3. Briefly, this method involves dissolving 0.2 g of latex film, which is cast at room temperature and dried under vacuum for ten hours, in 25 ml solvent, e.g., toluene or acetone, and mixing for 24 hours. The dissolved portion, i.e., the non-gel part, is determined gravimetrically from the amount of solids remaining in the supernatant after centrifugation of the swollen system at 5,000 rpm for 30 min. The gel fraction is the percentage of the insoluble polymer in the total film sample. The swelling ratio of a latex film was determined from the weight ratios of the film samples before and after a 24 h swelling process at room temperature.

6.3.6 Stress-Strain Mechanical Properties

The latex films were cut into dumbbell-shapes according to ASTM Standard D1708-84 and the tensile tests were carried out using an Instron Universal Testing Machine (Model-1011) with a crosshead speed of 25 mm/min.

6.4 Results and Discussions

To decrease the extent of hydrolysis of the isocyanate group in the TMI monomer during the second-stage polymerizations, the reactions were carried out at 40 °C using the redox initiator system. It was found that there were almost no isocyanate groups left after a polymerization at 70 °C.

Seeded emulsion polymerization was first carried out after the equilibrium-swelling process of the second stage monomers (Run 1, Table 6-2). The film formed from the resulting latex was severely cracked and brittle. Figure 2 shows the conversions of the of second-stage monomers and the increase in the gel fraction of the latex films formed from the latexes obtained at various conversions. The conversion of each monomer was measured by gas chromatography (GC). The TMI monomer exhibited a much higher conversion compared to n-BA, shortly after the reaction was started. After about 30 minutes, the conversion of TMI was 95 %, while the conversion for n-BA was only about 55%. As shown in Figure 6-2, the gel fraction increased soon after starting the reaction, and eventually reached 93%. This indicates the occurrence of grafting/crosslinking reactions during the P(Bd-S) seeded emulsion polymerization of the second stage monomers. In Chapter 3, the same tendency has been shown for a P(Bd-S)/BA seeded emulsion polymerization system without the presence of the TMI monomer. Similar results were obtained when a low gel fraction (2%) P(Bd-S) seed latex was used, i.e., the final gel fraction was still higher than 90%, and the latex film was cracked and brittle. In an

attempt to search for a process that could be used to suppress the increase of the gel fraction, the reactions were also carried out with various addition rates of the second stage monomers, e.g., from monomer-flooded to monomer-starved, or with the addition of a chain transfer agent such as n-dodecyl mercaptan. Nonetheless, the gel fractions of the latex films were always above 90 %.

This process describing the development of the highly grafted/crosslinked core/shell interphase zone has been reported in Chapter 3. Because of the existence of the large number of residual double bonds, especially the vinyl double bonds, and allylic hydrogens in the P(Bd-S) seed latexes, the continuing reactions of these radical-reaction-active double bonds, which would cause crosslink and graft formation on the P(Bd-S) polymer chains, seemed to be inevitable during the second stage polymerization. Hydrogenation of these double bonds has been considered to be an effective mean for controlling the development of the highly grafted/crosslinked interphase zone.

Figure 6-3 shows the gel fractions and swelling ratios of the films cast from the latexes obtained from the seeded emulsion polymerizations, in which the semi-continuous mode of addition of the second stage monomers was used. The unfilled marks represent the data for control latex film samples in which no TMI monomer is present. Extremely high gel fractions for the latex films prepared with or without the TMI present, were obtained when the non-hydrogenated P(Bd-S)-S seed latex was used. The low swelling ratios for this seed system indicate a very high degree of crosslinking in the polymer. The latex films exhibited many cracks and were easily fragmented. When the modestly hydrogenated (74%) H-P(Bd-S)-1 latex was used as seed, the latex films exhibited a lower

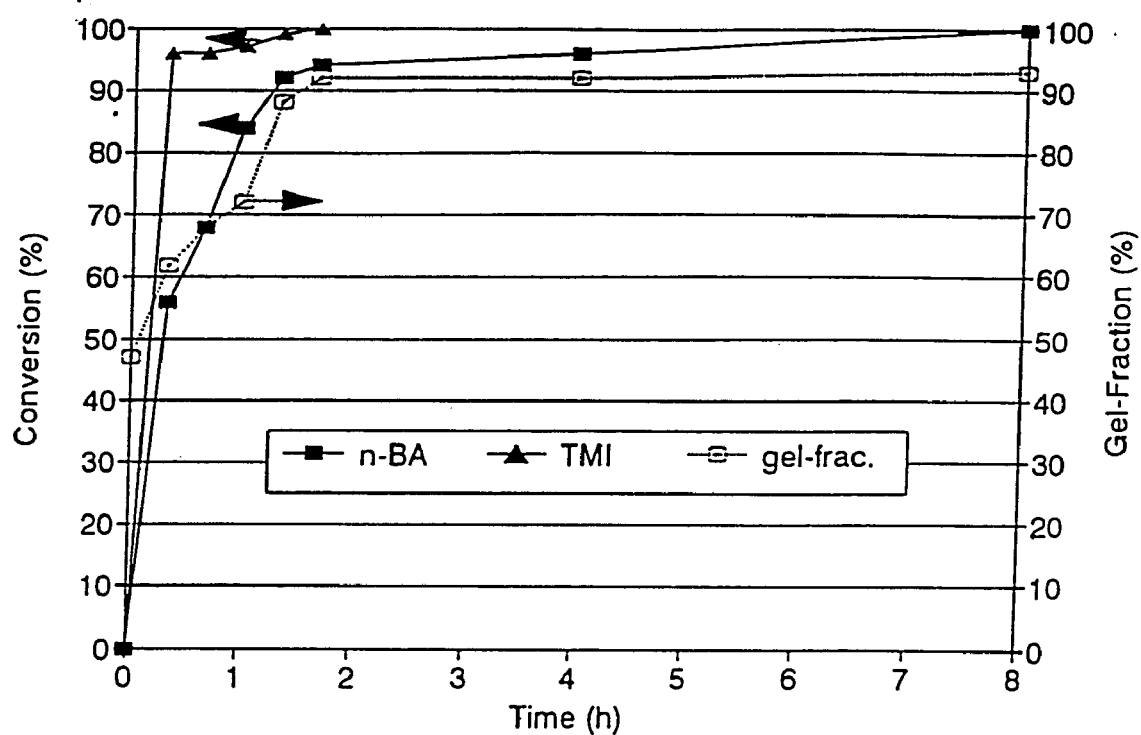


Figure 6-2: Percentage of second-stage monomers converted, and the total gel fraction of the latex vs. reaction time obtained using a SBR seed latex (run 1 in Table II) polymerized to 57 % conversion.

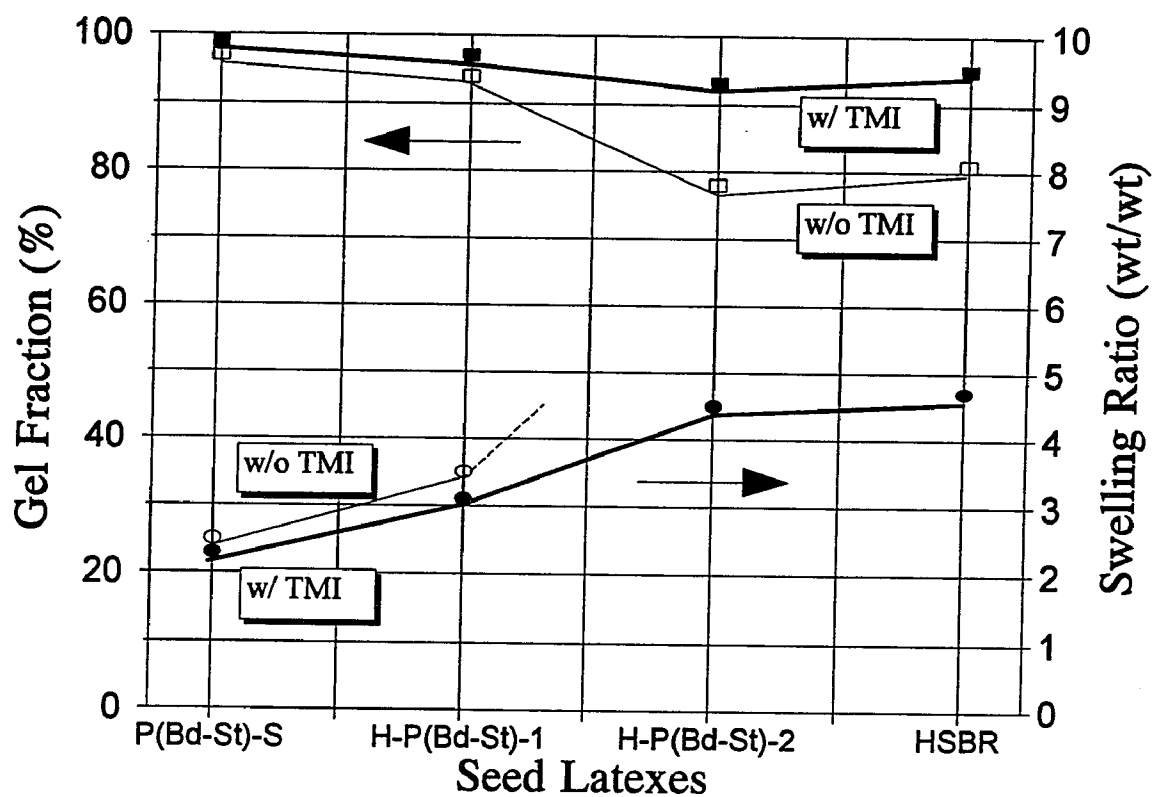


Figure 6-3: Gel fractions and swelling ratios of the films cast from latexes obtained by using the different seed latexes.

number of cracks but still did not exhibit any elasticity. This result suggests that even with a degree of hydrogenation of 74%, the remaining 26% of the double bonds in the H-P(Bd-S)-1 seed latex can still be crosslinked to such a high level that polymer chain interdiffusion is greatly restricted between adjacent particles and prevent the formation of a continuous film.

By using the highly hydrogenated (>90%) seed latexes, i.e., H-P(Bd-S)-2 and HSBR, the gel fractions of the control film samples decreased significantly. The gel fractions for the samples prepared with TMI present only decreased slightly, while the swelling ratios increased from 2.2 and 3.1 for the P(Bd-St)-S and H-P(Bd-St)-1 seed systems, to 4.5 and 4.7 for the H-P(Bd-St)-2 and HSBR seed systems, respectively. The swelling ratios for the control film samples prepared by using the latter two seed latex systems were not obtainable due to the relatively high soluble fractions (>20%). For the gel part of these two film samples the swelling ratios were higher than 8.

The mean molecular mass between two crosslinks, M_c , can be estimated from the well-known Flory-Rehner equation^{23,24}:

$$\ln(1-v_p) + v_p + \chi v_p^2 + (\rho/M_c)V_l(v_p^{1/3} - v_p/2) = 0 \quad (6-1)$$

where v_p is the volume fraction of the polymer in the swollen film, V_l the molar volume of solvent, χ the Flory-Huggins polymer-solvent parameter, and ρ is the density. For the swelling ratios obtained in this experiment, i.e., 2.2, 3.1, 4.5, and 4.7, the M_c 's can be calculated as 7×10^2 , 2×10^3 , 5×10^3 , and 6×10^3 g/mol, respectively. It has been

demonstrated¹⁴ that latex films formed from particles so highly crosslinked that the M_c becomes smaller than the critical entanglement chain length, M_E , which is about 3×10^4 g/mol,^{14,25,26} remained brittle upon annealing because the interdiffusion of polymer chains and the formation of interparticle entanglement were impossible in these films. It is noticeable that all of the M_c values obtained in the present experiment are far below the M_E value. During the film formation process, additional crosslinks would form in those films which incorporated the isocyanate groups which would result in higher gel fractions and degree of crosslinking, compared with the control film samples. The additional crosslinks which were formed during film formation could be either intraparticle (inside the latex particle), or interparticle, depending on the extent of interdiffusion of polymer chains and/or the degree of crosslinking in the original particles for the systems where the polymer glass transition temperature is much lower than the film formation temperature. Polymer chains in highly crosslinked latex particles would undergo very little interdiffusion, thus, the majority of additional crosslinks arising from the isocyanate groups would result from “intraparticle crosslinking”. Consequently, the resulting films are as cracked and brittle as those latex films formed using P(Bd-St)-S and H-P(Bd-St)-1 as the seed latexes. On the other hand, the continuous films formed from the latexes prepared with H-P(Bd-St)-2 and HSBR as seeds exhibit good elasticity, which indicates that both chain interdiffusion and crosslinking via the isocyanate groups have played positive roles in the film formation process, i.e., the major part of the crosslinks derived from the isocyanate groups are formed among those polymer chains that have interdiffused beyond the original boundaries of particles, which would form “interparticle” crosslinks and

strengthen the film.

Figure 6-4 shows the results of tensile testing for HSBR/P(BA-TMI)-1, HSBR/P(BA-TMI)-3 (1 wt% and 3 wt% of TMI in shell, respectively). A non-hydrogenated P(Bd-St) latex film was also used as a control sample. A continuous film could not be formed from the non-modified HSBR seed latex in the temperature range used for casting films in this study (25 to 70 °C), and thus, no testing was carried out with this latex. Table 6-3 lists the swelling ratios for film samples used in the tensile tests.

Figure 6-4 shows that both HSBR/P(BA-TMI) structured latex films exhibited typical stress-strain properties for elastomers, i.e., the stress increased gradually with an increase in strain without a yield point and the film samples were broken at the point where the highest stress was reached. The film having the lower TMI content (1% by wt) showed both higher stress and strain values than those obtained for the film with the higher TMI content (3% by wt). From the swelling ratio data in Table 6-3, it is seen that the HSBR/P(BA-TMI)-3 latex film has a higher average degree of crosslinking (i.e., lower swelling ratio), which should normally result in a higher stress value or modulus in a uniformly crosslinked film. In the latex film systems using thermally crosslinkable functional monomers^{11,12}, it has also been shown that both the stress and modulus increased with an increase in the concentration of the functional monomers. However, unlike the thermal crosslinking system where the crosslinking resulting from the thermal activation of functional groups occurs during the annealing process after the formation of the latex film, in our latex system both polymer chain interdiffusion and crosslinking (from reactions of isocyanate groups) occurred at the same time during the final stage of the film

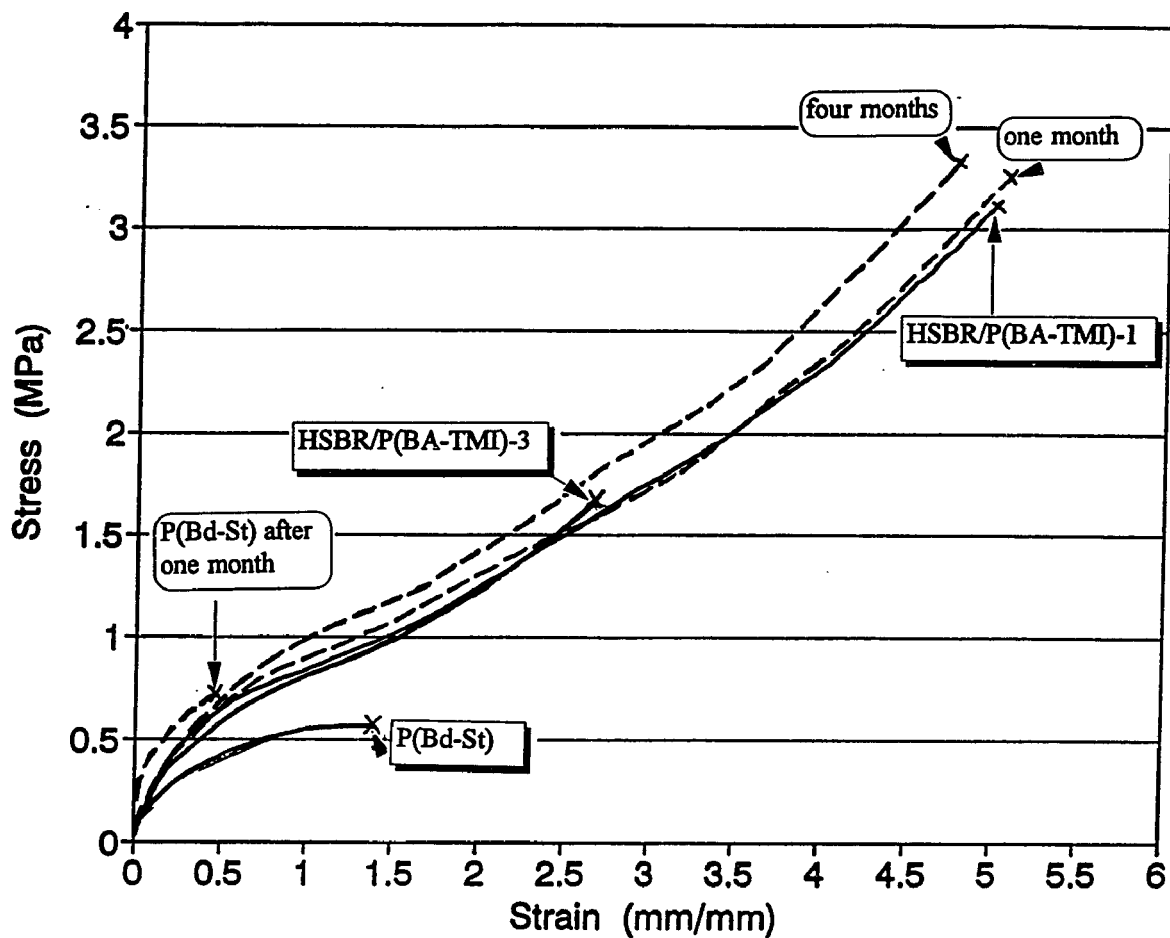


Figure 6-4: Stress-strain behavior for HSBR/P(BA-TMI) structured latex films and P(Bd-St) latex film; solid lines, freshly prepared latex film; dashed line, latex film after aging. (Swelling ratios of the freshly prepared latex films are shown in Table 6-3).

Table 6-3: Film Swelling Ratios for Samples Used in Stress-Strain Measurements
(24 h in toluene)

Latex Films	Swelling Ratios (W_t/W_o) [†]
Non-hydrogenated P(Bd-S)	5.1
HSBR/P(BA-TMI)-1	4.7
HSBR/P(BA-TMI)-3	4.0

[†] W_o and W_t are weight of films before swelling and after 24 h swelling in toluene, respectively.

Thus, the relative extent of the intraparticle and interparticle crosslinking obtained via the isocyanate group are dependent on both the relative rates of polymer chain interdiffusion and the crosslinking reaction of the isocyanate groups. At high isocyanate concentrations, the crosslinking from the isocyanate groups during the film formation takes place too rapidly and polymer chain interdiffusion would be slowed. This premature crosslinking would restrict the further interdiffusion of polymer chains and reduce the extent of interparticle crosslinking. Therefore, the higher degree of crosslinking in the system with the higher TMI content is caused by an increased number of crosslinks inside the latex particles (formed before or during the film formation process). As a result, the HSBR/P(BA-TMI)-3 latex film has shown inferior mechanical properties to that of the HSBR/P(BA-TMI)-1 latex film.

Nonetheless, compared with the P(Bd-S) latex film, which was cast from the unmodified P(Bd-S) latex, both structured latex films showed much better properties. The P(Bd-S) latex film broke at low stress and strain values, although the average degree of crosslinking was lower than those obtained for the two structured latex films. An M_c of 7×10^3 g/mol can be calculated by using equation (1) from the swelling ratio data shown in Table 6-3. Since there is no additional crosslinking which may arise from the presence of isocyanate groups in this latex film, this M_c value can be used to represent the M_c inside the original latex particles, which is much lower than the critical entanglement chain length M_c ($\sim 3 \times 10^4$ g/mol). This indicates that the degree of crosslinking inside the P(Bd-S) latex particles is too high to develop enough molecular interdiffusion between adjacent particles. At the same time, it is further shown that for both structured latex films, which have an

even higher average degree of crosslinking (i.e., lower swelling ratio), that there is a contribution from interfacial crosslinking which occurs during the film formation process.

Another significant difference between the modified HSBR latex film and the non-hydrogenated P(Bd-S) latex film is their aging properties. Obvious deteriorations in film properties were found for the P(Bd-S) film after one month of aging. On the other hand, there was very little change in the mechanical behavior of HSBR/P(BA-TMI)-1 film after one month of aging; a slight improvement in the stress-strain properties was even observed after four months of aging.

Figure 6-5 shows the influence of the film formation temperature on the stress-strain properties of HSBR/P(BA-TMI)-1 latex films. Significant improvements in the mechanical properties were observed when the temperature increased from 25 °C to higher than 45 °C. The higher film formation temperature promoted better polymer chain interdiffusion, and also enhanced interfacial crosslinking during the film formation process.

In Chapter 5, the consumption mechanism of the isocyanate groups from the TMI monomer was investigated using an Attenuated Total Reflectance-FTIR technique. By applying this technique, the IR spectra are able to be recorded during the entire latex film formation process, and the change in the concentration of functional groups in the latex film system can be followed.

Figure 6-6 shows the absorbance intensity profiles for the isocyanate groups and water during the film formation process of the HSBR/P(BA-TMI)-3 latex. After the time (~ 60 min) at which the absorbances of water and the -NCO group reached their minimum

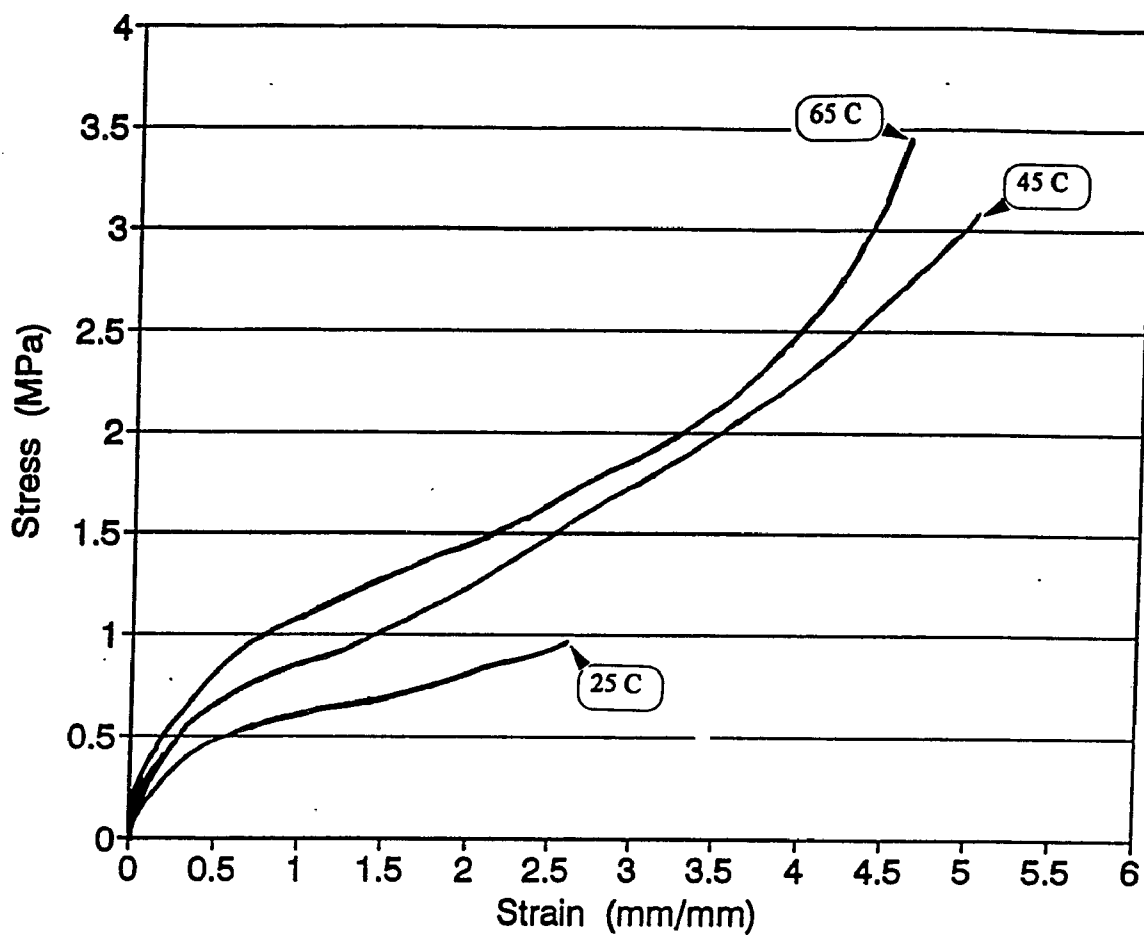


Figure 6-5: Stress-strain behavior for HSBR/P(BA-TMI)-1 structured latex films cast at various film formation temperatures with film formation times as: 4 days at 25 °C, 1day at 45 °C and 65 °C.

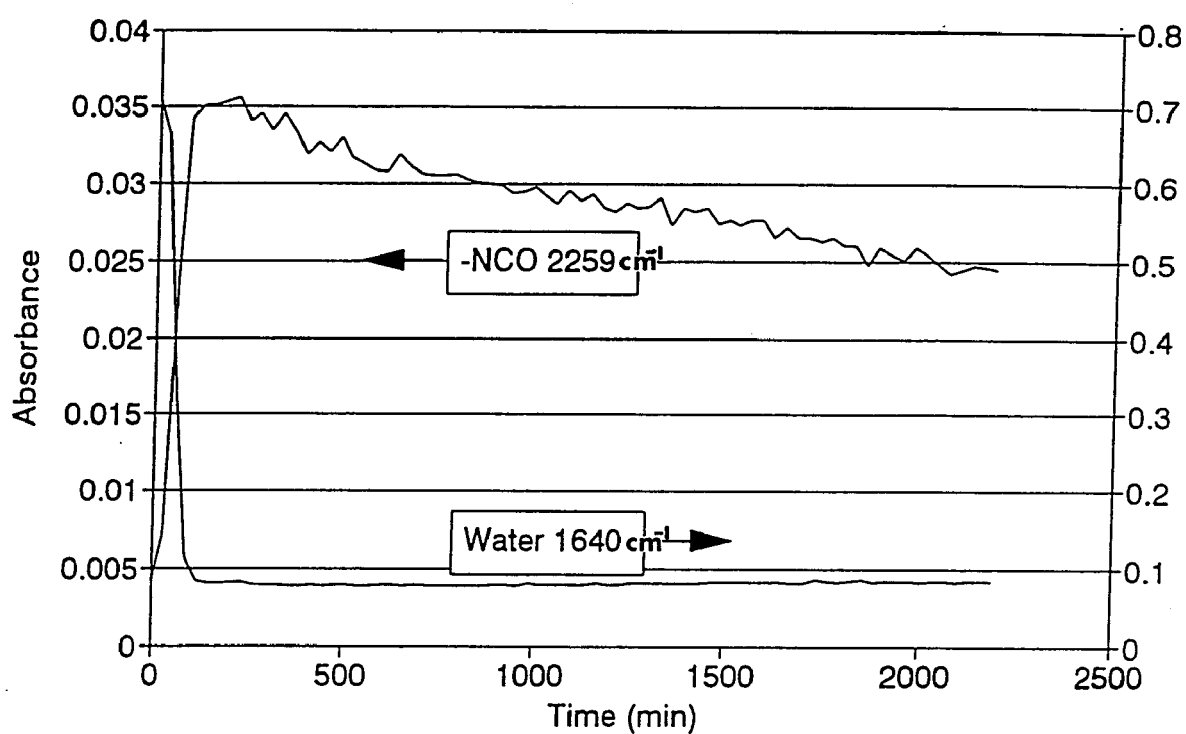


Figure 6-6: ATR-FTIR absorbance profiles of water and isocyanate groups in the HSBR/P(BA-TMI)-3 latex system during a 24 h film formation process.

and maximum points, respectively, the latex system became converted from an extremely concentrated latex into a latex film. After this point, the amount of water in the latex film remains almost constant, while on the other hand, the absorbance for the isocyanate group decreases gradually. This experiment demonstrates the formation of crosslinks (both intraparticle and interparticle) via isocyanate groups during the latex film formation process. Since the crosslinking network is formed in the entire shell polymer phase between core polymer domains, this kind of crosslinking may be, more appropriately, defined as "interphase crosslinking" to distinguish it from "interfacial crosslinking", which is generally used to represent a rather thin crosslinked layer of crosslinking at the particle interfaces. Obviously, a more uniformly crosslinked latex film can be formed from the interphase crosslinking structure, which would lead to better elastomeric properties for the latex film.

6.5 Summary and Conclusions

In summary, the development of the highly grafted/crosslinked core/shell interphase zone in a PBd-based structured latex can effectively be suppressed by the hydrogenation of the PBd-based seed latex. A high degree of hydrogenation (>90%) is necessary for the purpose of this study. Besides controlling the extent of crosslinking in the core/shell interface zone, another great benefit from the hydrogenation of the PBd-based seed latex is the significant improvement in the anti-aging properties of the latex

film, which has been a severe problem in numerous applications using PBd-based latexes.

These model structured latex particles are appropriate for developing high performance elastomeric films, in terms of the formation of an "interphase crosslinked" network in the latex film. It is very important to have a controlled rate of crosslinking of the functional groups (not restricted to the functional groups system used in this work) so that the crosslinking could occur primarily among interdiffused polymer chains. Premature crosslinking inside the latex particles themselves would greatly restrict interdiffusion and lead to the formation of poor latex film.

References

1. Bradford, E.B., *J. Appl. Phys.*, **23**, 609 (1952).
2. Vanderhoff, J.W., *Br. Polym. J.*, **2**, 161 (1970).
3. Linne, M.A., Klein, A., Sperling, L.H., and Wignall, G.D., *Polym. Mat. Sci. and Eng.*, **54**, 593 (1986).
4. Hahn, K., Ley, G., and Oberthur, R., *Coll. Polym. Sci.*, **266**, 631 (1988).
5. Yoo, J.N., Sperling, L.H., Glinka, C.J. and Klein, A., *Macromol.*, **24(10)**, 2868 (1991).
6. Kim, K.D., Sperling, L.H., Klein, A., and Hommonda, B., *Macromolecules*, **27**, 6841 (1994).
7. Bufkin, B.G., and Grawe, J.R., *J. Coat. Tech.*, **50**, 644 (1978).
8. Distler, D. and Kanig, G., *Coll. Polym.Sci.*, **256**, 1052 (1978).
9. Stanislawczyk, V., and Lake, S., U.S. Pat. No. 4,879,364 (1989).
10. Moles, P.J., *Polym. Paint Colour J.*, **178**, 154 (1988).
11. Yeliseeva, V.I., *Br. Polym. J.*, **7**, 33 (1975).
12. Fryd, M., U.S. Pat. No. 4,956,252 (1990).
13. Bassett, D., Sherwin, M., and Hager, S., *J. Coatings Tech.* **51(657)**, 65 (1979).
14. Zosel, A., and Ley, G., *Macromolecules*, **26**, 2222 (1993).
15. Okubo, M., Nakamura, Y., and Matsumoto, T., *J. Polym. Sci., Polym. Chem. Ed.*, **18**, 2451 (1980).
16. Chapter 3.
17. Keskey, W. H., Schuetz, J. E., and Hickamn, A., U.S. Pat. No. 4,644,032,

- (1988).
18. Freakley, P.K., "Rubber Processing and Production Organization", Plenum Press, New York and London (1985).
 19. Parker, D. K., and Poberts, R. F., *Rubber Chem. and Technol.*, **65**, 245 (1991).
 20. Chapter 4.
 21. Dexter, R.W., Saxon, R., and Fiori, D.E., *J. Coatings Tech.*, **58**, (737), 43 (1986).
 22. Spitzer, W.C., *Offic. Dig. Federation Soc. Paint Technol.*, **36**, 52 (1964).
 23. Flory, P.J., *J. Chem. Phys.*, **10**, 51 (1942).
 24. Flory, P.J., and Rehner, J., *J. Chem. Phys.*, **11**, 521 (1943).
 25. Fox, T.G., Gratch, S., and Loshaek, S., in "Rheology" Eirich, F.R. Ed., Academic Press, Orlando, Vol. 1, Chap 12 (1956).
 26. de Gennes, P.G., "Scaling Concept in Polymer Physics" Cornell University Press, Ithaca, New York. Chap. 8 (1979).

Chapter 7

Conclusions and Recommendations

The conclusions drawn from this study of "Elastomeric Films from Structured Latexes" are summarized as follows:

1. Polymerization of BA monomer using P(Bd-S) as seed latex exhibited some unique properties in regards to the formation of a highly crosslinked/grafted P(Bd-S)/PBA interphase zone. The amount of the second stage BA monomer consumed to form this interphase zone could be as much as 1 to 1.5 times the weight of the P(Bd-S) seed latex particles when the gel fraction of the seed is low. A pure PBA phase would be formed only after the interphase zone was completely formed. The formation of a gradient in the grafting and crosslinking density, i.e., high to low grafting/crosslinking level from the surface to the center of the P(Bd-S)/PBA composite particles could be hypothesized. The development of these grafted composite particles would be followed by the formation of a much less grafted PBA phase with further polymerization of BA.
2. Among the four monomers used for the grafting study, i.e., BA, MMA, S, and *i*-

BMA, BA monomer showed the highest degree of grafting and exhibited the most dramatic increase in the degree of crosslinking during the emulsion polymerization using P(Bd-S) as seed. The formation of the P(Bd-S)/PBA interphase zone led to a great increase in the degree of crosslinking in the latex particles and the resulting films remained brittle.

3. The high degree of grafting and crosslinking during the second stage emulsion polymerization using P(Bd-S) as seed could only be decreased slightly by controlling polymerization parameters such as type of initiator, polymerization temperature, mode of addition of the second stage monomer, and the addition of chain transfer agent (dodecyl mercaptan) during the period that the core/shell interphase zone was being formed.

4. Hydrogenation of the P(Bd-S) seed latexes has proven to be an effective way to decrease the degree of grafting and crosslinking during the second stage polymerization using the hydrogenated P(Bd-S) as seed.

5 It can be concluded that, in addition to other parameters such as temperature, pH, and addition rate of the hydrogen peroxide, the surface area density of copper ions at the latex particle surface is a key factor which influences the optimum conditions for hydrogenation. The optimum surface area density is estimated as $2 \text{ Cu}^{2+}/1000 \text{ nm}^2$. The hydrogenation reaction does occur radially from the particle surface inward. The gel fraction in the latex particles does not influence the diffusion of diimide molecules very much, but greatly influences the mobility of polymer chains within the particles.

Therefore, the LG latex system fits the uniform model description of the hydrogenation reaction while the HG latex is better described by a layer model. The hydrogenation zone (thickness) from the particle surface inward where diimide molecules can diffuse before disproportionation reactions occur among themselves is about 20 nm.

6. Attenuated Total Reflectance FTIR (ATR-FTIR) has proven to be a useful technique to study the mechanism of the consumption of isocyanate groups from TMI monomer during emulsion polymerization and film formation. The consumption of isocyanate groups could occur during both polymerization and the film formation process. In most of the systems studied, the percentage of isocyanate groups consumed during the polymerization stage is about 10 to 20%, depending on the particle size or the shell thickness in which the isocyanate groups are incorporated. During the film formation process, a greater number of isocyanate groups could be consumed for a thin shell layer latex system, some of which form interfacial crosslinks. When the particle size is larger than 60 nm, or the shell layer is thicker than 30 nm, interfacial crosslinking from the reactions of isocyanate groups would not take place in a short period of time.

7. Although the development of the highly grafted/crosslinked core/shell interphase zone in a PBd-based structured latex can effectively be suppressed by the hydrogenation of the PBd-based seed latex, a high degree of hydrogenation ($> 90\%$) is necessary for the purpose of this study. Besides controlling the extent of crosslinking in the core/shell interface zone, another great benefit from the hydrogenation of the PBd-based seed latex

is the significant improvement of the anti-aging properties of the latex film, which has been a severe problem in numerous applications using PBd-based latexes.

8. The model structured latex particle is appropriate for developing high performance elastomeric films, in terms of the formation of an “interphase crosslinked” network in the latex film. H-P(Bd-S)/P(BA-TMI) structured latex films which showed satisfactory mechanical properties were obtained by using highly hydrogenated P(Bd-S) seed.

9. It is very important to have a controlled rate of crosslinking of the functional groups (not restricted to the functional groups system used in this work) so that the crosslinking could occur primarily among interdiffused polymer chains. Premature crosslinking inside the latex particles themselves would greatly restrict interdiffusion and lead to the formation of poor latex films.

Finally, in addition to the important data and results that have been provided in this dissertation, this study can be extended for further investigations in several aspects.

1. Through the study on the grafting/crosslinking behaviors of PBd-based structured latexes, it was understood that the degree of crosslinking in the PBd-based structured latex particles increased dramatically during the seeded emulsion polymerization. The high degree of crosslinking not only could obstruct the formation of the elastomeric films, which is the primary objective of this study, but may also influence the outcome for

applications where the PBd-based structured latex particles are used as impact modifiers. It is worthwhile to carry out a series of studies on the effect of the hydrogenated PBd (H-PBd)-based structured latex particles as impact modifiers. Compared with the conventional PBd-based impact modifier, such as SBR/PS or SBR/SAN structured latex particles, the use of H-PBd-based structured latex particles are expected to result in improvements both in the energy absorption (due to the relatively low degree of crosslinking in the structured latex particles) and anti-aging capabilities (from the saturation of the residual double bonds) of the impact modifiers.

2. The ATR-FTIR technique has proven to be very useful for studying the reaction of functional groups in a latex system during the film formation process. Further studies should be conducted on the crosslinking reaction kinetics by investigating such parameters as the distribution of functional groups in the particles, the type of crosslinking agent or reaction catalyst, and the film formation temperature. By combining these studies with the mechanical property measurements, the relationship between the “interparticle” and “intraparticle” crosslinking in latex films can be further determined and understood.

3. A systematic study should be carried to investigate the relationship between the “interparticle” and “intraparticle” crosslinking during latex film formation. Specifically, the distribution of the isocyanate moieties in the latex particles can be controlled via preparation of a series of structured latex particles, e.g., multilayered particles in which the isocyanate groups are incorporated in a certain layer(s). The polymer components used

in different layers should possess similar MFT (Minimum Film Temperature) while exhibiting phase separation. The mechanical properties of the latex films prepared from these structured latex particles with different distributions of the isocyanate groups could provide some important information on the relationship between the mechanical properties of latex films and the relative extents of interparticle v.s. intraparticle crosslinking.

4. The model structured latex particle proposed in the present work can possibly be used in other functional monomer systems. By choosing appropriate types of functional groups in the hydrophobic functional monomer and the hydrophilic crosslinker, the rate of crosslinking reactions and polymer interdiffusions during the film formation can be well balanced to attain optimum "interphase crosslinking" in the latex film.

VITA

Yuan He was born on May 21, 1961, in Beijing, China, the youngest son of Wenjun He and Jing Sun.

In 1984, Mr. He earned a B.S. degree in Chemical Engineering in Tsinghua University, where he met his classmate Danni Wang who became his wife in 1986.

In 1987, Mr. He went to Japan and studied in Dr. M. Okubo's laboratory in Kobe University. After three year's study, Mr. He received his M.S. degree in Department of Chemical Engineering. Upon graduation, Mr. He came to Boston, Mass. USA. He spent eight months in Boston University and then enrolled in Lehigh University and joined the Emulsion Polymers Institute. In July 28, 1992, Mr. Yuan He and Ms. Danni Wang were gifted a baby girl and she was named Shanni, means "mountain girl" in Chinese.

After receiving his Ph.D. from Lehigh, Mr. He has accepted a position as a research scientist with the Cooperate Research of Lord Co.